University of Alberta

Microbiologically Influenced Corrosion in the Stress-Corrosion Cracking of Steels

by

Peter Pingxiao Sheng ©

A thesis submitted to the Faculty of Graduate Studies and Research in partial

fulfillment of the requirements for the degree of Master of Science

in

Metallurgical Engineering

Department of Mining, Metallurgical and Petroleum Engineering

Edmonton, Alberta

Fall 1996

ISBN   0-612-18324-6

Canada

Microfilming Copie

(copyright materials removed)

University of Alberta

Library Release Form

Name of Author: Peter Pingxiao Sheng
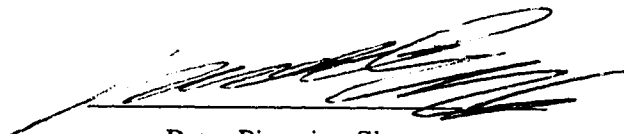
Title of Thesis: Microbiologically Influenced Corrosion in the Stress-Corrosion Cracking of Steels

Degree: Master of Science

Year This Degree Granted: 1996

Permission is hereby granted to the University of Alberta Library to reproduce single copies of this thesis and to lend or sell such copies for private, scholarly, or scientific research purposes only.

The author reserves all other publication and other rights in association with the copyright in the thesis, and except as hereinbefore provided, neither the thesis nor any substantial portion thereof may be printed or otherwise reproduced in any material form whatever without the author's prior written permission.

Peter Pingxiao Sheng

606 Chemical/Mineral Engineering
Building
116 Street - 92 Avenue
Edmonton, Alberta T6G 2G6

Date: _June 12, 1996_

University of Alberta

Faculty of Graduate Studies and Research

The undersigned certify that they have read, and recommend to the Faculty of Graduate Studies and Research for acceptance, a thesis entitled Microbiologically Influenced Corrosion in the Stress-Corrosion Cracking of Steels submitted by Peter Pingxiao Sheng in partial fulfillment of the requirements for the degree of Master of Science in Metallurgical Engineering.

Dr. S. A. Bradford
Supervisor

Dr. M L. Wayman

Dr. J. Luo

Dr. P.M. Fedorak

Date: May 28, 1996

Dedication

To my parents and my wife Ying.

Abstract

One grade of stainless steel and one of carbon steel were tested in two environments containing microorganisms for stress-corrosion cracking with C-ring specimens. Although no specimens ever cracked during the test period of 96 days, their corrosion behavior could still be studied through corrosion potential monitoring, cyclic polarization, scanning electron microscopy and energy dispersive spectroscopy.
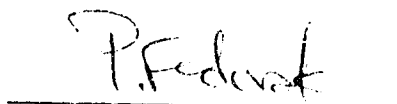
The stainless steel specimens did not undergo microscopically detectable corrosion during the immersion test. However, microorganisms lowered their resistance to localized corrosion and lowered corrosion potential.

Microorganisms also lowered the corrosion potential and caused more vere general corrosion for the carbon steel specimens. In addition, they affected the composition of various elements in the deposits on the carbon steel specimens.

It is also found that almost all the stainless and carbon steel specimens reached a similar corrosion potential which may suggest that this potential is heavily affected by the passive film, corrosion products, biofilm or a combination of them.

Acknowledgements

I would like to express my sincere gratitude to my supervisor Dr. S.A. Bradford for his excellent vision, help and guidance.

I would also like to thank Dr. P.M. Fedorak and Dr. W.J. Page in the ltment of Biological Sciences for valuable discussions and advice.

My appreciation is also extended to the technical staff for their ready help, and amongst them especially: Mrs. Christina Barker, Mr. Shiraz Merali, and Mr. Henry Skrzypek in the Department of Mining, Metallurgical and Petroleum Engineering, Ms. Sara Ebert in the Department of Biological Sciences, and Ms. Christine Hereygers in the Department of Civil Engineering.

Also, I would like to thank Dr. K. Barron, Chairman of Department of Mining, Metallurgical and Petroleum, for financially supporting this research.

Table of Contents

List of Tables

List of Figures

List of Abbreviations

ATCC	American Type Culture Collection
CS	carbon steel
DD	medium containing a viable, pure culture of SRB
EDS	energy dispersive microscopy
EIS	electrochemical impedance spectroscopy
ENA	electrochemical noise analysis
ESEM	environmental scanning electron microscopy
MIC	microbiologically influenced corrosion
MUD	medium containing mud
SCC	stress-corrosion cracking
SCE	saturated calomel electrode
SDD	sterile medium containing heat-killed *D. desulfuricans*
SHE	standard hydrogen electrode
SMUD	medium containing mud sterilized by heat
SRB	sulfate-reducing bacteria
SS	stainless steel
SVET	scanning vibrating electrode technique
TEM	transmission electron microscopy
ZAF	a calculation or correction procedure to improve the accuracy of results by correcting the errors caused by atomic number effect (Z), X-ray absorption effect (A) and X-ray fluorescence effect (F) in quantitative X-ray analysis

1. Introduction

Corrosion is generally thought of as the deterioration of a metal by chemical or electrochemical reaction with its environment. It has long been realized that corrosion is a serious problem in industry. Corrosion can result not only in direct economic loss but also environmental problems, as well as human life and safety issues. However, it is relatively recently that microorganisms have been realized as one of the major causative factors of corrosion.

Microbiologically influenced corrosion (MIC), or biocorrosion or biological corrosion, is defined as the deterioration of metals that is initiated, accelerated, or otherwise influenced by the presence and/or metabolic activities of bacteria and other microorganisms (Walch, 1992). Simply, MIC refers to the corrosion of metals induced by the activity of one or more microorganisms (Iverson, 1987; Ford and Mitchell, 1990). MIC is of considerable concern to the power-generation. chemical-processing, oil, shipping, and pulp and paper industries. Bacterial activity, for instance, is thought to be responsible for more than 75% of the corrosion in productive oil wells and for more than 50% of the failures of buried pipelines and cables (Walch, 1992).

The involvement of microorganisms in metal corrosion was first suggested in 1891, that corrosion of lead could be due to the bacteria products such as ammonia, nitrates, and nitrites (Walch, 1991). Since then, there have been a growing number of reports describing the effects of microorganisms on metal corrosion. The early work was mainly focused on sulfate-reducing bacteria (SRB) and corrosion of iron and steel in soils. Relatively recently, much extensive work has been done by including more bacteria, environments and metals. However, the

possible effects of microorganisms on stress-corrosion cracking (SCC) have not attracted much attention.

SCC usually refers to the failure by cracking under combined action of corrosion and stress, either external (applied) stress or internal (residual) stress. It is one of the most subtle corrosion-related causes of premature fracture of structures, especially in the pipeline industry. Although the relationship between microorganisms and SCC has not been extensively studied, it is reasonable to assume that some microorganisms may have effects on SCC for some metals under certain environments based on the understanding of mechanisms of MIC and SCC. This study focuses on the effects of microorganisms (mainly SRB) on SCC of some steels. Some basic theories related to MIC and SCC are given in the following section

2. Theory

2.1. Basics on Microorganisms

Microorganisms are generally thought of as those organisms that cannot be seen individually with the unaided human eye. Fungi, algae and bacteria are major groups involved in MIC.

Fungi   Fungi are eucary   ave true nuclei). Their cells have a distinct nucleus that contains the genetic   d of cells and is surrounded by a special enveiope called the nuclear membra... (ortora et al.. 1989a).

Fungi may be u... ellular or multicellular. Large multicellular fungi. such as mushrooms. may look somewhat like plants except that they cannot carry out photosynthesis. Even the unicellular fungi. such as oval-shaped yeasts are larger than bacteria. The most typical fungi are molds. They can form mycelia which are long filaments that branch and intertwine. Fungi can reproduce sexually or asexually. They obtain nourishment by absorbing solutions of organic material from their environments.

Fungi may contribute to the biofouling which will establish concentration cells and thus localized corrosion. Furthermore. the consumption of oxygen by fungi may strengthen the concentration cell. However, from the point of view of MIC, fungi seem to be of minimal importance. This is because fungi are rarely found in large numbers in most aquatic systems (NACE, 1984). But, they are important in systems containing wood which will be quickly deteriorated by fungi.

Algae   Algae are eucaryotes with a wide variety of shapes and both sexual and asexual reproductive forms. They carry out photosynthesis and thus produce oxygen and carbonates (Tortora et al.. 1989b). They are relatively large

and can withstand a wide range of conditions from dark to very high light intensity, pH from 5.5 to 9.0, temperatures from less than 0°C to somewhat over 40°C.

Algae generally require light, water, air and a few inorganic nutrients such as phosphorus or nitrogen for nutrition.

Bacteria   Bacteria have received the most attention for their presence and activities within the biofilms which play a very important role in MIC. They are very small, relatively simple, single-celled organisms whose genetic material is not enclosed in a special nuclear membrane. Thus, they are also called procaryotes (have no true nucleus) (Tortora et al., 1989a). Bacterial cells generally have one of several shapes. They may be bacillus (rodlike), coccus (spherical or ovoid), spiral (or helical, corkscrew) and even star-shaped or square-shaped (Tortora et al., 1989c) . Individual bacteria may form pairs, chains, clusters, or other groupings; such formations are usually characteristic of a particular species and thus can be used as identification. Some important properties of bacteria are as follows (NACE, 1984):

(1). They are generally small, usually about 0.2 to 5 μm wide by 1 to 10 μm in length, although some filaments may be several hundred microns in length.

(2). Various types can live in the range of pH 0 to 12, temperatures from -10°C to +99°C, and oxygen concentrations 0 to 100%.

(3). They can migrate to more favorable conditions or away from less favorable conditions.

(4). They may use almost any available carbon molecules as food.

(5). They have specific receptors for certain chemicals which can be adsorbed onto metal surfaces. This makes the metal surface a good place for bacteria to survive and grow.

(6). They can form "colonies" by growing together to cross-feed the individuals.

(7). Most reproduce very quickly by binary fission in which the cell is divided into two halves.

(8). They can adapt to new conditions quickly by genetic mutation.

(9). They can be dispersed widely and quickly by wind, water, animals, aircraft, etc.

(10). "...... are resistant to many chemicals by either degrading them, or by being impenetrable to them (due to slime, cell-wall or cell-membrane), or by adaptation through mutation.

(11). Many produce organic acids such as formic or succinic acids.

(12). Many can form biofilms which play so important a role that a separate part to follow will address this problem.

Many microorganisms play a role in corrosion processes, but by far the most attention has focused on SRB. Anaerobic corrosion by SRB is one of the most important types of MIC documented in the field. There are many cases of SRB-induced corrosion in the pulp and paper, petroleum, chemical, marine and general engineering industries.

SRB are obligate (or strict) anaerobes, which will not function in the presence of oxygen. SRB reduce sulfate to sulfide, which usually shows up as hydrogen sulfide or, if iron is available, as black ferrous sulfide. SRB fall into fourteen genera with each genus containing one or more species of organisms which are very similar (Singleton, Jr., 1992). The best known genus is *Desulfovibrio*. The well known organism *Desulfovibrio desulfuricans* is most wide-spread and easy to isolate (NACE., 1984). SRB have the main responsibility for anaerobic corrosion. They can be found in anaerobic mud and sediments of

freshwater, brackish water and marine environments, soils, and the gastrointestinal tract of man or animals. Most common strains of SRB grow best at temperatures from 25°C to 35°C although a few thermophilic strains can grow at more than 60°C. SRB have the ability to circulate (probably in a resting state) in unfavorable environments such as aerated waters even with chlorine and other oxidizers to find a site to their liking. Furthermore, SRB can thrive in anaerobic microenvironments beneath deposits on metals, within colonies, or under biofilms, where release of secondary nutrients and scavenging of oxygen by the respiration of aerobic bacteria favors growth of SRB. In addition, hydrogen sulfide (H_2S) produced by SRB is a reducing agent that removes oxygen, thereby protecting established colonies of sulfate reducers from its harmful effects. Thus, even in aerated environments, highly active populations of SRB are frequently found on metal substrata (Walch, 1992).

2.2. Biofilms and Biofouling

Microbial cells usually do not grow individually but rather grow together and form biofilms. A biofilm is the microbial community that develops at the interface of two phases (Walch, 1992). Biofilms of most concern in the case of MIC are those at the interface of water and a metal.

Fouling refers to the undesirable formation of deposits on equipment surfaces (Videla and Characklis, 1992). Several types of fouling and their combinations may occur, including biological, corrosion, particulate and precipitation fouling. In most operating plant environments, more than one type of fouling will occur simultaneously. The biofouling is the result of biofilm accumulation. It covers two phenomena, i.e., physical obstruction or fouling and MIC (Cloete and Brözel, 1992).

According to Little et al. (1991b), biofilms can develop on all engineering materials placed in biologically active liquids. Biofilms can be either beneficial or detrimental in actual situations. For example, they can remove dissolved and particulate contaminants in fixed film biological systems such as trickling filters, rotating biological contactors, and fluidized bed wastewater treatment plants. Biofilm reactors can be used for commercial fermentation processes. It is also well known that microorganisms within biofilms have been used to recover minerals and to remove sulfur from coal. However, biofilms can form undesirable deposits on industrial equipment causing reduced heat transfer, increased fluid frictional resistance or plugging. They also enhance or cause MIC. Many reports have been available in this field.

According to Videla and Characklis (1992), net biofilm accumulation results from the combination of (Figure 1):

(1). Transport through the bulk liquid and adsorption of organics onto the water/metal interface.

(2). Transport of microbial cells to the substratum.

(3). Adsorption of cells by the substratum.

(4). Growth and other metabolic activities within the biofilm.

(5). Detachment of portions of the biofilm.

Among these steps, the metabolic production of extracellular polysaccharide (EPS) by all kinds of microorganisms is a key factor. The EPS materials, when accumulated, form sticky slimes. Biofilms tend to be spotty, rather than have continuous surface coverage. It is rare to find a biofilm that is both thin and continuous; thin biofilms are also usually quite spotty, while those which are nearly continuous are thick (Dexter et al., 1991). These films can vary widely in thickness. According to Characklis (1983), biofilm thickness in turbulent flow

seldom exceeds 1000 µm. Biofilms, usually containing 98% to 99% water, have conductivity similar to that of stationary water, thus usually act as an insulator (Characklis, 1983; Dexter et al., 1991).

Walch (1992) summarized the effects of EPS on interfacial processes in biofilms as follows:

(1). Immobilization of water at the biofilm-water interface.

(2). Entrapment of metals and corrosion products at the substratum.

(3). Decrease in rates of diffusion of chemical species to and away from the substratum.

(4). Immobilization and inactivation of corrosion inhibitors and/or biocides.

From the unique properties of biofilms we can conclude that biofilms, where they exist, may play an important role in MIC.

2.3. Mechanisms of MIC

There exists a vast variety of bacteria capable of directly or indirectly influencing the corrosion process. Bacteria are ubiquitous and are able to colonize surfaces and, by genetic mutation, to acquire the ability to adapt to environmental changes. Because of this they represent a dynamic system which is able to change with time. The other important feature associated with colonization of metal surfaces is the subsequent formation of biofilms as discussed before. Adherence of these biofilms is brought about by the release of extracellular polymers. Biofilms up to 100 µm thick are not unusual and in nearly all cases contain bacteria. Such films encourage the growth of these bacteria and this results in the formation of complex biological systems comprising active bacteria, their metabolites and the chemical changes generated by the system. Because of this complexity there will be

numerous corrosion processes and mechanisms, although it is generally accepted that these do not involve any new form of corrosion process.

2.3.1. Iron and Steel

There are many kinds of microorganisms involved in the MIC of iron and steel. The best known are probably SRB. Another kind of anaerobic bacteria that can cause corrosion problems are iron-reducing bacteria.

The other microorganisms have been extensively studied are aerobic bacteria in the genus *Thiobacillus*. These bacteria can oxidize the reduced forms of sulfur and produce sulfuric acid which will cause corrosion (NACE, 1984,). The iron bacteria which fall into the genera *Gallionella*, *Leptothric*, *Sphaerotilus*, *Crenothric*, *Clonothrix* and *Lieskeela* are also important in the MIC of iron and steel (NACE, 1984). Aerobic iron-oxidizing bacteria have also been extensi ely studied with regard to MIC (Jones, 1992c). Corrosion of iron and ste ' un de: the influence of bacteria can proceed in the forms of anaerobic, aerobic and concentration cells.

2.3.1.1. Anaerobic MIC

The best documented case for MIC so far is that for mild steel and iron under anaerobic conditions by SRB. Iron and carbon steel usually undergo very slow corrosion in deaerated neutral water and dilute salt solutions because the only available cathodic reduction reaction,

$$2H_2O + 2e^- \longrightarrow H_2 + 2OH^-$$
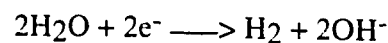
occurs very slowly. However, saturated soils and deaerated cooling waters may support relatively fast corrosion due to anaerobic SRB (Jones, 1992a). Many

studies of MIC have been related to this kind of corrosion (Dexter, 1992). A number of hypotheses have been put forward on the mechanism(s) of anaerobic corrosion by SRB.

Cathodic Depolarization by SRB   This is the first and, until recently, most widely accepted hypothesis which was proposed by von Volzogen Kuhr and van der Vlught (Seed, 1990). In this theory, SRB are postulated to depolarize corroding metals by removing cathodic hydrogen that accumulates on the metal surface, thus accelerating the whole corrosion process. The main features of this theory are as follows.

$$4Fe \longrightarrow 4Fe^{2+} + 8e^-$$ (anodic reaction)

$$8H_2O \longrightarrow 8H^+ + 8OH^-$$ (water dissociation)

$$8H^+ + 8e^- \longrightarrow 8H(ads)$$ (cathodic reaction)

$$SO_4^{2-} + 8H \longrightarrow S^{2-} + 4H_2O$$ (bacterial consumption)

$$Fe^{2+} + S^{2-} \longrightarrow FeS$$ (corrosion product)

$$3Fe^{2+} + 6OH^- \longrightarrow 3Fe(OH)_2$$ (corrosion product)

$$4Fe + SO_4^{2-} + 4H_2O \longrightarrow 3Fe(OH)_2 + FeS + 2OH^-$$ (overall reaction)
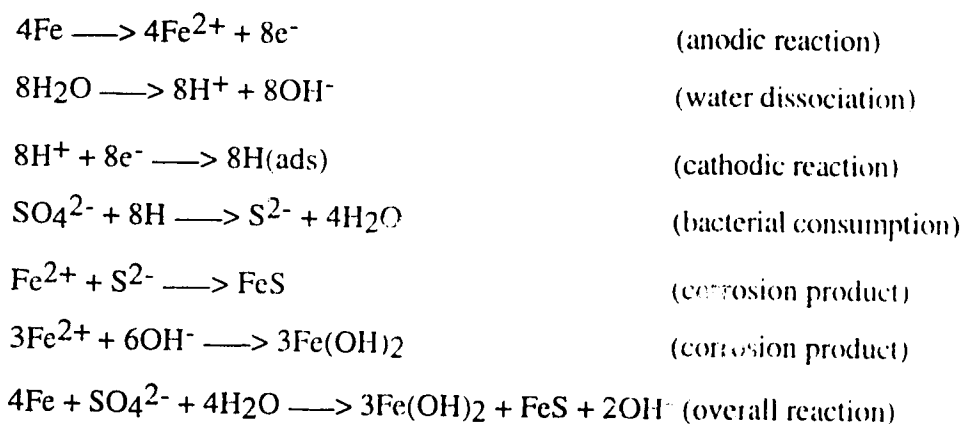
This theory has been supported by some experimental results, for example, the removal of cathodic hydrogen by bacterial hydrogenase, an enzyme produced by most SRB. At present the utilization of cathodic hydrogen by SRB seems to be accepted (Cloete and Brözel, 1992). Nevertheless, not all the anaerobic corrosion by SRB can be explained by this theory. This theory has been modified and some new theories have also been proposed.

Depolarization by Iron Sulfide FeS   In this theory the corrosion product FeS cannot provide any protection for the metal, but rather, as a deposit on

the metal it can act as an additional cathode to utilize the cathodic hydrogen and thus enhance corrosion (Pankhania, 1988).

Depolarization by H2S In anaerobic, neutral environments the concentration of H^+ is extremely small. Therefore additional cathodic reactions must be considered:

$$2H_2S + 2e^- \longrightarrow 2HS^- + H_2$$
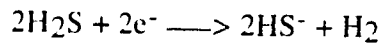
The dissolved H_2S produced by SRB receives electrons to form H_2, thus depolarizing the cathodic reaction (Pankhania, 1988; Little et al. 1991a).

Production of Sulfuric Acid The argument is that corrosion product sulfide may react with oxygen at the aerobic/anaerobic interface to produce elemental sulfur which can then be oxidized to highly corrosive sulfuric acid by sulfur-oxidizing bacteria (Pankhania, 1988).

$$2S + 3O_2 + 2H_2O \longrightarrow 2H_2SO_4$$
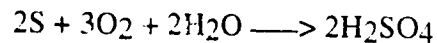
This process will be discussed in more detail in the aerobic corrosion section as the effect of aerobic sulfur-oxidizing bacteria.

Production of Highly Corrosive Metabolic Products It is postulated that the SRB can produce highly corrosive and volatile phosphorous metabolic products which enhance the metal corrosion. The experimental evidence is the identification of iron phosphide Fe_2P as a major corrosion product in addition to FeS (Pankhania, 1988; Weimer et al., 1988).

Anodic Stimulation by Sulfide Ion, S^{2-} The corrosion can be accelerated by S^{2-} because S^{2-} can react with Fe^{2+} at the anode.

Depolarization by Iron-Reducing Bacteria   Besides SRB.

iron-reducing bacteria can also play a role in MIC under anaerobic conditions. These bacteria can reduce ferric (Fe^{3+}) to ferrous iron (Fe^{2+}) (Arnold et al., 1990; Obuekwe et al., 1981). As we know, ferric iron (Fe^{3+}) is insoluble except at very low pH. The deposited ferric compounds can protect the metal from further corrosion due to chemical activity. Ferrous compounds are mostly soluble and, therefore, reduction of ferric compounds to ferrous compounds results in the breakdown of the protective rust layer and indirectly causes corrosion problems. The genera considered to include iron-reducing bacteria are *Bacillus, Pseudomonas, Paracoccus, Micrococcus, Corynebacterium, Escherichia, Enterobacter, Citrobacter, Serratia, Proteus, Alcaligenes, Vibrio, Clostridium, Bacteroides* and *Desulfovibrio* (Cloete and Brözel, 1992).

2.3.1.2. Aerobic MIC

The following are two major MIC mechanisms related to aerobic bacteria:

Acid Production   The aerobic, sulfur-oxidizing bacteria of the genus *Thiobacilus* obtain their energy by oxidizing sulfur, sulfate, hydrogen sulfide or other sulfur compounds, leading to the production of highly corrosive sulfuric acid (Bos and Kuenen, 1983; Iverson, 1987; Purkiss, 1971). The mechanisms are described below in terms of chemical reactions (Purkiss, 1971).

$$2H_2S + 2O_2 \longrightarrow H_2S_2O_3 + H_2O$$

$$5Na_2S_2O_3 + 4O_2 + H_2O \longrightarrow 5Na_2SO_4 + H_2SO_4 + 4S$$

$$4S + 6O_2 + 4H_2O \longrightarrow 4H_2SO_4$$
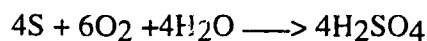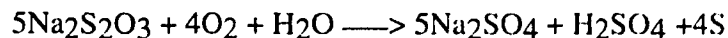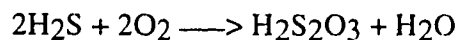
Among the sulfur-oxidizing bacteria *Thiobacillus ferroxidans* have been well known for their ability to recover metals from low grade ore, produce sulfuric acid from the mineral pyrite, or iron sulfide, and oxidi. ferrous ion to ferric iron. The proposed mechanism is as follows (LeRoux, 1971).

$$2FeS_2 + 7O_2 + 2H_2O \longrightarrow 2FeSO_4 + 2H_2SO_4$$

$$4FeSO_4 + O_2 + 2H_2SO_4 \longrightarrow 2Fe_2(SO_4)_3 + 2H_2O$$

$$FeS_2 + Fe_2(SO_4)_3 \longrightarrow 3FeSO_4 + 2S$$

$$2S + 3O_2 + 2H_2O \longrightarrow 2H_2SO_4$$
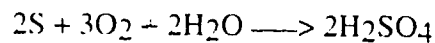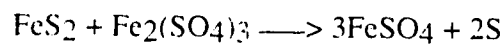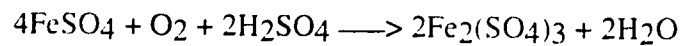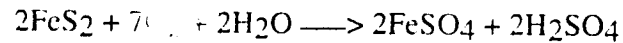
According to LeRoux (1971), the second reaction would be very slow in the absence of *T. ferroxidans* since ferrous ions are relatively stable in acid solution. The presence of the bacteria also makes the third reaction possible.

Similarly the production of many other acids, including organic acids, by a variety of different organisms will also corrode iron and steel. Acetic and butyric acids are examples of such metabolic products (Ford and Mitchell, 1990). It might be noted that the organic acids will also tend to break organic coatings, providing good environments for microorganisms to grow creating anaerobic condition for SRB.

Corrosion by Iron Oxidizing Bacteria   The usually cited iron oxidizing bacteria causing MIC are genera *Gallionella, Sphaerotilus, Crenothrix, Pedomicrobium and Leptothrix* (Little et al., 1991a; Cloete and Brözel, 1992). These bacteria oxidize soluble ferrous ions (Fe^{2+}) to less soluble ferric ions (Fe^{3+}), jointly causing the formation of tubercles with microbial slime (Ford and Mitchell, 1990). Underdeposit corrosion is extremely important because it initiates a series of events that are extremely corrosive (Little et al., 1991a). The sheltered area

under the tubercle acts as an anode in a differential aeration cell, with oxygen being reduced to OH^- at the cathodic surrounding area and on deposit surfaces to cause a series of reactions.

$$O_2 + 2H_2O + 4e^- \longrightarrow 4OH^-$$

$$Fe^{3+} + 3OH^- \longrightarrow Fe(OH)_3$$

or $\quad 2Fe^{3+} + 3CO_2 + 6OH^- \longrightarrow 3H_2O + Fe_2(CO_3)_3$
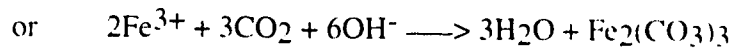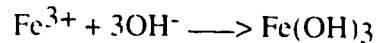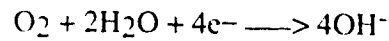
Because of the shortage of oxygen, SRB may grow under the deposit and cause anaerobic corrosion. In addition, migration of chlorides into the anode area (to neutralize the positive charge) may also accelerate the corrosion.

2.3.1.3 Concentration Cells

As discussed above, biofilms are usually nonuniform. Biofilms result in different diffusion rates of many particles and ions and thus can lead to the formation of concentration cells involving oxygen and various ions. A biofilm 15 μm thick may be thick enough to prevent the oxygen from diffusing through it (Walch, 1991). Besides, a biofilm may also lead to macrofouling (barnacles, etc.) which may also provide corrosion sites (NACE, 1984). In addition, because of the anaerobic condition resulting from the oxygen depletion under the biofilm (or barnacles), SRB can grow and introduce anaerobic corrosion.

It should be noted, however, that fungi and algae may also play a role in concentration cells. As mentioned above, fungi can strengthen the concentration cells by contributing to the biofouling and consumption of oxygen, but algae may cause a more complicated situation than fungi (NACE, 1984).

Along with bacteria, algae are widely recognized as important biofoulers and thus MIC promoters. Another way in which algae affect the MIC is that they

are one of the food producers for bacteria and fungi, and therefore may increase or cause MIC problems. In addition, they can also produce corrosive organic acids and slimes (Cloete and Brözel, 1992). For algae, however, the major concern is probably their production of oxygen. As mentioned before, algae can carry out photosynthesis to produce oxygen, which will be accumulated within the biofilm (Little et al., 1991a; Tortora et al., 1989b). Increased oxygen concentration then may depolarize the cathodic oxygen reduction reaction,

$$O_2 + 2H_2O + 4e^- \longrightarrow 4OH^-$$
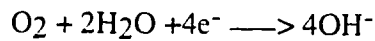
resulting in increased corrosion rates (Little et al., 1991a).

2.3.2. Stainless Steels and Nickel Alloys

These alloys have usually a thin passive surface film which is resistant to corrosion. This film requires oxidizing conditions for both initiating passivity and repairing subsequent chemical or mechanical damage to the film. It is generally accepted that for this reason these kinds of alloys are particularly susceptible to pitting and crevice corrosion. Among these alloys, stainless steels are the most documented with regards to MIC.

Although there are not as many reports available on MIC of stainless steels as on iron and mild steel, it can be concluded that microorganisms are involved in the corrosion of stainless steels, especially for the heat-affected zones of austenitic stainless steel weldments (Borenstein, 1988, 1991; de Mele et al., 1991). The MIC is often in the form of pitting and may be in the weld, in the heat-affected zone, along the fusion line, or in the base metal near the weld. Either or both phases,

austenite and delta ferrite, may be susceptible to MIC. However, reasons for this phenomenon are still not well understood (Borenstein, 1991).

Unlike MIC of iron and steel, MIC of stainless steels and nickel alloys may involve more aerobic bacteria such as iron-oxidizing bacteria rather than anaerobic SRB. Nevertheless, there is not much information available on the microorganisms involved in this kind of corrosion. As for mechanisms, cathodic depolarization of oxygen reduction,

$$O_2 + 2H_2O + 4e^- \longrightarrow 4OH^-$$
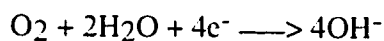
seems to be the most accepted (Little et al., 1991a; Mollica, 1992).

Based on experimental results, Mollica (1992) concluded that the depolarization of the above reaction induced by biofilm growth on stainless steels and nickel alloys was due to a catalyst produced by settled bacteria, probably linked to their exopolymers, that raised the pH above 8 on the surface. Algae may also contribute to the depolarization by production of oxygen through photosynthesis as discussed before. Other hypotheses to explain the reason for depolarization of the oxygen reduction include the surface acidification (Dexter and Gao, 1988) and increase of exchange current density of oxygen reduction due to the effect of a catalyst generated by the bacterial metabolic activity (Gallagher et al., 1988).

2.3.3 Other Metals and Alloys

Many people do not think MIC of copper alloys to be a serious problem as they believe that copper ions and salts formed by corrosion are always lethal to the causative organisms. Unfortunately, this is not the case.

It is well known that corrosion products of copper and copper alloys are toxic to marine organisms and therefore suppress the attachment of these fouling organisms (NACE, 1984). However, evidence shows that many bacteria may tolerate very high levels of copper, e.g., *Thiobacillus*, which can produce very corrosive sulfuric acid, can tolerate as high as 2% copper (NACE, 1984). *Aspergillus* and *Penicillium* are both noted for their ability to corrode copper (Seed, 1988). Anaerobic SRB may also play an important role in MIC of copper and copper alloys under anaerobic conditions.

Many reports have suggested the involvement of microorganisms in corrosion of copper alloys (NACE, 1984: Little et al., 1991a). For example, a first incidence of failure within a copper plumbing system recorded only two months after installation was thought to be due to MIC (Fischer et al., 1992).

Although not as well understood as MIC of iron and steel, MIC of copper and copper alloys may employ one or many of the mechanisms similar to anaerobic and aerobic corrosion of iron, e.g.,

(1). Direct corrosion through corrosive products such as carbon dioxide, hydrogen sulfide, ammonia, organic or inorganic acids (NACE, 1984: Pope et al., 1984). Ammonia may be responsible for stress corrosion of copper and brass (Pope et al., 1984).

(2). Production of organic products which can act as depolarizers or catalysts of corrosion reactions (Pope et al., 1984).

In addition, differential aeration, selective leaching, and underdeposit corrosion are also considered possible mechanisms (Little et al., 1991).

Aluminum and its alloys are highly susceptible to bacteria. and fungal attack, a well-known phenomenon in aluminum alloy fuel tanks which has long been recognized as a problem (Seed, 1990). Many bacteria and fungi have been

found involved in MIC of aluminum and its alloys. The attack by these microorganisms may occur under both aerobic and anaerobic conditions. The most common species have been *Pseudomonas*, *Cladosporium*, and *Desulfovibrio* (NACE, 1984).

The proposed possible mechanisms for MIC of aluminum and its alloys are as follows (NACE, 1984; Little et al., 1991a):

(1). Depletion of natural inhibitors.

(2). Production of corrosive compounds, e.g., water-soluble organic acids.

(3). Formation of differential aeration cells.

(4). Cathodic depolarization.

(5). Extracellular enzyme activity and metabolism of alloy constituents.

Among engineering alloys, titanium employs unparalleled resistance to MIC. A literature review indicates no evidence of titanium failure related to MIC. The resistance of titanium to MIC is thought to be due to its highly stable, tenacious, adherent, and protective surface oxide film (TiO_2) (Schutz, 1991).

2.4 Mechanisms of SCC

As previously stated, SCC is the failure of materials by cracking resulting from the combined and synergistic interaction of mechanical stress and corrosion reactions. A sensitive material, high enough tensile stress but usually below the macroscopic yield point, and a corrosive environment constitute the basic requirements for SCC to occur.

SCC is material (usually metal)/environment specific; that is, it is the direct result of a specific metal in an environment with specific chemical component(s). SCC is of the greatest concern in corrosion resistant alloys, which usually form a film on the metal surface exposed to aggressive aqueous environments.

The SCC process includes three consecutive stages:

(1). Crack initiation at surface discontinuities such as grooves, laps, burrs, corrosion pits, or slip bands. Some discontinuities are pre-existing such as fabrication defects and some are created afterwards such as corrosion pits or intergranular corrosion produced when metal is exposed to an environment. Not all surface discontinuities can cause crack initiation. Crack initiation actually has not been precisely defined and it is difficult to determine at what point a pit is actually a crack (Jones and Ricker, 1992). Although it is convenient to view the SCC process in separate stages from an engineering point of view, there may be a gradual transition from localized corrosion to crack initiation and growth with no separation of stages, or there may be a repeated succession of short steps of initiation and growth (Sprowls, 1992). Few models have successfully depicted this stage.

(2). Crack propagation through the synergistic stress-corrosion interaction at the crack tip. Many models have been put forward to deal with this process. This is still a very active field for research. Basically they can be classified into either anodic or cathodic mechanisms. The point is that the crack propagation may be associated with either anodic or cathodic reaction of the corrosion which occurs at the same time as crack propagation. For example, simple chemical dissolution and removal of material from a crack tip is an anodic mechanism, and hydrogen evolution, absorption, diffusion, and embrittlement is a cathodic mechanism (Jones and Ricker, 1992). While environmental action may be dominant only at the initiation stage, tensile stress becomes dominant as subcritical cracking advances with the proceeding of SCC (Sprowls, 1992).

Crack propagation can also be classified into dissolution and mechanical fracture categories. While a crack advances by preferential dissolution at its tip in dissolution models, stress concentration at the base of corrosion slots or pits

increases to the point of ductile deformation and fracture, or brittle fracture, in the mechanical models (Jones and Ricker, 1992).

Dissolution Models   In this category, the film-rupture model and active-path intergranular SCC are most accepted (Jones and Ricker, 1992).

In the film-rupture model (Treseder and Swanson, 1968; Dvoreček, 1970), stress acts to open the crack and rupture the protective surface film. It is postulated that localized plastic deformation at the crack tip ruptures the passivation film, exposing bare metal. This bare metal then dissolves rapidly, resulting in crack extension. This model tends to explain intergranular SCC in some systems.

In the active-path intergranular SCC model, an active-path process that results from a difference in the microchemistry of the material at grain or interface boundaries causes SCC (Jones and Ricker, 1992).

Mechanical Fracture Models   In this category, corrosion tunnel, tarnish-rupture, adsorption-enhanced plasticity, adsorption-induced brittle fracture and hydrogen embrittlement are more prominent and often cited (Jones and Ricker, 1992).

The corrosion tunnel model (Azhogin, 1966) assumes that a fine array of small corrosion tunnels forms at emerging slip steps. These tunnels grow in diameter and length until the stress in the remaining ligaments causes ductile deformation and fracture. The crack thus propagates by alternating tunnel growth and ductile fracture. It was concluded that transgranular SCC can be explained with this model.

In the adsorption-enhanced plasticity model (Campbell, 1970; Haufman and Rouls, 1965; Walter and Chandler, 1971), cleavage fracture is not an atomically brittle process, but occurs by alternate slip at the crack tip in conjunction with formation of very small voids ahead of the crack. Chemisorption of environmental

species facilitates the nucleation of dislocations at the crack tip, promoting the shear processes responsible for brittle, cleavage-like fracture. This theory promises to explain m iy similarities among SCC, liquid metal embrittlement and hydrogen embrittlement.

In the tarnish-rupture model (Williams and Nelson, 1970), a brittle surface film forms on the metal, fracturing under the applied stress. Fracture of the film exposes bare metal, which rapidly reacts with the environment to re-form the surface film. The crack propagates by alternating film growth and fracture. This model is mainly used to describe intergranular SCC.

The adsorption-induced brittle fracture (Ishizuki and Onishi, 1967) involves adsorption of environmental species which lowers the interatomic bond strength and the stress required for cleavage fracture.

For hydrogen embrittlement, the enhanced-plasticity theory as described above and the decohesion theory are the the two most widely accepted models (Marsh and Gerberich, 1992). In the decohesion theory (Troiano, 1960), electrons donated from dissolved hydrogen atoms enter the incompletely filled bond of metals. The cohesive strength of the metal lattice is reduced by the increased electron density acting to increase the interatomic spacing of the lattice. At any locality of the lattice where hydrogen concentrates under the thermodynamic effect of hydrostatic tension, cohesive strength is reduced. Externally applied stress is magnified in the crack-tip region and overcomes the resistive-cohesive force between atoms. The resistive-cohesive force is diminished by the stress-induced local hydrogen concentration.

(3). Final failure through almost pure mechanical fracture. This is due to the act that with the progress of SCC, the true stress (the load divided by actual cross section area in the necked-down region) of the material will increase due to the

decrease of the cross section which actually withstands the stress (Jones and Ricker, 1992).

2.5 Relationship Between MIC and SCC

Despite many published reports on the effects of microorganisms on general corrosion, much less information is available with respect to SCC. Based on the understanding of MIC and SCC, we can easily conclude that microorganisms may play a role in SCC under some circumstances. What microorganisms may affect corrosion in MIC may also affect SCC considering that corrosion is also involved in SCC. However, the extent to which microorganisms may play a role may be different for MIC and SCC.

Izumiya et al. (1988) reported a case of SCC of mild steel in a cooling system due to nitrofying bacteria. The proposed mechanism is the microbial oxidation of nitrite ion NO_2^- to nitrate ion NO_3^- which accelerates corrosion through lowering pH by hydrolysis in pits. Due to the existence of residual stress from welding, final cracking results.

A 6-year field study by TransCanada Pipelines Ltd. (Delanty and O'Beirne, 1992) of SCC suggests that the severity of SCC for pipelines appears to increase with the presence of bacteria and the absence of oxygen. The involved bacteria include sulfate-reducing and acid-producing bacteria. The result shows that the colony size, crack length, and crack depth increases with increasing bacterial concentrations within a given area. It is suggested that the bacteria could generate such by-products as CO_2, H_2S, and organic acid and thus promote corrosion or SCC. Laboratory results indicate that the existence of bacteria can create reduced conditions thus promoting formation of the iron carbonate corrosion deposit which is most predominantly associated with SCC.

Gangloff and Kelly (1994) reported that a SRB (*Desulfovibrio vulgaris*) greatly enhanced fatigue crack propagation in a martensitic alloy steel HY130 under cathodic protection. The suggested mechanism includes metabolic sulfide-enhanced H uptake and hydrogen embrittlement.

Tatnall (1994) reported fa 'ure case of type 304 stainless steel condenser tubes. Metallographic examination showed the cracks with a branched, transgranular appearance typical of chloride SCC The biological deposits correlated directly with the crack locations. However, there was no concentration of chloride in the biodeposits although a minute concentration of chloride was detected at each crack. The metal temperature was $40^{\circ}C$ which is well below the $60^{\circ}C$ usually considered the minimum temperature for Cl^- SCC to occur. The cracks were circumferential, although the residual stresses in the tubes should have been in the circumferential direction. The inconsistency with normal Cl^- SCC led the author to suspect it was microbiologically-induced SCC.

The most studied aspect of a relationship between microorganisms and SCC is probably the effect of H2S on SCC. although in most cases H_2S is not from bacteria. However, some bacteria, especially SRB. may produce H_2S as a major metabolic product which may play a big role in SCC.

Hydrogen sulfide SCC has been reported in carbon and low-alloy steel applications such as pipelines, process piping, pressure vessels. gas and oil well tubulars, and wellhead ipment and is often termed "sulfide stress-cracking" (SSC) although its mechani.. 's consistent with hydrogen embrittlement.

The most harmful environments regarding SCC for high-yield-strength steels are those with cathodic poisons which prevent the association of atomic hydrogen to molecular hydrogen and thus increase the supply of atomic hydrogen

to cause hydrogen embrittlement (Marsh and Gerberich, 1992). The most common cathodic poison is sulfur in the form of H_2S.

Hydrogen embrittlement of high-strength stainless steels due to hydrogen sulfide is well known. The presence of hydrogen sulfide in various environments decreases the hydrogen embrittlement resistance of high-strength stainless steels.

Hydrogen sulfide will definitely play a role in SCC under some circumstances. However, differences in effect on corrosion fatigue of some high strength micro-alloyed steels in natural seawater between biologically and abiologically produced H_2S have been reported (Thomas et al., 1987). The authors claimed that the microbially-produced H_2S was less potent than synthetic, abiological H_2S with   in promotion of corrosion fatigue, and that the exact reason for this phenome   own.

3. Literature Review on Commonly Used Methods in MIC and SCC Studies

There has been virtually no consensus on how to conduct an MIC test or how to interpret the test results due to the complexity involved. First of all, MIC involves a dynamic system due to the activity of microorganisms during corrosion. Secondly, MIC deals with a complex biofilm which may involve many kinds of processes. Finally, people usually do not have enough expertise in both microbiology and corrosion at the same time.

The forms of corrosion which can be stimulated by the interactions of bacteria with metals are numerous and range from general, pitting, crevice corrosion and SCC, to enhancement of corrosion fatigue, intergranular stress cracking of sensitized austenitic stainless steels, and hydrogen embrittlement and cracking. Because of the complexity, microbially related corrosion problems are seldom straightforward and require a considerable amount of investigation often involving sophisticated methodology and equipment.

Many kinds of techniques from different fields, e.g., metallurgy, microbiology and electrochemistry, have been employed in the study of MIC. But, none of these can solve the problem alone. The interpretation of the data obtained is tricky even with the combination of a few techniques. The correlation between the data and the mechanism of MIC is still far from satisfactory although some techniques can monitor the process of MIC. Future work should be focused on the interpretation of the data and/or development of new techniques. The following techniques are those most commonly used by corrosion researchers and microbiologists for MIC and SCC studies.

3.1 Methods for MIC Studies

3.1.1 Physical and Metallurgical Methods

Physical and metallurgical methods include identification of the type of corrosion (uniform corrosion, crevice attack, pitting, etc.) and metallographic, microscopic, and electron microscopic techniques. These methods have been used to determine if the corrosion was MIC or not. Among these techniques, the optical microscopic and electron microscopic techniques are most useful.

3.1.1.1 Optical Microscopy

The microscopic techniques constitute some of the easiest, fastest, and most precise techniques available for the detection and enumeration of microbes. The major difficulty with brightfield microscopy is discriminating the bacteria from the surrounding nonmicrobial materials.

Certain stains, such as methylene blue or gram stain, can be used to stain the microbial cells and help differentiate cells from debris. However, much of the debris also reacts with these stains. The advantages of this technique are that it is inexpensive, relatively quantitative, and both live and dead cells are counted, regardless of whether they can be routinely cultured (grown on agar plates or other such media that allow the cells to be counted and help in their identification).

The situation can be much improved by staining of the biological materials with dyes that are fluorescent and react specifically with molecules found only in biological materials since they react less with noncellular materials. Consequently, there is much less interference from debris when viewed with the fluorescence microscope. Examples of such dyes are fluorescein isothiocyanate, which reacts with proteins in the microbial cell, and acridine orange, which reacts with nucleic

acids in the cells. These techniques have the advantages of the brightfield microscopic techniques and, in addition, allow discrimination of cells from debris. However, these methods still do not differentiate between live and dead cells.

3.1.1.2 Electron Microscopy

Many electron microscopic techniques have been used to study the MIC. The commonly used methods include scanning electron microscopy (SEM) with energy dispersive spectroscopy (EDS), transmission electron microscopy (TEM), X-ray photoelectron spectroscopy, Auger electron spectroscopy, scanning Auger microscopy, etc. More recently, Environmental SEM (ESEM) has been employed.

The conventional SEM has been extensively employed in the study of microorganisms because of its well-known advantages (high resolution, depth of field, microanalysis) with flexibility. However, the conventional SEM can only be operated with a high vacuum in the chamber. Any vacuum lowering due to the introduction of gas into the chamber can cause a variety of serious problems with filament, imaging, electron detector, specimen contamination, etc. Therefore, special preparation of the microorganisms is needed due to their high water content. The preparation of these biological materials for SEM requires extensive work in manipulation, including fixation, dehydration, and either air drying or critical-point drying. In addition, the microorganisms must be coated or stained with a conductive film of metal before being viewed. These preparation procedures not only are time consuming, but also may cause contamination and distortion.

Chemical analysis for corrosion products, or deposits on specimens can be done either qualitatively or quantitatively by EDS in the SEM by measuring the energy and intensity distribution of the x-ray signal generated by a focused electron beam. EDS can also be used to determine the elemental composition of

microorganisms in the SEM. However, the disadvantages of the SEM in manipulating microorganisms are also a problem for EDS analysis. Scientists have long explored ways to modify the SEM in order to allow the direct examination of moist biological specimens without the need to resort to tedious and often damaging conventional preparation techniques. This has led to the development of the so-called ESEM recently.

The ESEM has been defined as an SEM capable of maintaining a minimum water vapor pressure of 609 Pa in its specimen chamber (Danilatos, 1991). This pressure corresponds to the saturation pressure of water vapor at 0^oC and constitutes a natural threshold, above which water can be maintained in its liquid phase. Then, the moist specimen can be kept wet in the chamber. The ESEM can be also operated at room temperature and higher pressures. The "environmental" thus really refers to the truly wet and almost natural condition of the specimen. The microorganisms are therefore more ideally examined under the ESEM than SEM.

The ESEM operates under basically the same principles as the SEM except that the former employs a high pressure of water vapor (or other gases) environment for the specimen. It is this water vapor (or other gases) that will cause a series of effects modifying or changing the behavior of electrons, and thus affect ESEM operation. This constitutes the most significant difference between ESEM and SEM. One of the most important phenomena for the ESEM operation is the interaction between electrons and water molecules which causes scattering of electrons and ionization of water vapor. Fortunately, the scattering of the electrons will not strongly affect the focusing. Further, the ionized gas can neutralize the accumulated charge on the surface of the specimen. These basic characteristics of interaction between electrons and water vapor (or other gases) thus make ESEM possible.

For microo.ganisms, one aspect of most concern is their behavior and relationship with their environment under natural condition. Usually, the microorganisms will produce a biofilm, thus leading to a extremely complicated situation. The ESEM can offer an almost natural environment for the microorganisms, and thus can contribute much to this kind of study.

Much work has been done on biofilms. However, microscopic examination under natural conditions is actually impossible with conventional methods such as SEM and TEM. Almost all examinations have been done by traditional preparation methods and thus may cause many problems as previously stated.

Little et al. (1991b) reported some results of the application of ESEM to a biofilm. They used an ElectroScan Type II ESEM with a secondary electron detector capable of forming high resolution images at pressures in the range of 13 to 2660 Pa.

The specimens were maintained at 4°C and the pressure of water vapor at 266 to 665 Pa to maintain materials in a hydrated state. The accelerating voltage was 20 kV. The EDS data were obtained with a Tracor Northern System II analyzer equipped with a diamond window light element detector.

As shown in Figure 2, ESEM micrographs of a surface can show bacteria within the corrosion layers, while an SEM image indicates the presence of a monolayer of cells attached to the corrosion layer (Little et al., 1991). The TEM has been used to demonstrate that bacteria were intimately associated with the corrosion products and, on copper-containing surfaces, the bacteria were found between alternate layers of corrosion products and attached to base metal. This basically coincides with the ESEM result that the SRB are distributed through the sulfur-rich corrosion layers.

Gerristead and Link (1992) reported in situ corrosion studies of corrosion within an ESEM. Concentrated HCl was deposited on and evaporated from the specimen surfaces in situ at set intervals. Any corrosion product, when present, was washed away in situ for observation of underlying corrosion. This experimental procedure allowed the observation of the corrosion process in a nearly continuous fashion when the sample surface was not obscured by liquid.

The applicability and advantages of ESEM/EDS in studies of MIC have also been discussed in other literature (Jones-Meehan et al., 1992; Wagner, 1992).

3.1.2. Biochemical Methods

3.1.2.1. Detection of Bacteria

Bacterial detection methods are designed to detect molecules that are a part of the microbial cells themselves (for example, cell wall materials and long-chain fatty acids) (Pope and Zintel, 1989). The techniques by which molecules common to most bacteria (for example, cell wall materials called murein) are detected can give an estimate of the total amount of all bacteria obtained, and those techniques in which molecules are specific to a particular group of microbes (for example, specific membrane fatty acids) can detect specific microbes (Pope and Zintel, 1989).

Some specific bacteria can be detected through fatty acid fingerprinting, because some bacteria have fatty acids in their cells that seem unlike those in other cells. Fourier-transformation infrared spectroscopy has also the potential for identifying "fingerprints" for specific bacteria on a surface. However, these techniques have some serious drawbacks, including very expensive equipment, a need for well-trained operators, and difficulty with preparation of field samples for such analysis without disrupting the sample to be analyzed (Pope and Zintel, 1989).

DNA analysis is another useful method to detect SRB (Voordouw, 1994;
Voordouw et al., 1994).

3.1.2.2. Metabolic products analysis

This group of methods is designed to detect metabolic products (for
example, hydrogen sulfide, organic acids, short-chain fatty acids, and hydrogen)
directly. For example, gas chromatography, ion chromatography, high-pressure
liquid chromatography, fast protein liquid chromatography, nuclear magnetic
resonance, and electron spin resonance can be used to analyze metabolic products
including gases, organic acids, and specific marker proteins characteristic of certain
bacteria or to indicate that specific metabolic pathways are being used in the
community (Pope and Zintel, 1989). Gas chromatography is usually used to
analyze metabolic gases or organic acids, and ion chromatography is usually used
for organic acid analysis. Some of the gases (hydrogen, carbon dioxide, hydrogen
sulfide) and the organic acids can be identified with radiotracer materials. Specific
marker proteins (hydrogenases, cytochromes) can be identified by extracting the
proteins from the sample and separating them using high-pressure liquid
chromatography or fast protein liquid chromatography, then detecting them using
gel electrophoresis, or nuclear magnetic resonance.

For example, if it is determined that the community at an MIC site is adapted
to using hydrogen, then it could support the idea that MIC is caused by "cathodic
depolarization" or that the hydrogen being produced by cathodic protection is
actually promoting the growth of SRB and /or other microbes that use hydrogen as
an energy source for growth. If the community is, however, showing a net
production of organic acids and hydrogen, then it would suggest that organic acid-
producing bacteria are the dominant organisms present, that the SRB and

methanogens and other hydrogen consumers may be low in number, and that the acids may be responsible for much of the corrosion at the site. This could be confirmed by analyzing the corrosion product and surrounding water and sediment for hydrogen, organic acids, carbon dioxide, hydrogen sulfide, methane, and possibly, the presence of periplasmic hydrogenases, cytochromes, ubiquinones, etc., which are markers for certain bacteria and metabolic pathways. If they are present in large amounts, then certain bacteria must be present, and certain pathways are being used and, therefore, producing certain end products. These end products include H_2S, H_2, CO_2, or organic acids.

3.1.3. Electrochemical Methods

3.1.3.1. Corrosion Potential

The corrosion potential (or open-circuit potential) E_{corr} of a corroding metal can be measured by determining the voltage difference between that metal immersed in a corrosive medium and an appropriate reference electrode. The magnitude and sign of the corrosion potential are functions of the metal itself, as well as the composition, temperature, and hydrodynamics of the electrolyte. The corrosion potential can be measured by a potentiometric circuit, a high-impedance voltmeter, or an electrometer. These instruments are capable of accurately measuring small voltages without drawing enough current to polarize either the reference electrode or the test electrode. Among the electrochemical techniques, measurement of corrosion potential is probably the easiest. It has been therefore used in MIC studies for many years. However, it provides the least amount of mechanistic information (Mansfeld and Little, 1991). The main problem with the use of E_{corr} measurements is the overinterpretation of such data, such as predicting corrosion rates. Based on the information obtained with E_{corr} alone it is not possible to determine whether

corrosion rates have increased or decreased. Mansfeld and Little (1991) recommended determining not only E_{corr}, but also the polarization resistance R_p at the same time. The changes of both parameters can then be interpreted in terms of changes in the rates of the anodic and/or the cathodic partial reactions which determine the corrosion rate.

Some early results of E_{corr} for steel in the presence of SRB showed changes of E_{corr} in the negative direction. These changes were explained by a reduction of the rate of cathodic reaction (Hadley, 1943) and by an increase of the rate of the anodic reactions (Wanklin and Spruit, 1952). Although these are the two simplest possibilities which can be expected to lead to the observed result, it is necessary to have additional data in order to draw valid conclusions. Only when the exact mechanism of MIC has been established for a given system will it be possible to use E_{corr} data for monitoring purposes such as the detection of an increase of uniform corrosion rates or the initiation of localized corrosion due to the presence of bacteria.

For stainless steels in natural seawater, most published data show a rapid ennoblement of E_{corr} during the first couple of days of exposure. Figure 3 is a representative example of potential-time curves (Johnson and Bardal, 1985).

Different authors have offered different interpretations for the cause of the observed ennoblement of E_{corr}, but many have speculated that this effect was caused by a change of the cathodic properties of the stainless steels as a result of microbiological activity on the surface (Mollica et al., 1984; Johnson and Bardal, 1985; Dexter and Gao, 1988). Mansfeld and Little (1991) suggested that the ennoblements of E_{corr} for stainless steels in seawater did not demonstrate directly an increased susceptibility to corrosion. In fact, the sustained noble potentials show that the stainless steel surface retained its normal corrosion resistance in seawater

for the time of the experiment used by different authors. If localized corrosion had occurred, E_{corr} would have dropped to more active potentials (very negative) typical of pitted stainless steels. As far as the mechanism responsible for the ennoblement of E_{corr} is concerned, it is not possible from the experimental data for E_{corr} or the polarization curves to decide whether the increase of E_{corr} is due to thermodynamic effects, kinetic effects or both.

3.1.3.2. Direct Current Polarization

Polarization is a change in the potential of an electrode during electrolysis, such that the potential of an anode becomes more noble (anodic polarization), and that of a cathode more active (more negative, cathodic polarization), than their respective reversible potentials. Slow electrochemical reaction or low diffusion rate of ions can result in accumulation of either electrons at the cathode thus lowering the electrode potential (cathodic polarization) or deficiency of electrons at the anode thus increasing the electrode potential (anodic polarization). Additionally, sometimes deposits or a protective film such as a passive film on stainless steels can be formed on metallic anodes thus causing a very slow diffusion of metallic ions into the bulk solution which results in a very positive anodic potential. The reverse process is called depolarization.

The general procedure for direct current polarization is to use a potentiostat in conjunction with a reference electrode to measure the corrosion potential, and then to polarize the specimen (working electrode) from the corrosion potential, in either the active (cathodic) direction, or the noble (anodic) direction, or both. A potentiostat is a widely used electrical device in corrosion study which can automatically adjust the applied polarizing current to control the potential between the working electrode and the reference electrode at any prescribed value.

Depending upon the method to be used, these polarizations may be large (several hundred mV) or small (e.g., 10 to 20 mV). Polarizations may also be done either quasi-statically in discrete steps at some appropriate time interval (25 mV every 5 minutes is common) or dynamically at a constant scan rate for MIC study (Dexter et al., 1991).

3.1.3.2.1. Tafel Polarization

In theory, the cathodic and the anodic curves should intersect at a point representing the corrosion potential and the corrosion current density. Both measured cathodic and anodic curves deviate from linearity in the vicinity of the corrosion potential; nevertheless, both often contain linear segments or Tafel regions. Extrapolating the linear segments of either the anodic or cathodic curve back to the corrosion potential yields the corrosion current density as is shown in Figure 4 (Jones, 1992b). The corrosion current density can be converted to corrosion rate. Strictly speaking, such extrapolations give a valid value for the corrosion current density only when the linear Tafel region extends for several decades of current. Extrapolations from the linear segment of the cathodic curve are generally preferred, since the latter is often easier to measure experimentally and is less affected by corrosion-product and biological films.

These methods have been used with considerable success. However, several limitations should be noted.

(1). Electrolytes in which more than one reduction reaction takes place or in which concentration polarization occurs, exhibit less distinct linear regions. This greatly decreases the validity of the extrapolated values. These disadvantages can sometimes be overcome by the linear polarization resistance technique as will be discussed later.

(2). For systems in which the corrosion potential drifts or fluctuates with time (e.g., the 300 series stainless steels in natural seawater), Tafel polarization measurements are nearly meaningless.

(3). The rather large polarizations required may change the electrochemical conditions at the metal surface in such a way as to be deleterious to microorganisms in the biofilm.

(4). These measurements alone give no information on either the distribution of corrosion on the metal surface (MIC is usually localized) or on the relative contribution to corrosion of the bic .m as compared to that of other parameters.

3.1.3.2.2. Cyclic Polarization

The potential scans for cyclic polarization can range from several hundred mV to several volts. The potentiodynamic techniques are most useful in characterizing, and sometimes predicting, the corrosion behavior for metal-electrolyte systems in which e metal passivates by the formation of a protective (or passive) film. The recording of a polarization curve as described below provides an ove: v of the types of reactions which occur for a given corrosion system such . transfer or diffusion controlled reactions, passivity, transpassivity and localized corrosion phenomena.

An idealized polarization diagram for a passivatable metal which can form a protective film (passive film) in a certain electrolyte system is shown in Figure 5. Starting with the corrosion potential E_{corr} (related corrosion rate i_0) (or sometimes start with a lower potential than E_{corr} in the cathodic region) and moving upward (by anodic polarization or increasing applied potential) on the diagram, one encounters first the active region, in which general corrosion takes place, with the

corrosion rate increasing rapidly with potential. Upon reaching the primary passivation potential E_{pp}, protective and stable oxide films can form in oxidizing environments. Under these conditions, the metal is said to passivate and the corrosion current density drops from a maximum of i_{crit} to the very low passive current density i_p, and one enters the passive region, in which the corrosion behavior is independent of potential. In electrolytes of more neutral pH, the corrosion potential is already within the passive range, and the active current peak is not observed. At more noble or positive potential, the transpassive region is encountered, in which the corrosion rate increases once again, accompanied by oxygen evolution. The starting potential of this region E_{pit} is called pitting potential due to the fact that new pits initiate from this point. Pitting corrosion is a type of localized attack in an otherwise resistant surface. To study pitting corrosion, reversed or cyclic scanning may be used in which the polarization direction is reversed (potential decreasing) from a potential within the transpassive region and a hysteresis is observed. The intersection at the passive current density gives protective potential E_{prot} below which established pits cannot continue to grow. However, between E_{prot} and E_{pit}, new pits cannot initiate, but old ones can still grow. Further reversed polarization beyond E_{prot} may give a new corrosion potential E_{corr}' and related corrosion current i_c.

The recording of potentiodynamic polarization curves seems to be very simple. However, the experimental conditions have to be tailored to the electrochemical characteristics of the system under study to obtain optimum results. The choice of the correct sweep rate and the elimination of the ohmic drop during the experiment are important considerations. The use of excessive sweep rates will change the shape of the polarization curves, but does not result in any meaningful mechanistic data. Polarization over wide potential ranges can drastically alter the

properties of the surface under investigation. Therefore separate samples should be used for the recording of anodic and cathodic polarization curves and each sample should only be used once (Mansfeld and Little, 1991). While some quantitative information can be obtained, interpretation of the results sometimes is difficult. The potentiodynamic polarization techniques have been widely used to determine the effects of microorganisms on the electrochemical properties of metal surfaces and the resulting corrosion behvior (Mansfeld and Little, 1991). While there is no general agreement concerning the details of the corrosion mechanisms, most authors suggest that the observed increase of corrosion rates observed from polarization curves for mild steels is due to the influence of the microorganisms on the rates of the anodic and/or cathodic reactions involved in the corrosion process (Tiller, 1986).

The polarization techniques have also been used in attempts to determine the mechanism by which microorganisms induce localized corrosion in the forms of pitting or crevice corrosion. In most cases the pitting potential E_{pit} has been determined in the presence and absence of bacteria. At this point it has to be stated that the pitting potential E_{pit} provides only the tendency for pitting, but does not give information concerning the rate at which pits propagate.

Figure 6 shows examples of potentiodynamic curves with a reversed scan for stainless steels in sterile medium and in a medium with SRB (Ringas and Robinson, 1987). In the sterile medium, the alloy was passive and displayed a large passive range. No hesterisis loop was found from the reverse scan which indicated that active pits were not formed. The shape of the anodic polarization curve was very different in the bacterial culture. E_{corr} was more active, an active-passive transition was observed and the passive c.d. was higher, suggesting that the passive film formed in the bacterial culture was less protective. The hesterisis loop

formed during the reverse scan showed that active pits had been formed which did not repassivate above the protection potential.

3.1.3.2.3. Potentiostatic Technique

It has to be remembered that the experimental conditions used to record a pitting scan can affect the value of pitting potential, E_{pit}, which has been defined in the previous section. If the scan rate is too high, E_{pit} will usually be higher than the value determined under steady-state conditions. Likewise the experimental value of E_{prot} becomes more negative if the current density at which the scan is reversed is increased. Because of these problems, E_{pit} is sometimes determined by a constant-potential technique in which a series of increasing anodic potentials is applied and the current is measured as a function of time. If the current decreases continuously at an applied potential E, it is concluded that E is more negative than E_{pit}. By increasing E stepwise, E_{pit} can be determined. This is a very useful technique but not commonly used for the study of MIC (Mansfeld and Little, 1991).

This potentiostatic technique can be also used to determine the induction time for pit nucleation. The time it takes to form the first pit on a passive metal exposed to a solution containing aggressive anions (e.g., chlorides or sulfides) is called the induction time for pit initiation. At a constant potential noble to E_{prot} and or a given metal, the induction time depends on the chloride ion concentration, the quality of the passive film and on the experimental conditions. Usually, it is determined by recording changes in the current density vs. time at a constant applied anodic potential. When pitting is initiated, there is a sudden increase in current, and the time elapsed between potential application and the current increase is a measure of induction time.

Ringas and Robinson (1987) used these techniques to determine whether sulfide-induced pitting could occur in an SRB environment. A potential of -200 mV (vs. SCE) was applied to the specimens for one hour immediately after immersion in the solution. The potential was then increased to +500 mV and the current monitored for a further two hours. The more noble potential fell within the passive range of the alloy. Scans were performed in sterile solution and in strain 8303. Typical results are presented in Figure 7. During the initial potential of -200 mV, the current recorded is cathodic indicating that no metal dissolution is occurring. When the potential was raised to +500 mV in the sterile solution, the current decayed to a very low value in a short period of time, clearly indicating a passivation tendency (a). In contrast, (b) shows the potentiostatic curve of AISI 304L SS in medium with strain 8303. During the initial active potential, an anodic current was recorded indicating that some metal dissolution was occurring. After the application of the more noble potential, the current decreased slightly initially, but then increased again. From this, the authors deduced that pits formed during the application of the active potential were not able to repassivate at the more noble potential, even though the higher potential fell within the passive range of the alloy.

3.1.3.2.4. Polarization Resistance

This method is based on the nature of the linear relationship between changes in the applied potential and the resultant current density, when the applied potentials are within about ±10 mV of the corrosion potential as is shown in Figure 8 (Dexter et al., 1991). The polarization resistance R_p is defined as the slope of this linear section. The technique is based on the assumption that the interface behaves as a simple resistor. The main advantage of the polarization resistance technique is the possibility of continuously monitoring the instantaneous corrosion rate of a

metal exposed to a corrosive environment (Mansfeld, 1973). Therefore this technique is very suitable for the detection of changes in corrosion rates due to the presence of bacteria, inhibitors, sunlight, biocides, etc.

The polarization resistance R_p is thus (Mansfeld,1976):

$$R_p = \frac{\Delta E}{\Delta i}$$

Where DE and Di are changes of applied potential and resulting current density respectively.

The i_{corr} is calculated from R_p by:

$$i_{corr} = \frac{B}{R_p}$$

Where

$$B = \frac{b_a b_c}{2.303(b_a+b_c)}$$

and b_a, b_c are Tafel slopes (slopes of Tafel regions as defined in Figure 4) for anodic and cathodic curves respectively.

The exact calculation of i_{corr} for a given time during an experiment requires therefore the simultaneous measurements of R_p and the Tafel slopes b_a and b_c for this time.

The polarization resistance technique is most useful for systems undergoing uniform corrosion. However, patchy biofilms and localized colonization give rise to localized biochemical reactions and to anodes and cathodes that are fixed in space

and stable in time (Dexter et al., 1991). The other problems with this technique are large fluctuations of the R_p data with time for systems undergoing pitting or crevice corrosion (Mansfeld and Little, 1991), the error caused by IR drop, the introduction of capacitance in parallel with the resistance under the bacterial conditions, etc.

3.1.3.3. Redox Potential

The reduction-oxidation or redox or solution potential refers to the relative potential of an electrochemical reaction under equilibrium conditions where there is no net flow of electrical current. It is also referred as oxidation-reduction potential (ORP) in water systems. According to ASTM standard D 1498-93, ORP is defined as the electromotive force between a noble metal electrode and a standard reference electrode when immersed in a solution:

$$E = E^0 + 2.3\frac{RT}{nF}\log\frac{A_{ox}}{A_{red}}$$

where:

E = oxidation-reduction p   ial (ORP).

E^0 = constant that depend   n the choice of reference electrodes.

F = Faraday constant,

R = gas constant,

T = absolute temperature, $^0C + 273.15$,

n = number of electrons involved in process reaction, and

A_{ox} and A_{red} = activities of the oxidants and reductants respectively in the process.

The ORP of an aqueous solution is almost always sensitive to pH variations. It will increase when the pH of the test solution decreases and it will decrease if the test solution pH is increased. However, the ORP resulting from

interactions among several chemical systems present in mixed solutions may not be assignable to any single chemical.

The redox potential of an environment such as moist soi is actually the equilibrium potential of the oxygen reaction as measured on a platinum electrode immersed in the soil (Dexter et al., 1991). The redox potential is therefore an indicator of the oxidation power of the electrolyte if suitable calibration is provided.

Redox potential measurements have been used frequently to assess the suitability of a given environment for the growth of SRB. Since these bacteria grow only in the absence of oxygen, they require an environment with an active, or oxygen deficient redox potential (generally less than -400 mV SHE (standard hydrogen electrode)) (Dexter et al., 1991). In the field of MIC study, the redox potential has been used to estimate the aggressiveness of soils due to SRB. For example, at a given temperature and pH, a low redox potential means low oxidizing power or low dissolved oxygen concentration thus more aggressiveness due to SRB. However, the combined use of several parameters such as electrical resistivity, redox potential, and water content of the soils is believed to be more reliable. Another useful application of the redox potential would be in a combination with measurements of E_{corr} and R_p for monitoring purposes (Mansfeld and Little, 1991).

3.1.3.4. Dual-Cell Technique

The dual-cell or split-cell technique developed by Little et al. (1986) for the study of MIC allows continuous monitoring of the changes in the corrosion rate of a metal due to the presence of a biofilm (Gerchakov et al., 1986). In this technique two identical electrochemical cells are biologically separated by a semipermeable membrane. The two working electrodes are connected to a zero resistance ammeter

or a potentiostat set to an applied potential of 0 mV. Bacteria are then added to one of the two cells and the resulting net current is recorded on a strip chart recorder to provide a continuous record of the time dependence of the corrosion process. The sign and the magnitude of the net current can be used to determine details of the corrosive action of the bacteria. It has to be recognized that the net current is a measure of the increase of the corrosion current of the anode due to the coupling to the cathode and does not allow calculation to the corrosion rate of either electrode in a simple manner (Mansfeld and Little, 1991).

Inherent in this method is the assumption that the two electrodes can be made identical and that there would be no current flow as long as both half-cells were maintained in the sterile condition. This may be a reasonable assumption in the case of steady-state uniform corrosion, or for stable passivity where neither electrode undergoes potential fluctuations in the absence of the microorganisms. It is probably not valid for systems such as the 300 series stainless steels in seawater. In this latter case, the potentials of the two electrodes are sufficiently variable that currents could flow in either direction whether or not microorganisms are present. In such a system, interpretation of the data from split-cell experiments is not straightforward. Another problem with this technique is that the method does not separate the anodes and cathodes of local action or microcells, but only measures the effect of coupling. Thus, it is not a simple matter to relate the data obtained from this method to MIC on real structures covered with a spotty biofilm or with discrete biodeposits (Dexter et al., 1991).

3.1.3.5. Electrochemical Impedance Spectroscopy (EIS)

Unlike the direct current technique, the EIS employing alternate current measures not only the resistive but also the capacitive and possibly the inductive

components of the overall interfacial impedance, therefore being particularly useful in the presence of nonconducting and semiconducting surface films such as organic paints and many metal oxide films. Many of the organic and microbiological films that adsorb on surfaces immersed in natural aqueous environments are nonconducting, and EIS techniques are potentially useful in their presence. EIS techniques are most helpful, and easiest to interpret, for metal-electrolyte systems involving continuous thin films and low solution conductivity. Some caution should, therefore, be exercised in data interpretation from MIC systems because the adsorbed organic and biological films tend to provide spotty, rather than continuous surface coverage, and these films can vary widely in thickness as mentioned in section 2.2. Nevertheless, EIS should provide useful information on biofilm-covered electrodes and may be helpful in assessing the degree of coverage similarly to its use in determining the porosity of coatings (Kendig et al., 1986).

EIS techniques are able to distinguish between electrochemical reactions based on their relaxation times. A given electrochemical reaction will only respond to an alternating current signal whose period is longer than the characteristic time for the rate-limiting step for that reaction to occur across the interface. The evaluation of the impedance spectrum of an electrode over a wide range of frequencies can then be used to distinguish among the various processes taking place at the interface between the metal and the electrolyte or between the metal and a film or coating. One of the most successful uses of EIS has been for assessing the performance of various types of organic coating materials. Perhaps the most serious impediment to the widespread use of EIS for corrosion studies is the complexity and cost of the instrumentation needed and the sophisticated electrochemical expertise required for detailed data analysis (Dexter et al., 1991)

However, there are some limitations with EIS when MIC is involved. For example, the interfaces involving partial coverage are difficult to model: the dynamic microbial entities can cause fluctuations in electrochemistry at the metal-film interface, causing localized attack under the film that is not easily measured. (Lee. 1986).

The theory and the practice of EIS techniques have been reviewed elsewhere (Cooper, 1986) and can also be found in the proceedings of the First International Symposium on EIS which was held in France, 1989.

3.1.3.6. Electrochemical Noise Analysis (ENA)

ENA follows fluctuation of potential or current as a function of time or experimental conditions. In some cases the potential of a test electrode is measured versus a stable reference electrode whereas in others the noise data are recorded for two electrodes of the same material which are exposed under identical conditions. One of the advantages of this technique is that no external signal needs to be applied for the collection of the noise data (Mansfeld and Little, 1991). Information concerning the nature of corrosion processes and magnitude of corrosion rate can be obtained through analysis of the structure of the electrochemical noise (Little and Wagner, 1994). Theoretically, the higher the frequency and the amplitude of the potential fluctuations observed during corrosion, the greater the number of events participating in the corrosion process and thus, the higher the corrosion rate (Dexter et al., 1991). However, most analyses of electrochemical noise measurements have been qualitative and used to determine the occurrence of localized corrosion. Because of the importance of pitting attack in MIC, electrochemical noise techniques may play an important role in the study of microbial effects on corrosion in the future. The results reported so far for the application of

electrochemical noise measurements suggest that this technique at its present state of development is more suited for monitoring purposes than for mechanistic studies.

In addition, it should be noted that the magnitude of the noise fluctuations depends on the total impedance of the system. A corroding metal undergoing uniform corrosion with fairly high corrosion rates might be less noisy than a passive metal which shows occasional bursts of noise due to localized breakdown of the film followed by rapid repassivation.

3.1.3.7. Scanning Vibrating Electrodes Technique (SVET)

SVET is a method used to determine the magnitude and sign of current densities over freely corroding metals in solution (Isaacs and Ishikawa, 1985). As described in a study of pitting attack by bacteria on carbon steel (Franklin et al., 1991), the vibrating electrode, used to scan the working electrode, consisted of an insulated platinum wire. The platinum wire was attached to a piezoelectric reed which was activated by applying a 200 Hz, 10 V r.m.s. signal to the reed. The peak to peak vibration was 0.04 mm. The vibrating electrode was positioned at about 0.09 mm from the working electrode surface. Vibration of the electrode tip within a potential field converts the d.c. field to an a.c. signal. The signal resulting from the vibration of the electrode in nonuniform potential fields was measured with a PAR model 116 lock-in amplifier. The signal from the lock-in amplifier was passed to a data acquisition unit and to a computer, where the data were analyzed and plotted. The surface of the working electrode was scanned by moving the cell in 100- or 200-μm increments with computer controlled stepper motors.

The SVET provides a non-destructive means to define the magnitude and sign of current densities in solution over freely corroding metals. Current density maps have been utilized to define localized anodic and cathodic activities of regions

on stainless steel. The SVET applied to the MIC studies as a non-destructive technique to determine local anodic and cathodic sites on-line shows a good future.

Franklin et al. (1991) mapped the changes in current densities over carbon steel with time using SVET in the presence and absence of bacteria. In a sterile liquid medium, the maps showed highly localized anodic current densities, which subsequently became inactive (Figure 9). Analysis of current maps and the open circuit potential showed that the potential transients were due to pit initiation and repassivation processes. When in the same bulk fluid, an aerobic bacterium, isolated from a corrosion tubercle, was grown, similar trends of pit initiation and repassivation were observed for several hours. However, after extended exposure to bacteria, local anodic activity did not repassivate. The corrosion then propagated and spread, until a large area of the sample was anodic (Figure 10).

3.2 Methods for SCC Studies

Many techniques have been used for SCC studies. The most important requirements for SCC studies are the selection of an appropriate technique and interpretation of the test results. Standard test methods have been available from the National Association of Corrosion Engineers (NACE), the American Society for Testing and Materials (ASTM) and even the International Organization for Standardization (ISO). There are many methods of classifying the SCC techniques, generally into in three basic categories: static loading of smooth specimens, static loading of precracked specimens, and dynamic loading (slow-strain-rate-test). Sprowls (1992) gives a good review of the techniques used in SCC studies.

3.2.1. Static Loading of Smooth Specimens

This group of techniques is designed to predict the SCC performance of an alloy in a particular service application with a stress system similar to that anticipated in service. There are two sub-groups, elastic strain specimens and plastic specimens, based on the type of deformation of specimens.

3.2.1.1. Elastic Strain Specimens

Here the strain in the test materials is restricted to the elastic deformation range. The main advantage of this method is the control over the magnitude of tensile stress. If the stress goes beyond the elastic range, it will be impossible to tell precisely how much stress actually has been applied. There are a number of specimen types.

Bent-beam specimens offer the advantage of a relatively large area of material under a uniform stress. They are mainly used for sheet, plate, or flat extruded sections, which provide flat specimens of rectangular cross section. A tensile stress is applied to the outer surface of a specimen through bending. There are several configurations for this kind of specimens.

C-ring specimens offer the advantage of a large quantity of specimens from all types of alloys in a wide variety of product forms. They are especially well suited for testing tubing and for making short-transverse tests on various product forms. The tensile stress is applied to the outer surface of a specimen through squeezing the C-ring shaped specimen. The stress causing SCC for C-ring specimens is circumferential. It should be noted however that this stress is non-uniform. There is a gradient through the thickness, varying from a maximum tension on the outside surface to a maximum compression on the inside surface. In addition, the stress varies around the circumference of the C-ring from zero at each

bolt hole to a maximum at the middle of the arc opposite the stressing bolt; the nominal stress is present only along a line across the ring at the middle of the arc. Finally, the circumferential stress may vary across the width of the ring depending on the width-to-thickness and diameter-to-thickness ratios of the C-ring. This technique will be discussed in more details later in the experimental section since it is employed in this study.

O-ring specimens are used to develop a uniform and tensile hoop stress around the specimens. An O-ring type specimen is stressed by pressing it onto an oversized plug that is machined to a predetermined diameter to obtain the desired stress around the outside surface of the ring.

Tension specimens are similar to those used in determining tensile properties. They offer much versatility when dealing with the SCC test because of the flexibility permitted in the type and size of the test specimens, stressing procedures, and the range of stress level. However, test results can be significantly influenced by the cross section of the test specimen.

Tuning fork specimens are used occasionally when dealing with some special applications such as short-transverse tests on sections that are too thin for tensile specimens or C-rings. They are stressed by closing the specimen tines and restraining them in the closed position with a bolt placed at the tine ends.

3.2.1.2. Plastic Strain Specimens

These specimens usually contain large amounts of elastic and plastic strain and provide one of the most severe tests available for smooth SCC test specimens. This type of test is primarily used as a screening test to detect large differences between the SCC resistance of one alloy in several environments, one alloy in several metallurgical conditions in a given environment, and different alloys in the

same environment. However, they are sometimes claimed to be too severe and therefore unsuitable for many applications. One typical configuration is the U-bend specimen which is a rectangu'·· strip bent approximately 180° around a predetermined radius and maintained in this plastically and elastically deformed condition during the test.

3.2.2 Static Loading of Precracked (Fracture Mechanics) Specimens

As the name implies, these specimens are precracked or machined with a groove which simulates flaws at the specimen surfaces. To sharpen the cracking tips, fatigue cracking is usually used. This technique is based on the engineering concept that crack-like flaws introduced during manufacture or subsequent service are generally present in thick structural components, and the flaws can contribute to the susceptibiliry of SCC. This technique is good for determining the critical flaw size for SCC to occur and the SCC propagation rate. However, it is not suitable for thin products because this technique needs to maintain elastically constrained conditions at the crack tip.

3.2.3 Dynamic Loading Slow Strain Rate Test

This is a tension test with a dynamic slow strain exceeding the elastic limit to assist in the SCC initiation. This technique is based on the concept of alternative plastic microstrain and film rupture during the progress of SCC. The major advantage of this method is its rapidity. Samples can be cracked in a relatively short time.

4. Experimental

4.1 Materials

One type of carbon steel and one stainless steel have been used to conduct the SCC tests. Both kinds of steels are sensitive to SCC given favorable conditions (Ciaraldi, 1992; Sedriks, 1992).

4.1.1 ASTM A513L REV Grade 1026 Carbon Steel

ASTM A513L REV Grade 1026 was supplied by Team Tube Ltd. in Edmonton. The tube size is 1.000 inch (25.40 mm) in outside diameter and 0.125 inch (3.18 mm) in wall thickness. It was received in the stress relief annealed condition. The chemical composition and mechanical properties of this steel are given in Tables 1 and 2 respectively.

This grade (AISI 1026) is a carbon steel. SCC of carbon and low-alloy steel is a significant problem in a variety of industries, such as those dealing with pipeline transmission, oil and gas production, and chemical processing (Ciaraldi, 1992). Both intergranular and transgranular SCC are possible depending on environments and microstructure. For those steels with higher strength, SCC in environments containing hydrogen sulfide is also common in the production, transmission and refining of oil and gas.

For carbon and low-alloy steels with yield strength lower than 620 MPa (90 ksi), ferritic-pearlitic structures are typical, and a tempered martensite structure is common for those with yield strength greater than 620 MPa (90 ksi).

For microstructure examination, a piece of the given steel was mounted in Bakelite thermoset material and ground down with successively finer SiC abrasive

paper to 600 grit. The specimen was then polished with diamond paste of 1 µm and an aqueous suspension of 0.05 µm gamma alumina. The microstructure of the given ASTM A513L REV Grade 1026 carbon steel with etchant of 1% nital (1 mL HNO_3 in 100 mL 95% ethanol) is shown in Figure 11. Obviously, this is a typical steel microstructure consisting of ferrite and pearlite which is a lamellar mixture of ferrite and carbide.

4.1.2 ASTM A312-89A Type 304L SMLS Stainless Steel

This is a seamless stainless steel tubing with an outer diameter of 1.000 inch (25.40 mm) and wall thickness 0.113 inch (2.87 mm). It was suppled by Atlas Alloys in Edmonton. The tubing has been bright annealed and quenched. The chemical composition and mechanical properties of this steel are given in Tables 3 and 4 respectively.

AISI type 304L is a very low-carbon, austenitic chromium-nickel steel. This grade has general corrosion resistance similar to that of type 304 but superior resistance to intergranular corrosion after welding or stress relieving. This is because of the lower carbon content of type 304L that thus reduces the sensitization which is the precipitation of carbide at austenite grain boundaries and is widely believed to be mainly responsible for SCC susceptibility. Both intergranular and transgranular SCC are possible depending mainly on whether or not the stainless steel is sensitized.

As with the carbon steel, a piece of the given stainless steel was mounted in Bakelite thermoset material for microstructure examination. The specimen was firstly ground down with successively finer SiC abrasive paper to 600 grit and then polished with diamond paste of 1 µm and an aqueous suspension of 0.05 µm

gamma alumina. The microstructure of this given stainless steel is shown in Figure 12. It is a typical austenitic structure with some manganese sulfide inclusions. The etchant used for this stainless steel was a mixture of 5 mL HCl, 1 g picric acid, and 100 mL of 95% ethanol.

4.2 Bacteria

4.2.1 *D. desulfuricans* Subsp. *desulfuricans* Strain NCIB 8307

The species *D. desulfuricans* has been widely studied regarding microbiologically influenced corrosion (MIC) not only because they are often found in MIC sites, but also because they can be easily cultured (NACE, 1984; Seed, 1990). According to Widdel and Pfennig (1984) and Singleton, Jr. (1992), this species is usually found in water, especially polluted waters showing blacking and sulfide formation. They are also found in soils, especially anaerobic or water-logged soils rich in organic materials, and in marine or brackish waters. Vibrioid is the typical shape. They are usually curved or occasionally straight rods with cell size of 0.5 - 1.0 by 3.0 - 5.0 μm. Figure 13 shows the typical morphology (Widdel and Pfennig, 1984).

The subspecies (ATCC number 29577) was received as a freeze-dried culture from the American Type Culture Collection (ATCC). Rehydration of this culture was done by aseptically Pasteur pipetting to the freeze-dried material 0.3 to 0.4 mL of a medium for detecting and culturing SRB as discussed below, mixing well and transferring the total mixture to a test tube of the same medium (5 - 6 mL). It made the medium turbulent in about one week at 30°C, which is an indication of active SRB.

4.2.2 Mixed Culture

In natural environments, many kinds of microorganisms may co-exist. It is more reasonable to apply the test results from a mixture rather than a pure culture to the practical situation. However, it is more difficult to study the behavior of mixed cultures due to the variety of microorganisms and possible interactions among them. In this study, a favorable condition for SRB genus *Desulfovibrio* was created by using the specially designed mass culturing solution as discussed below. Some mud from the North Saskatchewan River at Edmonton was put into a culturing vessel. SRB are supposed to be the major bacteria cultured by this method although many other kinds of microorganisms may exist in the mud and thus also be cultured.

4.3 Solutions

A specially designed medium must be used to detect, culture or massively culture SRB in a relatively short time. There have been many kinds of media developed for culturing SRB. For different purposes, different media may be used for best results. However, each laboratory has its 'pet' media and it is not always clear which details are crucial. The following media which have been proved to be successful (Postgate, 1984) were used during the study.

4.3.1 Medium for Detecting and Culturing SRB

Enumeration of SRB either in bulk liquids or in surface deposits by using a liquid or solid medium with sodium lactate as the carbon source has been extensively used as a method for MIC evaluation. When SRB are present in the sample, sulfate is reduced to sulfide which reacts with iron in solution to produce

black ferrous sulfide. It is generally accepted that blackening of the medium as a whole, or the zone around a colony, signals the presence of SRB.

Table 5 shows the composition of the general purpose medium used for detecting and culturing *Desulfovibrio* and *Desulfotomaculum* (Postgate, 1984). Most of the ingredients can be prepared and held as a stock, but the thioglycollate and ascorbate should be added and the pH adjusted just before autoclaving by using a 0.1 M NaOH solution. The autoclaving was done at 121°C for 30 minutes. The medium was used as soon as it was cooled down because the reductants could deteriorate in air at neutral pH values. The precipitate in this medium aids growth of tactophilic strains. It is recommended for long-term storage of strains.

4.3.2 Medium for Mass Culturing

Large amount of solutions were needed for SCC tests. For this purpose, a mass culturing solution (Postgate, 1984) was used. Table 6 gives the composition of the c.car medium which is suitable for mass culturing of *Desulfovibrio* and most *Desulfotomaculum*, for chemostat culture and for research in which a turbid medium is not desirable. The citrate serves to hold iron and other trace elements in solution. To indicate possible oxygen leaking into test vessels, 10 mL resazurin solution (0.1 g/L) was added to each litre of this solution. The pH was adjusted before autoclaving by using 0.1 M NaOH solution. The solutions were then autoclaved at 121°C for 30 minutes.

4.4 Test Methods

4.4.1 Standard C-ring Stress-Corrosion Specimens

A large number of specimens for SCC testing was needed for comparison purposes under different environmental conditions. As discussed before. C-ring specimens are versatile, economical for quantitatively determining the susceptibility to SCC of all types of alloys in a wide variety of product forms. They are especially well suited for testing tubing and for making short-transverse tests on various product forms. ASTM standard G38 - 73 (re-approved 1990) gives the standard practice for making and using C-ring stress-corrosion test specimens. Figure 14 shows the typical configuration of a C-ring type SCC specimen according to this standard. For this experimer'. the actual outside diameter (OD) and inside diameter (ID) will be given later in this section for both stainless steel and carbon steel C-ring specimens. All C-rings were machined directly from tubing materials as mentioned in section 4.1.

The desired tensile stress was produced on the exterior of the ring by tightening a bolt centered on the diameter of the ring. According to the ASTM standard G38-73 (re-approved 1990), the amount of compression required to give the desired stress can be calculated using the following equations:

$$OD_f = OD - \Delta , \text{ and}$$
$$\Delta = \frac{f\pi D^2}{4EtZ}$$

where:

OD = outside diameter of C-ring before stressing, mm.

OD_f = outside diameter of stressed C-ring, mm.

f = desired stress. MPa,

D = change of OD giving desired stress. mm,

D = mean diameter (OD -t), mm,

t = wall thickness. mm,

E = modulus of elasticity. MPa, and

Z = a correction factor for curved beams as shown in Figure 15.

The desired stress is usually around 80% of the yield stress to make the cracking fast enough under laboratory conditions and at the same time to avoid possible plastic deformation. A stress of 85% yield stress was chosen as the desired stress for both steels. This is equivalent to 76500 psi or 527 MPa for the stainless steel and 69700 psi or 481 MPa for the carbon steel specimens. The elastic modulus is 193 GPa or 2.8×10^7 psi for the type 304 stainless steel and 200 GPa or 2.9×10^7 psi for the carbon steel (Shackelford, 1992). Actual dimensions for the stainless steel C-ring specimens are shown in Table 7. For better accuracy, each dimension was measured four times around the middle of the specimen and an average was used. Similarly. Table 8 gives the measurements for the carbon steel C-ring specimens. The calculated results for stressing the stainless steel C-ring specimens by using a FORTRAN program CRING1 (see Appendix A) are shown in Table 9. Similar results for the carbon steel using the modified program based on CRING1 are shown in Table 10. In the FORTRAN programs, the relationship between correction factor Z and the ratio of mean diameter D over thickness t was tabulated.

When the nut had been tightened to apply the desired stress for a C-ring specimen, a similar additional nut was used to slightly tighten a copper wire which was attached to the end of the bolt in between the two nuts. The specimen thus

could be supported using this wire and also could be electrically connected to outside the test vessel. To avoid galvanic effects and crevice corrosion between the C-ring and the stressing bolt, the C-ring, bolt and wire were all coated with an insulating silicone coating except the critically stressed area for the C-ring.

Before immersion in test solution, the specimens were sterilized by immersion for 20 minutes in 70% ethanol prepared with distilled water which was boiled and then cooled to deaerate. The sterilized specimens were then immersed in 95% ethanol for about 10 minutes for degreasing. After drying, three similar specimens (parallel specimens for better accuracy) were immersed in a 1 litre glass flask with about 700 mL medium for mass culturing SRB as discussed in section 4.3.2 and were equally spaced about 3 cm from each other. In the middle of these three specimens was a Pt electrode which was a 0.1 mm thick Pt plate made from Pt wire; this was used as a reference electrode for monitoring the corrosion potential of the C-ring specimens. Deaeration was done by bubbling the solution for 15 minutes with 90% N_2 and 10% CO_2 gas mixture right after specimen immersion. Test flasks were made air tight with a rubber stopper and coated using epoxy adhesive where there was possible air (and thus oxygen) leaking. All tests were done at ambient temperature (about 22°C) except where otherwise clearly specified.

Four microbiological conditions were tested for each steel (Table 11): (1). Sterilized after adding 20 grams mud. This solution was supposed to contain no microorganisms and is only used for comparison with (2). (2). Solution was first sterilized and then 20 grams mud added to create a mixed culture condition. (3). Sterilized after adding 50 mL suspension of pure SRB culture. This was used to compare with (4). (4). Solution was first sterilized and then 50 mL pure SRB culture added. All sterilization was done at 121°C for 30 minutes by autoclaving.

The experimental setup for C-ring immersion tests is shown in Figure 16 and schematic configuration of this rig is shown in Figure 17. Due to the possibility of H_2S production, a three-stage processing system including two-stage $FeSO_4$ solution processing and one stage NaOH neutralization was used. A small glass bottle was put into the NaOH solution to collect the H_2S and other possible gases.

After the immersion and cyclic polarization test, the C-ring specimens were washed first with distilled water for about 5 minutes, then immersed in 70% ethanol for 20 minutes for sterilization, and finally immersed in 95% ethanol for 10 minutes for degreasing. All specimens were dried immediately with the compressed gas mixture of 10% CO_2 and 90% N_2 after washing, and kept in a desiccator.

4.4.2 Corrosion Potential

During the immersion tests, corrosion potentials for all the stainless and carbon steel specimens were monitored with a Model 273 Potentiostat/Galvanostat made by EG&G Princeton Applied Research. Reference electrodes were platinum plates placed in the solution as mentioned before. Final results were corrected to SHE potentials.

4.4.3 Cyclic Polarization

Cyclic polarization curves were obtained after the immersion tests and before removing samples from the medium by using the same Model 273 Potentiostat/Galvanostat as mentioned above in the section on corrosion potential. The data was processed with the Model 342 Softcorr Corrosion Measurement Software. A graphite auxiliary electrode was inserted into the flask while the flask was kept oxygen free by filling the flask with the gas mixture of 10% CO_2 and 90% N_2. The reference electrode was a saturated calomel electrode (SCE) but final

results were reported with reference to SHE through correction. The schematic cyclic polarization wiring diagram is given in Figure 18.

The initial potential at which the scans began was -100 mV below the corrosion potential E_{corr} to ensure that the cyclic scan passed through E_{corr} on the anodic scan and to give a complete and usable forward scan. The vertex potential at which the scan reversed direction was 100 mV SCE or 341 mV SHE. The final potential at which the scan ends was 0 mV fc sta:n'ess steel specimens and -100 mV for carbon steel specimens with respect .· &· · orrosion potential E_{corr}. The scan rate at which the appl:·rl potential was changed during the scans was 5 mV/s.

The threshold current ... which the scan reversed direction was 100 mA. It should be noted here that the threshold cui ·:.nt is not an enabling factor. In effect, the vertex potential acts as an enabling p ·ιι.meter, since the software looks for the threshold current only after it reaches the vertex potential. If the scan reaches the threshold current value before the threshold potential, it will not reverse at the current value; and if the scan reaches the potential first, it will continue to scan upward until it reaches the threshold current.

4.4.4 SEM with EDS

There was no evident deposit nor SEM-detectable corrosion on the stainless steel C-ring specimens. Therefore this section applies to only the carbon steel C-ring specimens.

Deposits were found on the carbon steel C-ring specimens under all four conditions tested. They were chemically analyzed by EDS on the Hitachi S-2700 SEM.

Steel surface morphology was analyzed with the SEM after removing corrosion products by immersion for 10 minutes in 1 L solution made of 500 mL

hydrochloric acid (HCl, specific gravity 1.19) and 3.5 g hexamethylene tetramine in distilled water according to ASTM standard G1-90.

5. Results and Discussions

5.1 Electrochemical Studies

5.1.1 Corrosion Potential

5.1.1.1 Stainless Steel Specimens
Figures 19 to 22 show the relationship between corrosion potential and exposure time for stainless steel C-ring specimens under various conditions. In the figures, SS stands for stainless steel and the numbers after them are specimen numbers.

Obviously, three specimens in each run performed similarly for all the tested conditions. However, specimens in the medium containing microorganisms (either pure SRB or those in the river mud) performed differently from those in the sterile medium. Those in the sterile medium did not have much change in corrosion potential over long time (20 to 90 days) although there was some initial oscillation during the first 10 to 15 days (Figures 19 and 21). As shown in Figures 20 and 22, specimens in the medium containing microorganisms performed differently. Corrosion potentials in these figures firstly decayed or dropped (decreased in the negative direction) rapidly within 5 days, then increased steadily with time. Further comparison with those in the sterile medium showed the difference more clearly in Figures 23 and 24 respectively. In these two figures, SS also stands for stainless steel, MUD and SMUD stand for medium containing mud and medium containing mud sterilized by heat respectively; SDD and DD stand for sterile medium containing heat-killed *D. desulfuricans* and medium containing a viable pure culture of SRB respectively. In Figure 23, the curves SS-SMUD and SS-MUD represent the average corrosion potential for the three specimens in each run from Figures 19 and 20 respectively. In Figure 24, the curves SS-SDD and SS-DD

represent the average corrosion potential for the three specimens in each run from Figures 21 and 22 respectively. One interesting thing found from this comparison is that corrosion potentials for specimens in the medium with microorganisms, although dropping significantly initially, steadily increased with time and finally approached a potential very similar to but below those in the sterile medium.

As for mechanisms for these changes in corrosion potentials, it is impossible to tell exactly what happened during the test based solely on corrosion potential. However, some conclusions still can be drawn.

For those specimens in the sterile medium, the initial oscillation in corrosion potential usually represent the construction period of a dynamic equilibrium between the steel electrode and the surrounding aqueous system. Once the construction of this dynamic equilibrium is complete, the corrosion potential then stays relatively constant with time. The rather positive and stable corrosion potential over a long period of time after the initial oscillation may indicate a high resistance to corrosion in the tested environments.

These phenomena may be related to polarization or depolarization of electrodes to some extent. For those specimens in the medium containing microorganisms, the initial decay of corrosion potential may be due to either cathodic polarization or anodic depolarization caused by microbiological activities. Figure 25 is a schematic polarization graph to explain these two possibilities. The first part (a) shows how a reduction of cathodic reaction rate (dotted cathodic line) due to reduction in electrochemical rate lowers a corrosion potential. This reduction of cathodic rate (cathodic polarization) results in a new equilibrium point at a new corrosion potential E_{corr}' and corrosion current density i_{corr}' compared with the original E_{corr} and i_{corr}. Obviously, E_{corr}' is lower than E_{corr} and i_{corr}' smaller than i_{corr}. The second part (b) indicates an increase of anodic reaction rate (dotted anodic

line) which lowers the corrosion potential. The increase of anodic rate (anodic polarization) also results in a new equilibrium point at a new corrosion potential E_{corr}' and corrosion current density i_{corr}' compared with the original E_{corr} and i_{corr} with E_{corr}' lower than E_{corr} but i_{corr}' larger than i_{corr}. One possible reason for this anodic polarization is due to production of sulfide which acts as an anodic stimulator. However, without further information, it is impossible to indicate which is correct, or how a factor would actually dominate. For a corrosion potential increase after an initial decay, it is usually accepted that this is caused by microbiological activities on the specimen surface (Johnsen and Bardal, 1985). Many people believe that a biofilm usually is formed on steel in the presence of the microorganisms (Johnsen and Bardal, 1985). This biofilm may change the cathodic properties of steel by forming a protective film as a result of microbiological activities on the surface. The final relatively stable corrosion potential may indicate a semi-protective and relatively stable biofilm. Without further information, it is impossible to predict which condition gives more susceptibility to corrosion based on corrosion potential alone.

5.1.1.2 Carbon Steel Specimens

Figures 26 to 29 show the relationship between corrosion potential and exposure time for carbon steel C-ring specimens under various conditions. In the figures, CS stands for carbon steel and the numbers after them are specimen numbers.

Similar to stainless steel specimens, three carbon steel C-ring specimens in each run performed very similarly. However, carbon steel specimens performed differently from stainless steel specimens. From Figures 26 to 29 we can also see that corrosion potentials from most specimens in all conditions increase rapidly

during the first few days (usually within 5 days), and then approach a relatively stable potential with time.

However, further study of the results show different corrosion potential change patterns for those in the medium containing microorganisms compared with those in the sterile medium. Figures 30 and 31 give the comparison of the behavior of carbon steel specimen in the sterile medium and the medium containing microorganisms (either microorganisms in the river mud or pure SRB). In these two figures, CS stands for carbon steel. MUD and SMUD stand for medium containing mud and medium containing mud sterilized by heat respectively; SDD and DD stand for sterile medium containing heat-killed $D.$ $desulfuricans$ and and medium containing a viable pure culture of SRB respectively. In Figure 30, the curves CS-SMUD and CS-MUD represent the average corrosion potential for the three specimens in each run from Figures 26 and 27 respectively. In Figure 31, the curves CS-SDD and CS-DD represent the average corrosion potential for the three specimens in each run from Figures 28 and 29 respectively.

As we can see from Figure 30, the initial rapid increase of corrosion potential for carbon steel in the medium containing mud sterilized by heat (CS-SMUD) is larger than that for the corrosion potential in the medium containing mud (CS-MUD). Also, we can see that the corrosion potential of carbon steel in the sterile medium becomes fairly stable for a certain amount of time and then slowly increases to a potential similar to that in the medium containing microorganisms. Figure 31 gives a comparison of the behavior of carbon steel in the sterile medium containing heat-killed $D.$ $desulfuricans$ (CS-SDD) with behavior in the medium containing viable $D.$ $desulfuricans$ (CS-DD). It shows that carbon steel in the sterile medium keeps a relatively stable potential after a big initial jump, while

carbon steel in the medium containing *D. desulfuricans* increases potential steadily through all the test period and finally approaches a similar potential.

For those specimens in the sterile medium, the initial big jump in corrosion potential is probably due to changes of either cathodic or anodic properties during the construction period of the dynamic equilibrium between the steel electrode and the surrounding aqueous system as is shown in Figure 32. The first part (a) shows how an increase of cathodic reaction rate (dotted cathodic line) due to increase in diffusion rate increases a corrosion potential. This increase of cathodic rate (cathodic depolarization) results in a new equilibrium point at a new corrosion potential E_{corr}' and corrosion current density i_{corr}' compared with the original E_{corr} and i_{corr}. Obviously, E_{corr}' is higher than E_{corr} and i_{corr}' larger than i_{corr}. The second part (b) indicates a decrease of anodic reaction rate (dotted anodic line) which increases the corrosion potential. The decrease of anodic rate (anodic polarization) also results in a new equilibrium point at a new corrosion potential E_{corr}' and corrosion current density i_{corr}' compared with the original E_{corr} and i_{corr}, with E_{corr}' higher than E_{corr} but i_{corr}' smaller than i_{corr}. One reason for this anodic polarization is probably due to lack of sulfide which acts as an anodic stimulator (Pankhania, 1988). Again, without further information, it is impossible to indicate which is correct, or how a factor would actually dominate. Once the construction of the dynamic equilibrium is complete, the corrosion potential tends to be relatively stable.

For specimens in the medium containing microorganisms, the initial increase of corrosion potential is also possibly caused partly by either anodic or cathodic property changes as with those in the sterile medium. As mentioned before, it is widely believed that microbiological activity on the surface can change the cathodic properties of steel, and the formation of a biofilm can increase the

corrosion potential. However, the introduction of microorganisms may create a corrosive environment for carbon steel due to microbiological activities such as the production of large amounts of hydrogen sulfide as evidenced by blackening of the medium due to the formation of FeS during the whole test (Figure 16). This may contribute to the smaller initial corrosion potential jump and relatively low corrosion potential during most of the test period in the medium containing microorganisms compared with those in the sterile medium. However, a steady build-up of biofilm and corrosion products may contribute to the slow increase in corrosion potential. The semi-protective layer of corrosion products and biofilm may finally give a relatively stable potential similar to those in the sterile medium.

5.1.1.3 Comparison Between Stainless and Carbon Steel Specimens

Figures 33 to 36 are all average corrosion potentials for stainless and carbon steel specimens under various tested conditions with the same notations as stated above. It is found that stainless steel specimens show more positive initial potentials under all four tested conditions. However, there is no big difference in stable corrosion potentials for most conditions after a certain amount of time, while in the sterile medium it may take a shorter time and in the medium with microorganisms take a longer time to reach that potential. This may indicate that the final stable corrosion potentials for both stainless and carbon steels were not the corrosion potentials for bare steels any more but potentials heavily affected by passive film, corrosion product, biofilm build-up or a combination of these factors. Although stainless and carbon steel specimens show similar stable corrosion potentials after a certain period, the mechanisms to reach that potential are not necessarily the same, as discussed before.

5.1.2 Cyclic Polarization

One specimen from each flask was chosen for the cyclic polarization. Figures 37 to 40 show cyclic polarization results for stainless steel specimens and Figures 41 to 44 give cyclic polarization results for carbon steel specimens.

Figure 37 was obtained in the medium containing mud sterilized by heat and Figure 38 from the medium containing mud. Compared with Figure 37, Figure 38 shows a larger hysteresis loop, much lower protection potential and much larger passive current. All these mean lower pitting resistance in microorganism-containing environments for the stainless steel specimens although without giving any information about corrosion rates.

Figure 39 was obtained in the sterile medium containing heat-killed SRB and Figure 40 from the medium containing viable, pure SRB. Compared with Figure 39, Figure 40 shows a larger hysteresis loop, lower protection potential and larger passive current. Similar to Figure 37 and Figure 38, these results again mean lower pitting resistance in microorganism-containing environments (containing pure SRB) for the stainless steel specimens although without giving any information about corrosion rate. Briefly, stainless steel specimens have lower pitting resistance in the two tested microorganism-containing environments.

Figure 41 was obtained from the medium containing mud sterilized by heat. Figure 42 from the medium containing mud, Figure 43 from the sterile medium containing heat-killed SRB and Figure 44 from the medium containing viable, pure SRB. From these figures we can see that carbon steel specimens performed very similarly to each other even under different conditions. No cyclic polarization graphs for carbon steel specimens have a passive region. This means that carbon steel specimens under all the tested conditions underwent active corrosion with increasing potential until a new anodic reaction other than corrosion took over.

Additionally, this means that the build-up of corrosion products or/and biofilm on carbon steel specimens does not give much protection compared with those passive films on the stainless steel specimens. Figure 43 shows a small hysteresis loop which may indicate a less protective corrosion product and/or biofilm layer in environments containing SRB compared with that in the sterile medium.
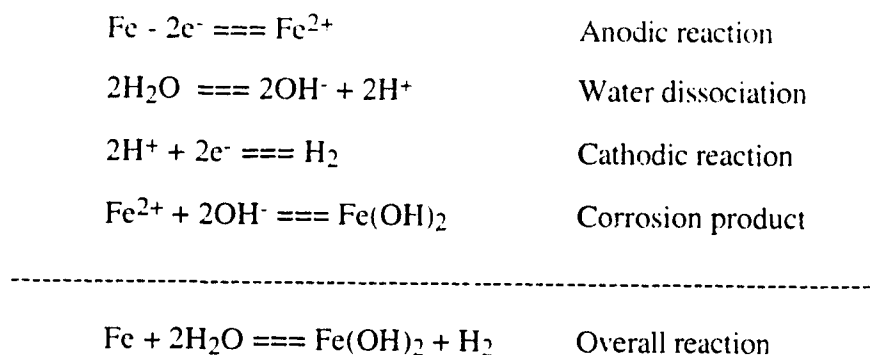
5.2 Scanning Electron Microscopy (SEM)

5.2.1 EDS Chemical Analysis

One specimen from each flask was chosen to undergo EDS chemical analysis. The analysis results for deposit of corrosion products on carbon steel specimens in all four tested conditions are shown in Table 12. The results have been corrected with ZAF calculation or correction and then normalized to bring the total concentration to 100%. The ZAF calculation or correction is a widely used procedure to improve the accuracy of results by correcting the errors caused by atomic number effect (Z), X-ray absorption effect (A) and X-ray fluorescence effect (F) in quantitative X-ray analysis (Goldstein et al., 1992). In Table 12, experimental numbers 5 and 6 represent the medium containing mud sterilized by heat and the medium containing mud (thus microorganisms) respectively, and experiment numbers 7 and 8 represent the sterile medium containing heat-killed SRB and and the medium containing the viable, pure SRB, respectively.

There are many elements in the deposit. Table 12 shows only major elements (Fe and O combined count for more than 90% from the normalized result) in the film. The minor elements such as Mn, Si, Ni, Cr, Cu, Al etc. which may be from the corroded steel and mechanically embedded into the deposit can be reasonably ignored regarding the mechanism for the deposit layer formation, due to their much lower concentration.

From Table 12 we can see that S is not a major element either in the deposit although H_2S was produced in the microorganism-containing environments during the test. This contradicts the generally accepted idea that SRB-created H_2S may react with Fe on the steel surface to create a FeS layer (Seed, 1990). Obviously, some kind of reaction resulted in the formation of a layer consisting mainly of Fe, O, and also probably H (which could not be analyzed by EDS). From experiment numbers 5 and 7 we can see that the atomic percentage of O is much higher than that of Fe in the sterile medium (around 2 to 1 in ratio). This is probably due to the following reactions:

$$Fe - 2e^- === Fe^{2+}$$ Anodic reaction

$$2H_2O === 2OH^- + 2H^+$$ Water dissociation

$$2H^+ + 2e^- === H_2$$ Cathodic reaction

$$Fe^{2+} + 2OH^- === Fe(OH)_2$$ Corrosion product

$$Fe + 2H_2O === Fe(OH)_2 + H_2$$ Overall reaction

$Fe(OH)_2$ is thus the major component in the deposit from the sterile medium.

From experiment numbers 6 and 8 we can see that the atomic percentage of Fe is much higher than that of O in the medium containing viable microorganisms (around 3 to 2 in ratio). While it is hard to determine a structure which represent this ratio, we can see the big difference between the components from the sterile medium and the medium containing viable microorganisms.

5.2.2 Morphology Studies

Considering that stainless steel specimens have not undergone microscopically detectable corrosion, only carbon steel specimens have been studied under the SEM. To find out whether the corrosion product cleaning process caused severe corrosion of carbon steel specimens so as to affect the morphology of immersion-tested specimens, three new, untested specimens were put into the solution used to remove corrosion products and underwent cleaning for different cleaning times. Figure 45 shows the effect of cleaning time on morphology for the carbon steel specin ens. Obviously, the specimens for 10 and 120 minutes immersion underwent corrosion to some extent. However, corrosion for 10 minutes which was used to remove corrosion product in all the actual experiments is not long enough to cause severe corrosion to distort the final result compared with results to follow. From this figure one can also see that even a 120 minutes immersion in the cleaning solution is not comparable to those from actual immersion tests regarding severity of corrosion.

Figures 46 and 47 show morphology for carbon steel specimens after immersion tests in the medium containing mud sterilized by heat and the medium containing mud, respectively. It is very clear that specimens in both solutions underwent corrosion but specimens in the medium containing mud underwent severe corrosion. Similarly, Figures 48 and 49 show morphology for carbon steel specimens after immersion tests in the medium containing heat-killed SRB and the medium containing viable, pure SRB, respectively. It is also clear that specimens in both solutions underwent corrosion but specimens in the medium containing viable, pure SRB underwent much more severe corrosion.

From these figures we can also see that although all specimens underwent general corrosion the pearlite phase in the pearlite-ferrite structure underwent faster

corrosion which is probably due to its lamellar structure of carbide and ferrite which creates a relatively anodic area compared with pure ferrite areas. The more severe corrosion for those specimens in the environments containing microorganisms is probably due to either a more corrosive environment caused by large amounts of H_2S or by the change of localized conditions under the biofilm. As mentioned in the section on biofilm and biofouling, a biofilm can cause entrapment of metals and corrosion products, and a decrease in rates of diffusion of chemical species to and away from the substratum. This may sometimes create a very corrosive condition through processes such as hydrolysis under the biofilm, much different from the condition of the bulk solution.

6. Conclusions

1. Microorganisms (either pure *D. desulfuricans* or those in river mud) have an effect on the corrosion potential of ASTM A312-89A type 304L SMLS stainless steel in the two tested environments, with the corrosion potential decreasing within 5 days and then increasing steadily with time until it reaches a potential similar to that in the sterile medium. The first drop is probably due to either cathodic rate reduction or anodic rate increase caused by microbiological activities. The later steady increase in corrosion potential may be due to the build-up of a semi-protective biofilm on the steel surface or the passive nature of the stainless steel.

2. Cyclic polarization graphs for the stainless steel specimens indicate a larger hysteresis loop, lower protection potential and larger passive current density in the medium containing microorganisms (either pure *D. desulfuricans* or those in river mud) than those obtained from the sterile medium. This means that the two tested kinds of microorganisms-containing environments actually lowered the localized corrosion resistance of the stainless steel.

3. Existence of the microorganisms (either pure *D. desulfuricans* or those in river mud) lowered the corrosion potential of the ASTM A513L REV Grade 1026 carbon steel specimens initially due to the corrosive environment caused by microbiological activities, and then caused a steady increase in corrosion potential, probably through biofilm build-up and also possibly corrosion product build-up.

4. With time, almost all the stainless and carbon steel specimens reached a similar corrosion potential. which may suggest that this potential is not due only to the bare steel but is heavily affected by a passive film. corrosion products. biofilm or a combination of them.

5. No cyclic polarization graphs for carbon steel specimens have a passive region. This means that the carbon steel is not a passive steel and will not passivate in the tested environments. This also means that the build-up of corrosion products or/and biofilm on the carbon steel specimens does not give much protection compared with those passive films on the stainless steel specimens. A small hysteresis loop in the cyclic polarization graph for the carbon steel in the medium containing pure SRB may tend to indicate a less protective corrosion product and/or biofilm layer in an environment containing pure SRB compared with those obtained from the sterile medium.

6. Sulfur (S) is not a major element in the deposits on the immersion-tested carbon steel specimens which contradicts the general belief that iron sulfide (FeS) is the major deposit for MIC. Iron (Fe) and oxygen (O) account for more than 90% of the deposit based on the normalized results. The major difference here regarding microorganisms is the ratio between Fe and O. The atomic percentage of O is much higher than that of Fe in the sterile medium (around 2 to 1 in ratio). This is probably due to the formation of $Fe(OH)_2$ based on the reaction between H_2O and Fe. The atomic percentage of Fe is much higher than that of O in the medium containing microorganisms (around 3 to 2 in ratio). Obviously, microorganisms caused the big increase in Fe in the deposits although the exact deposit composition is not known.

7. All carbon steel specimens underwent general corrosion in the tested conditions with the pearlite phase in the pearlite-ferrite structure undergoing faster corrosion which is probably due to the lamellar structure of pearlite. However, more severe corrosion was observed for those specimens in the environments containing microorganisms which is probably due to either a more corrosive environment caused by large amount of H_2S or by the change of localized conditions under the biofilm caused by the entrapment of metals and corrosion products and the decrease in diffusion rate of chemical species to and away from the substratum.

8. Stresses of the magnitude of 85% of yield strength on the surface of these metals are insufficient to initiate SCC under the tested conditions during the test period of 96 days.

7. Recommendations for Future Work

1. Considering the difficulty of cracking the C-ring specimens during SCC immersion tests, pre-notched specimens are recommended although it is difficult to predict the stress.

2. The pH value and content of H_2S of the batch test solution should be monitored. The exact effect of H_2S on corrosion or SCC should be investigated. In addition, differences between SRB-created H_2S and other types of H_2S may be studied.

3. The biofilm on the specimen should be investigated with ESEM or other methods to study the activity of microorganisms.

4. The exact composition of the corrosion deposit on the specimens should be identified to study the mechanism for the corrosion.

Table 1. Chemical composition of ASTM A513L REV Grade 1026 carbon steel in weight percent (supplied by Atlas Alloys, Edmonton, Alberta).

Elements	C	Mn	P	S	Si	Ni	Cr
wt%	0.23	0.63	0.009	0.003	0.028	0.020	0.040
Elements	Mo	Cu	Al	Ca	Ti	N	Fe
wt%	0.010	0.020	0.031	0.0014	0.0030	0.0061	balance

Table 2. Mechanical properties of ASTM A513L REV Grade 1026 carbon steel (supplied by Atlas Alloys, Edmonton, Alberta).

Yield Strength	Tensile Strength	Elongation in 2" (5.08 cm) (%)	Hardness (Rockwell, RB)
82000 psi (565 MPa)	92100 psi (635 MPa)	25	90

Table 3. Chemical composition of ASTM A312-89A type 304L SMLS stainless steel in weight percent (supplied by Team Tube Ltd., Edmonton, Alberta).

Elements	C	Si	Mn	P	S	Cr	Ni	Fe
wt%	0.019	0.360	1.790	0.018	0.015	18.680	10.490	Balance

Table 4. Mechanical properties of ASTM A312-89A type 304L SMLS stainless steel (supplied by Team Tube Ltd., Edmonton, Alberta).

Yield Strength	Tensile Strength	Elongation in 2" (5.08 cm) (%)	Hydrostatic Test
40000 PSI (276 MPa)	90000 psi (621 MPa)	66	2500 psi (17 MPa)

Table 5. Medium for SRB detection and cultivation.

Chemicals	Concentrations (g/L)
KH$_2$PO$_4$	0.5
NH$_4$Cl	1.0
CaSO$_4$	1.0
MgSO$_4$.7H$_2$O	2.0
Sodium lactate	3.5
Yeast extract	1.0
Ascorbic acid	0.1
Thioglycollic acid	0.1
FeSO$_4$.7H$_2$O	0.5
Note: Distilled water 1 litre, adjust solution to between pH 7 and 7.5.	

Table 6. Medium for SRB cultivation.

Chemicals	Concentrations (g/L)
KH_2PO_4	0.5
NH_4Cl	1.0
Na_2SO_4	4.5
$MgSO_4.7H_2O$	0.06
Sodium lactate	6.0
Yeast extract	1.0
$CaCl_2.6H_2O$	0.06
Sodium citrate.$2H_2O$	0.3
$FeSO_4.7H_2O$	0.004
Note: Distilled water 1 litre. pH 7.5 ± 0.2.	

Table 7. Outside diameter (OD) and thickness (t) measurements for the stainless steel C-ring specimens.

C-ring No.	OD (mm)				t (mm)			
	OD_1	OD_2	OD_3		t_1	t_2	t_3	t_4
1	23.86	24.13	24.00	23.92	1.88	1.91	1.90	1.88
2	24.80	24.81	24.77	24.79	1.77	1.78	1.77	1.79
3	24.80	24.79	24.82	24.79	1.67	1.65	1.68	1.68
4	23.37	23.47	23.87	23.85	1.90	1.89	1.92	1.94
5	24.78	24.70	24.77	24.77	1.82	1.88	1.84	1.89
6	24.81	24.83	24.77	24.88	1.75	1.94	1.80	1.88
7	24.58	24.62	24.66	24.70	1.83	1.80	1.79	1.80
8	24.81	24.84	24.80	24.83	1.83	1.98	1.92	2.01
9	24.76	24.76	24.75	24.79	1.96	1.98	2.00	1.95
10	24.83	24.81	24.82	24.83	1.65	1.66	1.68	1.69
11	24.88	24.85	24.81	24.75	1.65	1.66	1.63	1.64
12	24.91	24.92	24.94	24.91	2.00	1.96	1.94	2.06

Note: The subscript of OD_x means the xth measurement.

Table 8. Outside diameter (OD) and thickness (t) measurements for the carbon steel C-ring specimens.

C-ring	OD(mm)				t (mm)			
No.	OD_1	OD_2	OD_3	OD_4	t_1	t_2	t_3	t_4
1	22.69	22.71	22.67	72	1.76	1.84	1.79	1.78
2	22.68	22.67	22.71	.65	1.90	1.88	1.92	1.86
3	22.75	22.88	22.72	22.71	1.84	1.87	1.86	1.87
4	22.66	22.71	22.67	22.64	1.77	1.81	1.73	1.75
5	22.69	22.69	22.67	22.68	1.78	1.78	1.79	1.76
6	22.69	22.67	22.68	22.69	1.83	1.83	1.84	1.85
7	22.64	22.59	22.66	22.67	1.75	1.78	1.78	1.76
8	22.71	22.70	22.76	22.73	1.81	1.83	1.86	1.85
9	22.69	22.66	22.67	22.65	1.80	1.83	1.85	1.80
10	22.68	22.67	22.71	22.70	1.80	1.81	1.80	1.83
11	22.70	22.70	22.65	22.65	1.83	1.82	1.86	1.85
12	22.65	22.69	22.67	22.66	1.84	1.85	1.84	1.81

Note: The subscript of OD_x means the xth measurement.

Table 9. Calculated results for stressing the stainless steel C-ring specimens using
FORTRAN program CRING1.

C-ring No	OD (mm)	t (mm)	DT	Z	Δ (mm)	OD_f (mm)
1	23.98	1.89	11.67	0.94	0.26	23.72
2	24.79	1.78	12.95	0.95	0.30	24.49
3	24.80	1.67	13.85	0.95	0.32	24.48
4	23.64	1.91	11.36	0.94	0.25	23.39
5	24.75	1.86	12.33	0.95	0.28	24.47
6	24.82	1.84	12.47	0.95	0.29	24.53
7	24.64	1.81	12.65	0.94	0.29	24.34
8	24.82	1.94	11.83	0.95	0.27	24.55
9	24.77	1.97	11.56	0.94	0.27	24.50
10	24.82	1.67	13.86	0.95	0.32	24.50
11	24.82	1.65	14.09	0.95	0.33	24.50
12	24.92	1.99	11.52	0.94	0.27	65

Note: OD and t are average outside diameter and average thickness respectively based on the results from Table 7; DT is the ratio of D over t with D = OD - t; Z is the correction factor; Δ is the change of OD giving desired stress and OD_f is the outside diameter of stressed C-ring.

Table 10. Calculated results for stressing the carbon steel C-ring specimens using a modified FORTRAN program based on CRING1.

C-ring No	CD (mm)	t (mm)	DT	Z	Δ (mm)	OD_t (mm)
1	22.70	1.79	11.66	0.94	0.49	22.21
2	22.68	1.89	11.00	0.95	0.46	22.22
3	22.77	1.86	11.24	0.95	0.47	22.30
4	22.67	1.77	11.84	0.95	0.49	22.18
5	22.68	1.78	11.76	0.95	0.49	22.19
6	22.68	1.84	11.34	0.94	0.17	22.21
7	22.64	1.77	11.81	0.95	0.49	22.15
8	22.73	1.84	11.37	0.94	0.47	22.25
9	22.67	1.82	11.45	0.94	0.48	22.19
10	22.69	1.81	11.54	0.94	0.48	22.21
11	22.68	1.84	11.32	0.95	0.47	22.20
12	22.67	1.84	11.35	0.94	0.47	22.19

Note: OD and t are average outside diameter and average thickness respectively based on the results from Table 8; DT is the ratio of D over t with D = OD - t; Z is the correction factor; Δ is the change of OD giving desired stress and OD_t is the outside diameter of stressed C-ring.

Table 11. Test conditions for C-ring SCC immersion tests.

Test No.	Test Conditions
1 (SS) 5 (CS)	Medium containing mud sterilized by heat
2 (SS) 6 (CS)	Medium containing mud
3 (SS) 7 (CS)	Sterile medium containing heat-killed *D. desulfuricans*
4 (SS) 8 (CS)	Medium containing viable *D. desulfuricans*

Note: SS stands for stainless specimens and CS stands for carbon steel specimens.

Table 12. Major elements from normalized chemical analysis by EDS for deposits on the immersion tested carbon steel C-ring specimens.

Exp. No.	Elements (wt%)			Elements (atom.%)		
	Fe	O	S	Fe	O	S
5	61.4	30.3	1.7	34.1	58.7	1.7
6	77.5	15.9	1.4	54.4	38.9	1.7
7	56.8	35.3	1.9	29.4	63.7	1.7
8	79.0	14.0	2.7	56.9	35.1	3.4

Note: For experimental conditions, see Table 11.

Page 88 has been removed due to copyright restrictions. The information removed was Figure 1 which was a schematic summary diagram of processes contributing to biofilm accumulation and detachment (Videla and Characklis, 1992), and Figure 2 (a) which was a typical ESEM image of bacteria within sulfide corrosion layer (marker = 5 mm) (Little et al., 1991b).

Page 89 has been removed due to copyright restrictions. The information removed was Figure 2 (b) which was a typical SEM image of bacteria monolayer overlying a sulfide layer (marker = 2 mm) (Little et al., 1991b), and Figure 3 which was open-circuit potential vs. time for six stainless steels exposed to flowing natural seawater (Johnsen and Bardal, 1985).

Page 90 has been removed due t ..pyrig!n restrictio Th information removed was Figure 4 which was measui   nt   corrsion current densiy i_{corr} through extrapolation from Tafel regions on experimental polarizatior curves (Jones, 1992b).
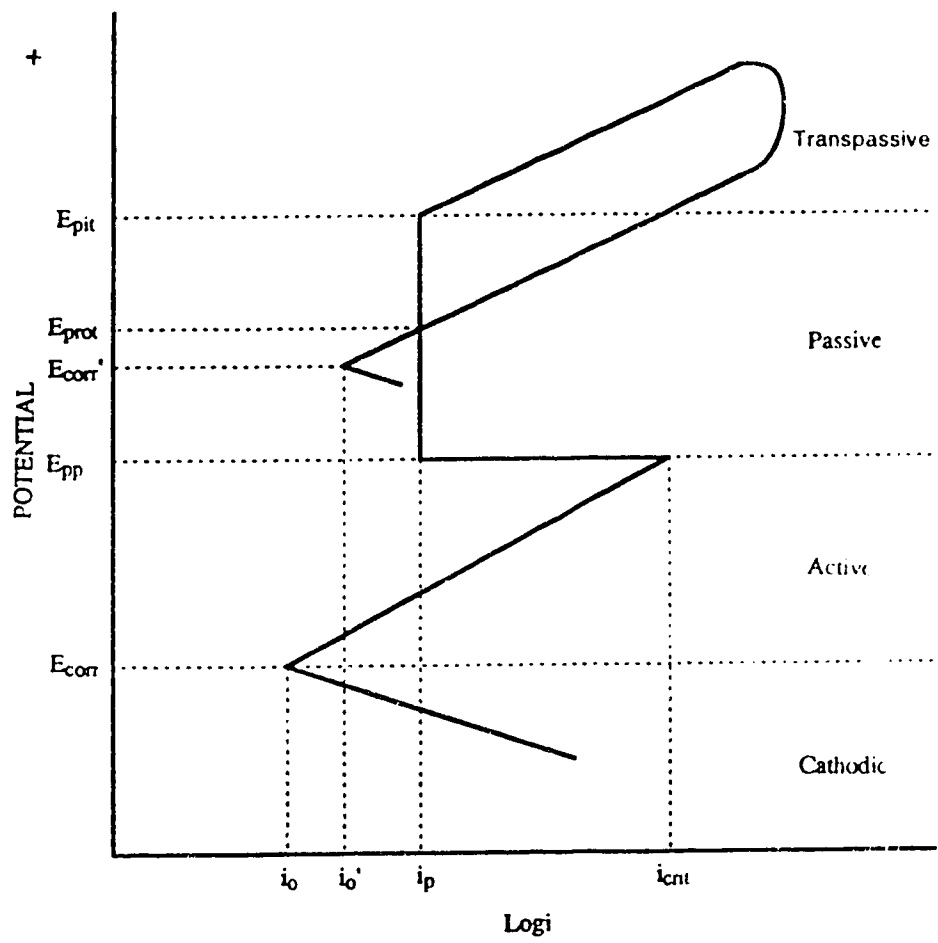
Figure 5. An idealized anodic polarization dia   ...n for a passivatable metal.

Page 92 has been removed due to copyright restrictions. The information removed was Figure 6 which was pitting curves of AISI 316 stainless steel in sterile medium and strain 8303 SRB (Ringas and Robinson, 1987).

Page 93 has been removed due to copyright restrictions. The information removed was Figure 7 which was potentiostatic curve of AISI 304L stainless steel in (a) sterile solution, and (b) strain 8303 SRB (Redrawn from Ringas and Robinson, 1987).

Page 94 has been removed due to copyright restrictions. The information removed was Figure 8 which was measurement of corrosion rate by polarization technique (Dexter et al., 1991).

Page 95 has been removed due to copyright restrictions. The information removed was Figure 9 which was current density maps over carbon steel electrode in sterile aerobic microbiological medium: (a) 1 minute; (b) 3 hours; (c) 32 hours (Franklin et al., 1991).

Page 96 has been removed due to copyright restrictions. The information

removed was Figure 10 which was current density maps over carbon steel electrode

in inoculated aerated medium: (a) 3 hours; (b) 7 hours; (c) 11.5 hours; (d) 23 hours

(Franklin et al., 1991).
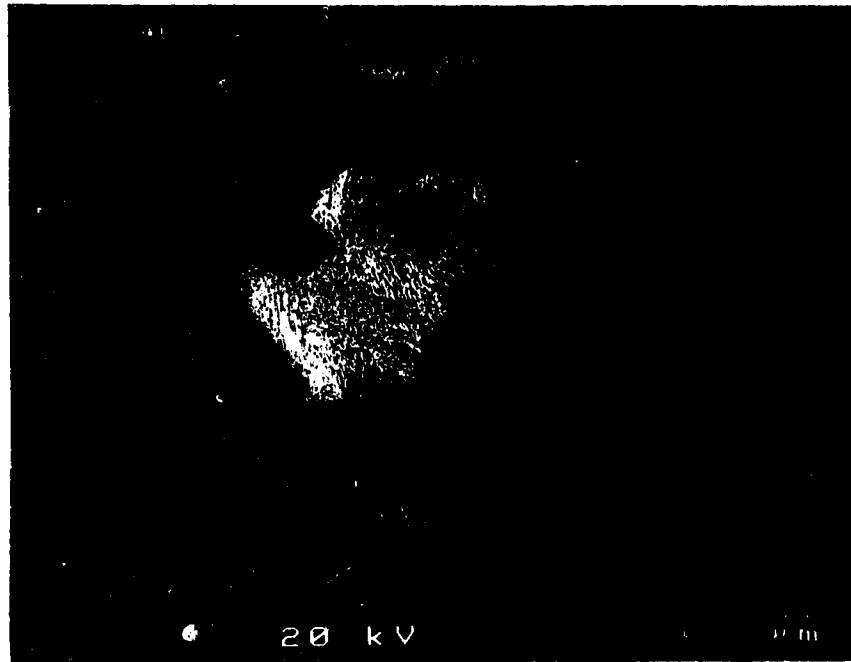
Figure 11. Microstructure of ASTM A513L REV Grade 1026 carbon steel under SEM.
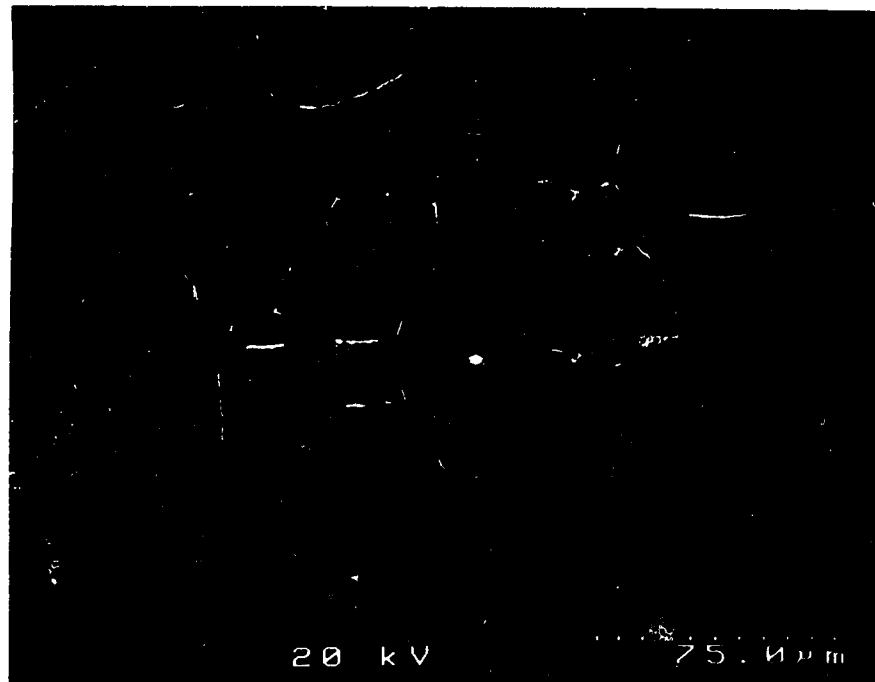
Figure 12. Microstructure of ASTM A312-89A type 304L SMLS stainless steel under SEM.

.

Page 98 has been removed due to copyright restrictions. The information

removed was Figure 13 which was a phase-contrast micrograph of *D. desulfuricans*

NCIB 8307 (x2000) (Widdel and Pfennig, 1984).

Page 99 has been removed due to copyright restrictions. The information removed was Figure 14 which was a typical configuration of C-ring type stress-corrosion cracking specimen (ASTM standard G38-73 (re-approved 1990)).

Page 100 has been removed due to copyright restrictions. The information removed was Figure 15 which was a correction factor for calculating the final diameter required to give the desired stress for curved beams (ASTM standard G38-73 (re-approved 1990)).

Figure 16. Experimental set-up for C-ring immersion SCC test.
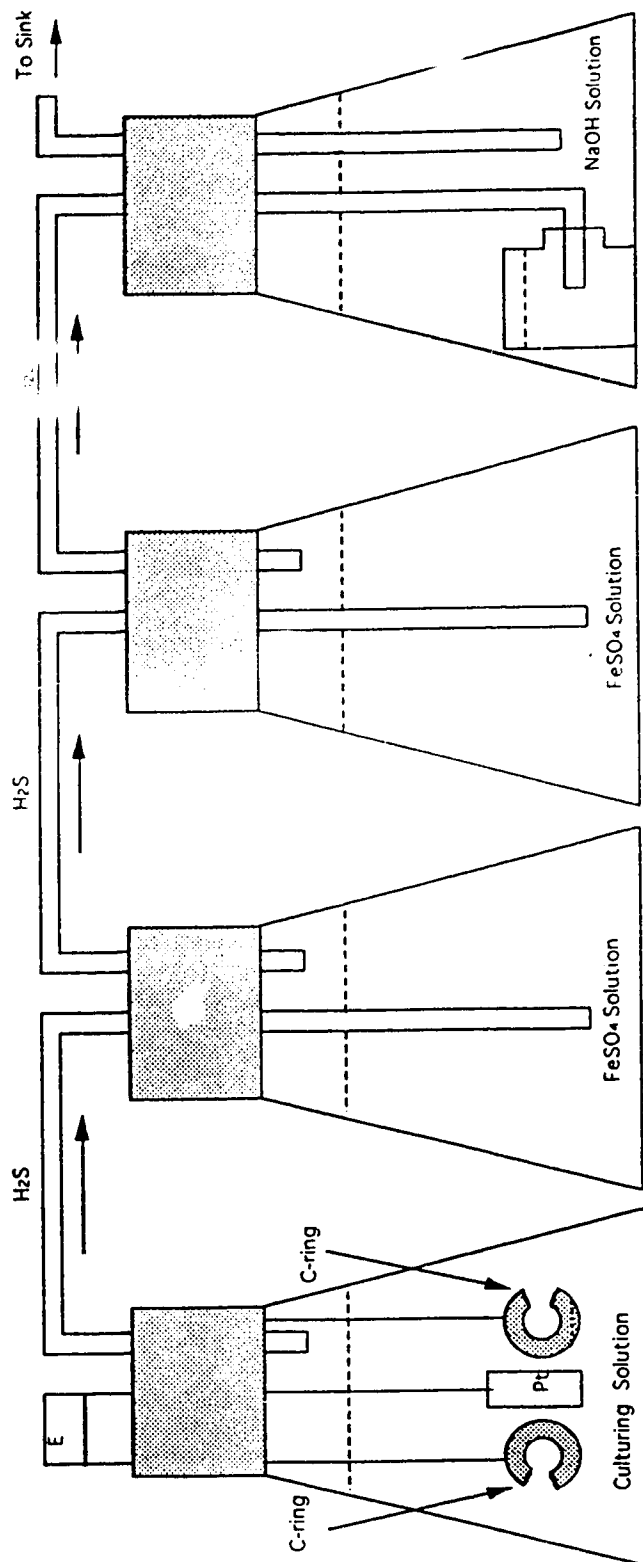
Figure 17. Schematic wiring diagram of C-ring immersion SCC test (E is a potentialstat and the bottle in the last flask is used to collect gases).
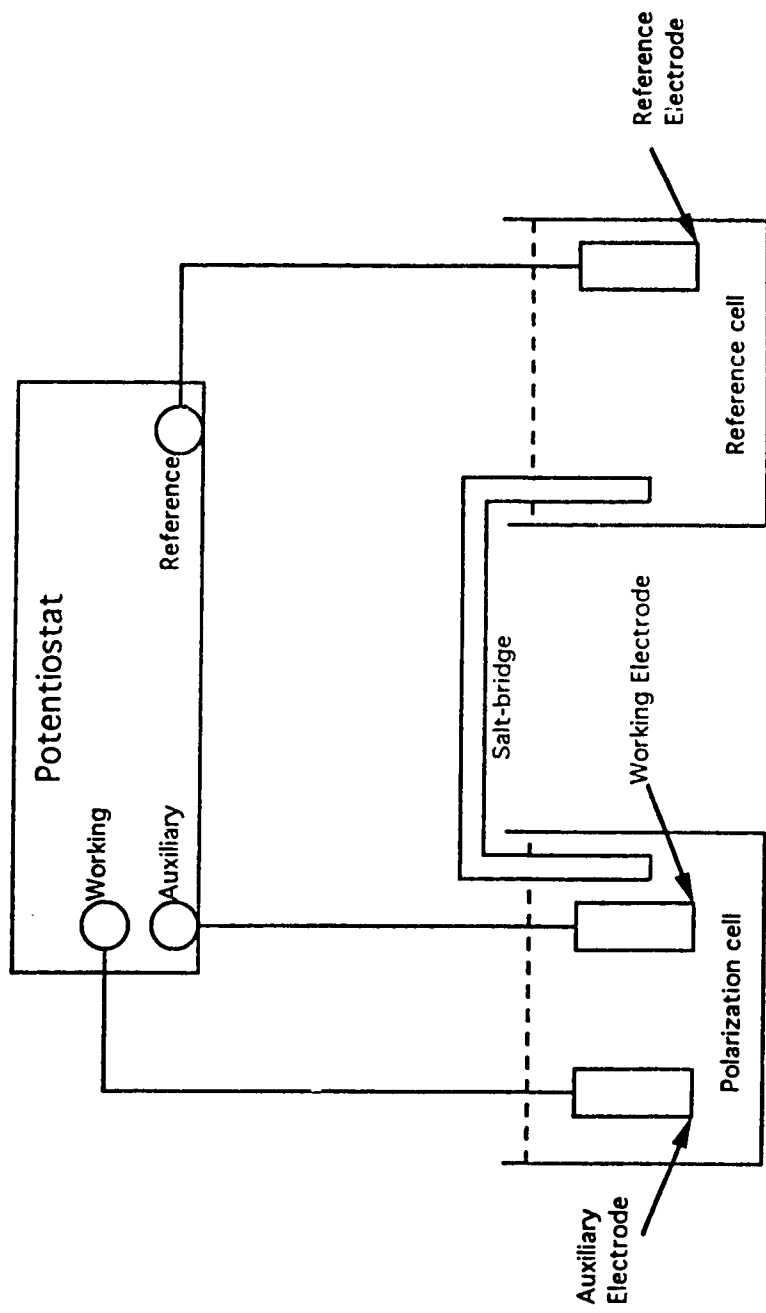
Figure 18. Schematic cyclic polarization wiring diagram.
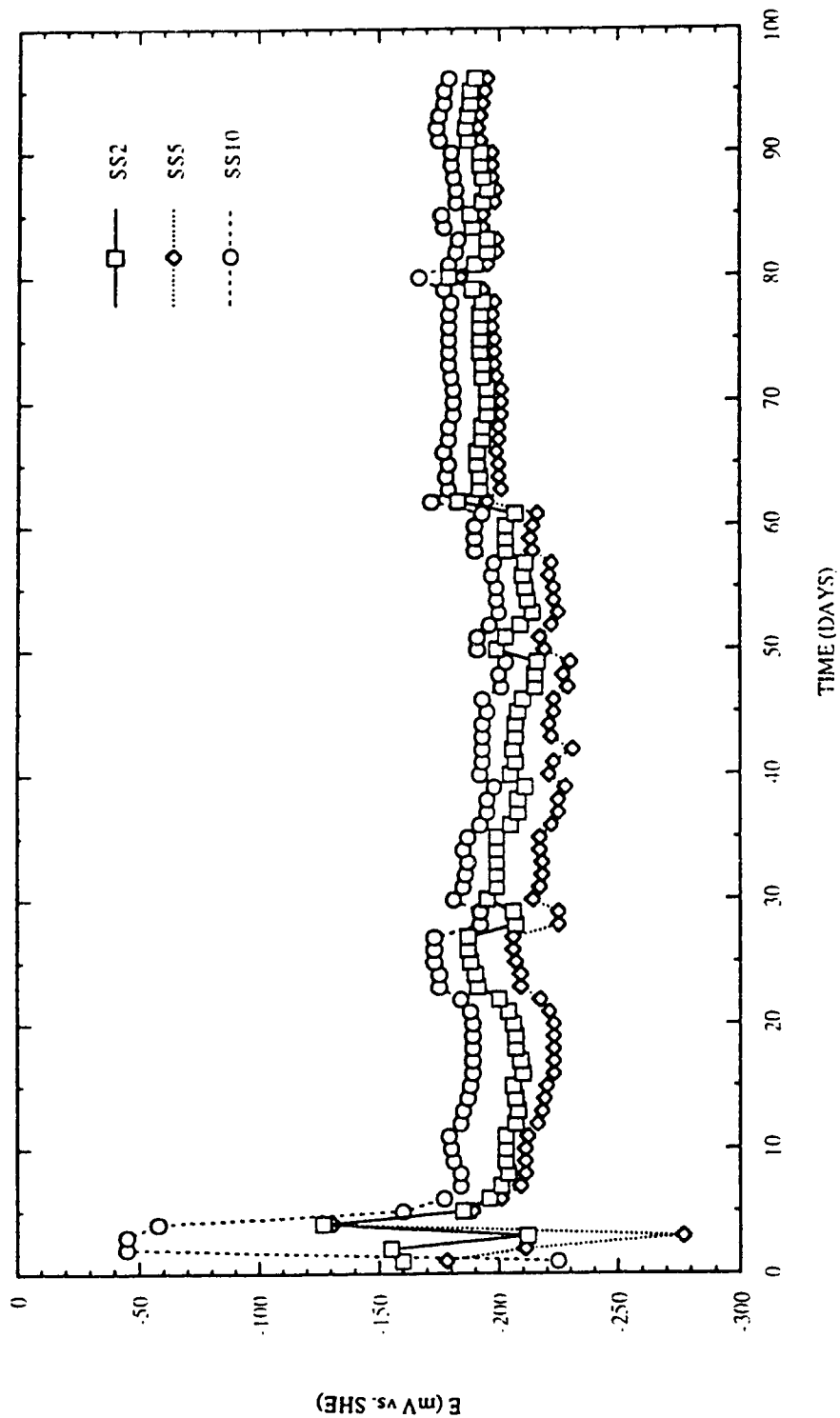
Figure 19. Corrosion potential *vs.* time for type 304L stainless steel in medium containing mud sterilized by heat.
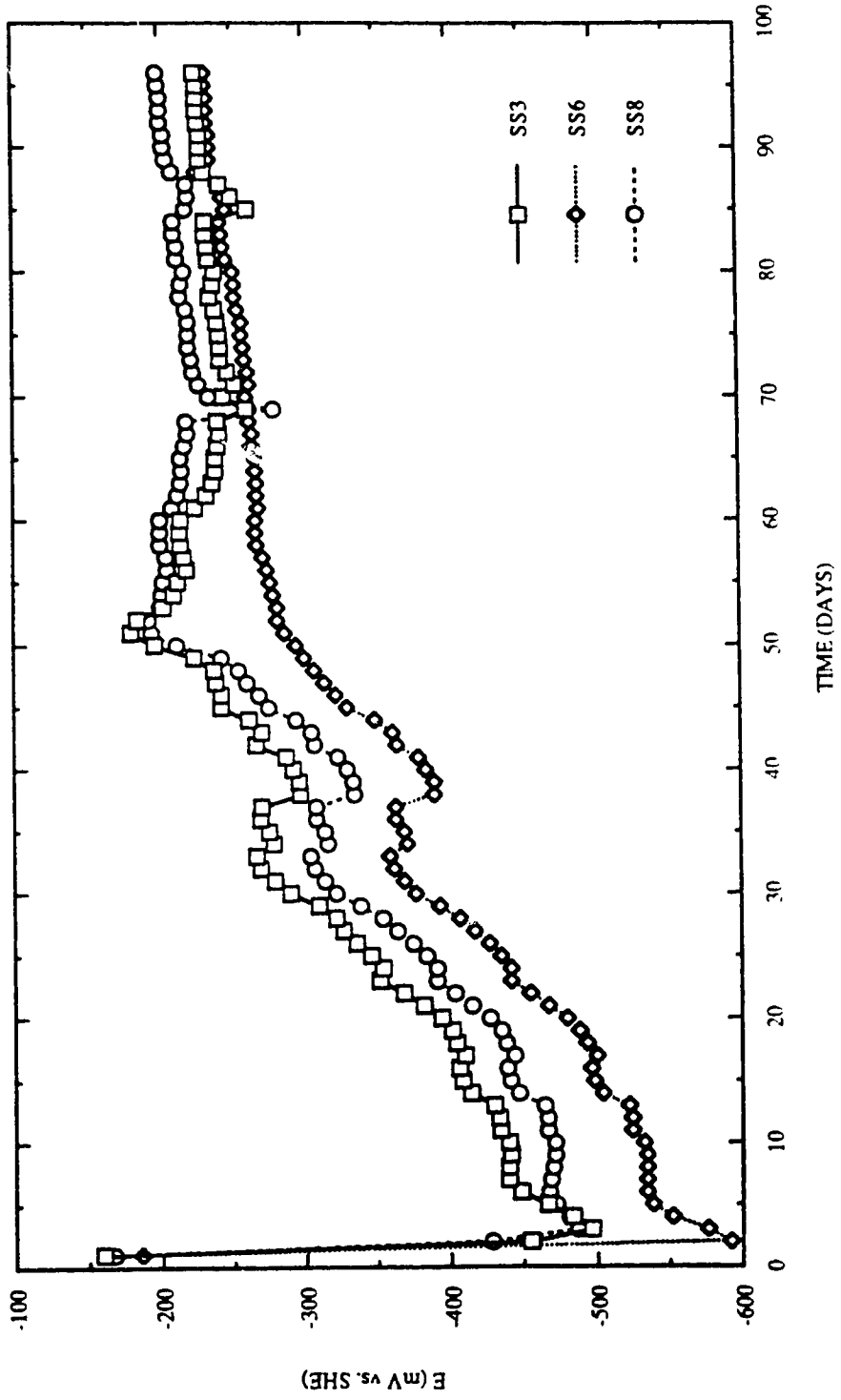
Figure 20. Corrosion potential vs. time for type 304L stainless steel in medium containing mud.
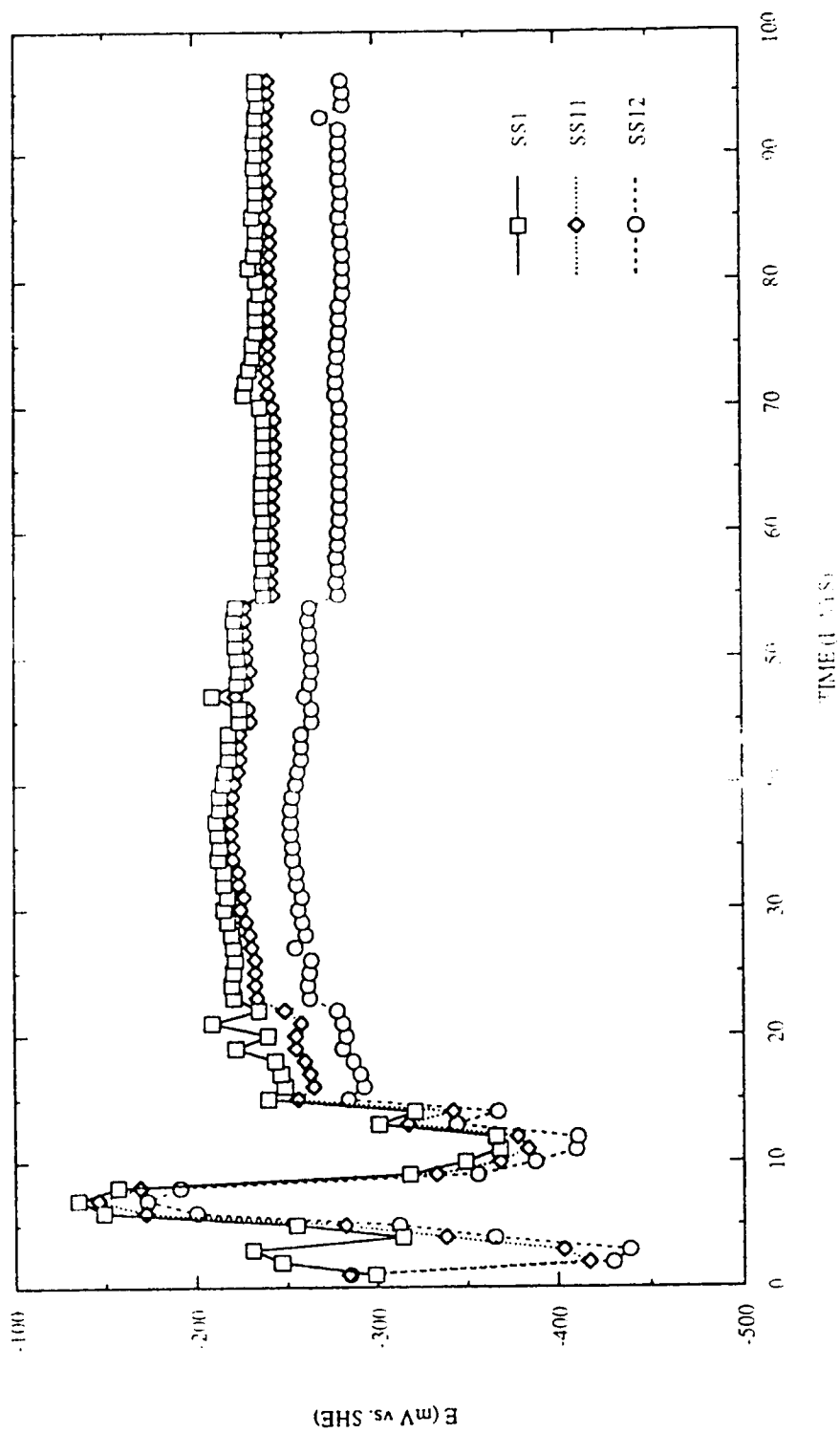
Figure 21. Corrosion potential *vs.* time for type 304L stainless steel in sterile medium containing heat-killed *D. desulfuricans.*
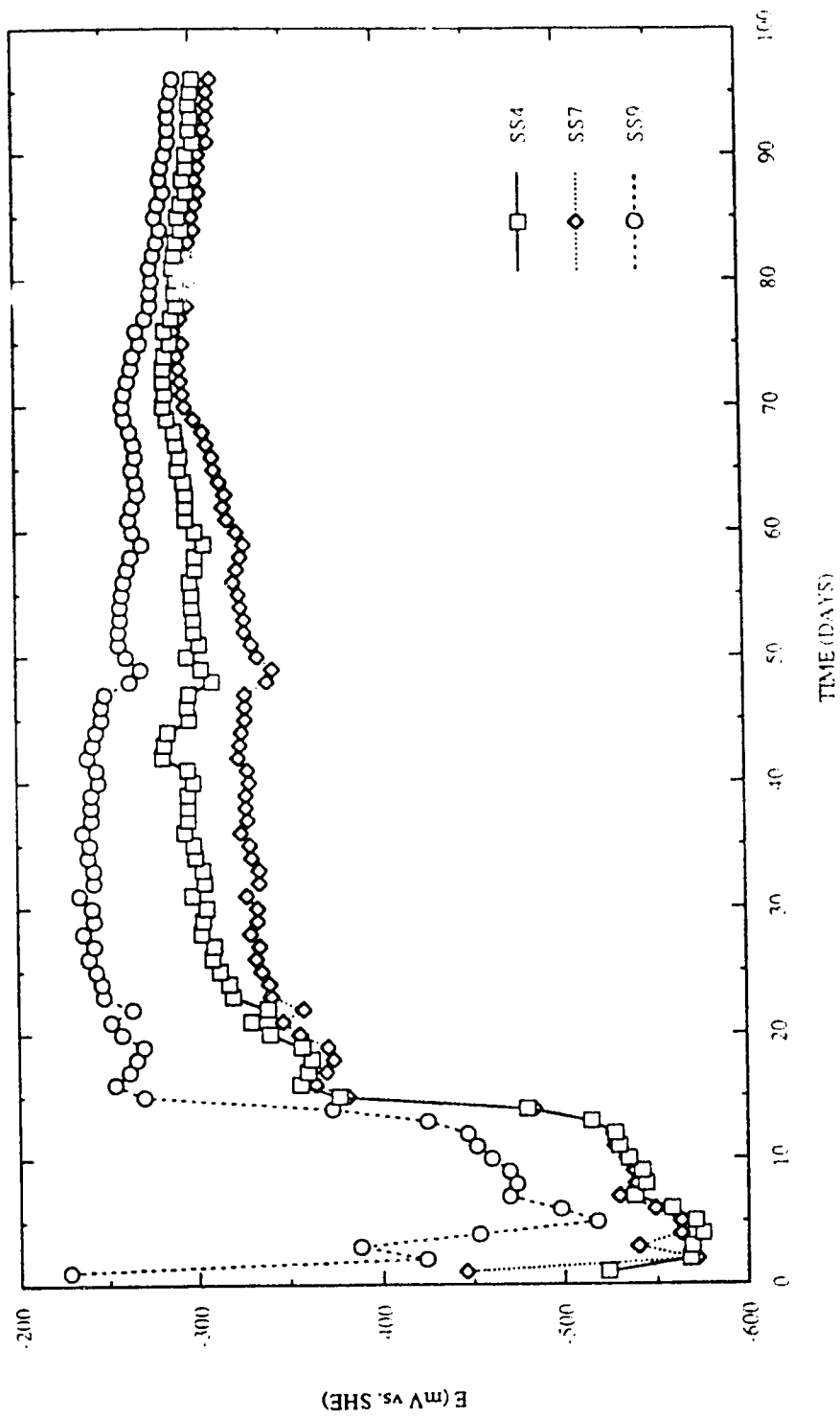
Figure 22. Corrosion potential vs. time for type 304L stainless steel in medium containing viable *D. desulfuricans*.
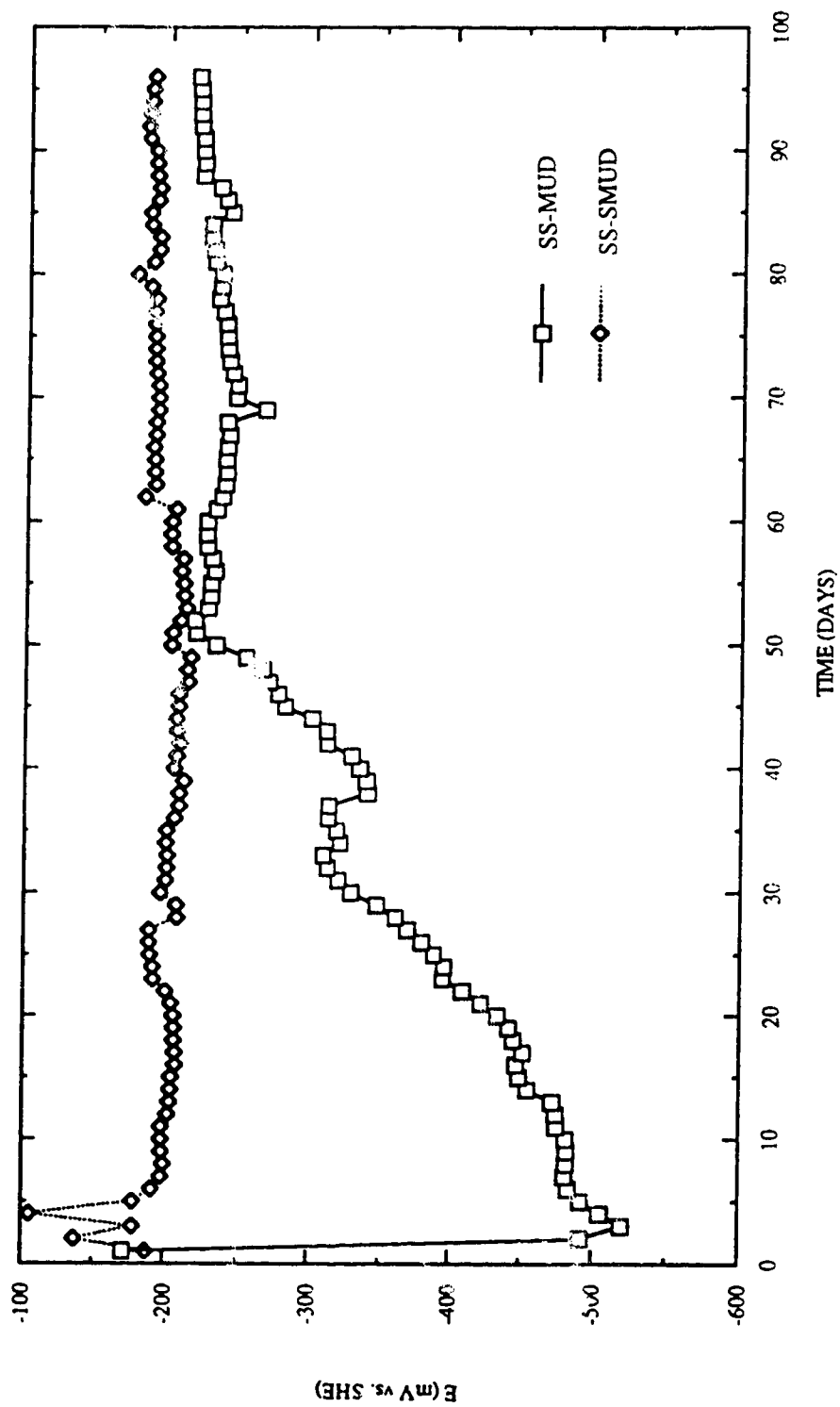
Figure 23. Corrosion potential *vs.* time for type 304L stainless steel in medium containing mud sterilized by heat (SS-SMUD) and in medium containing mud (SS-MUD).
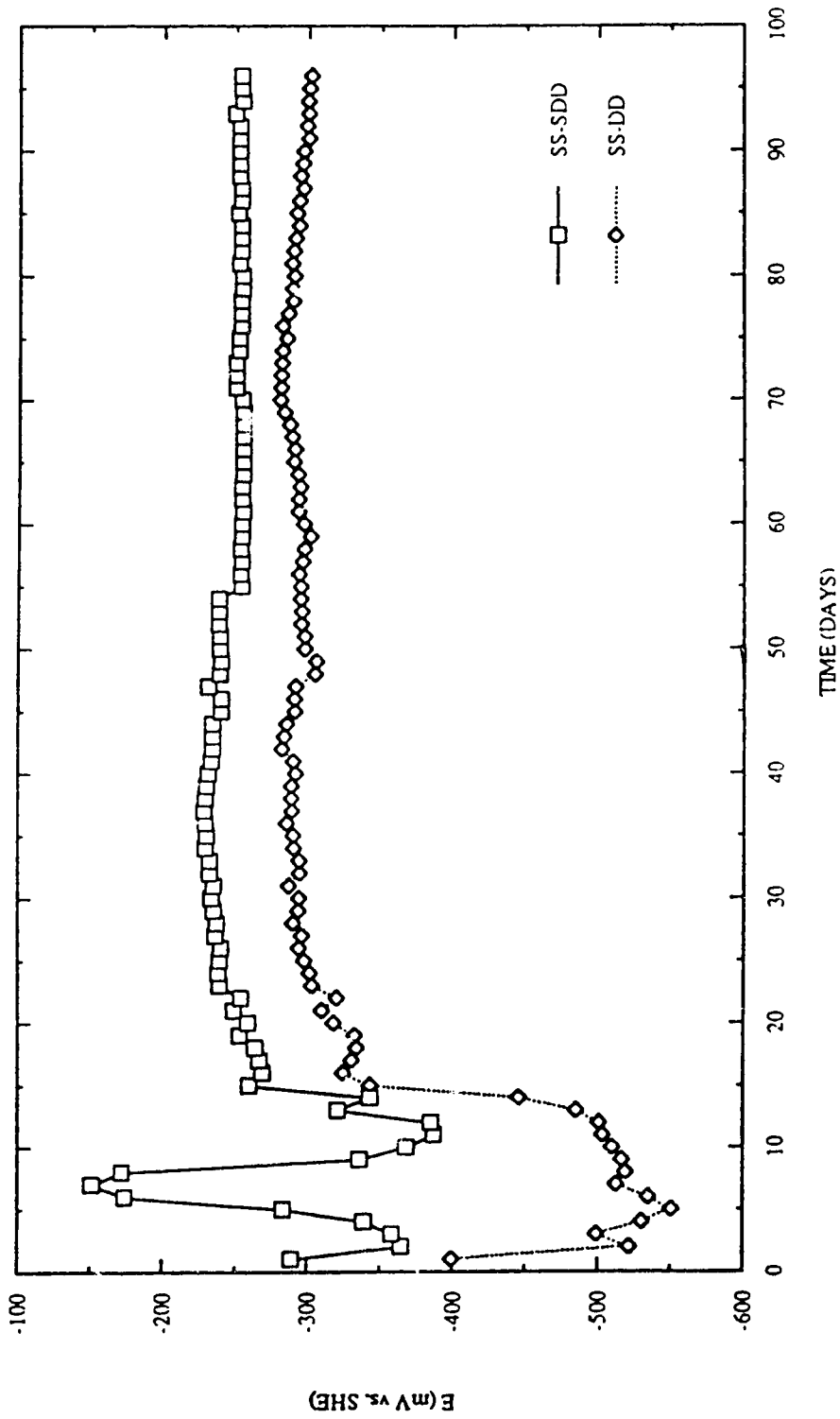
Figure 24. Corrosion potential vs. time for type 304L stainless steel in sterile medium containing heat-killed *D. desulfuricans* (SS-SDD) and in medium containing viable *D. desulfuricans* (SS-DD).
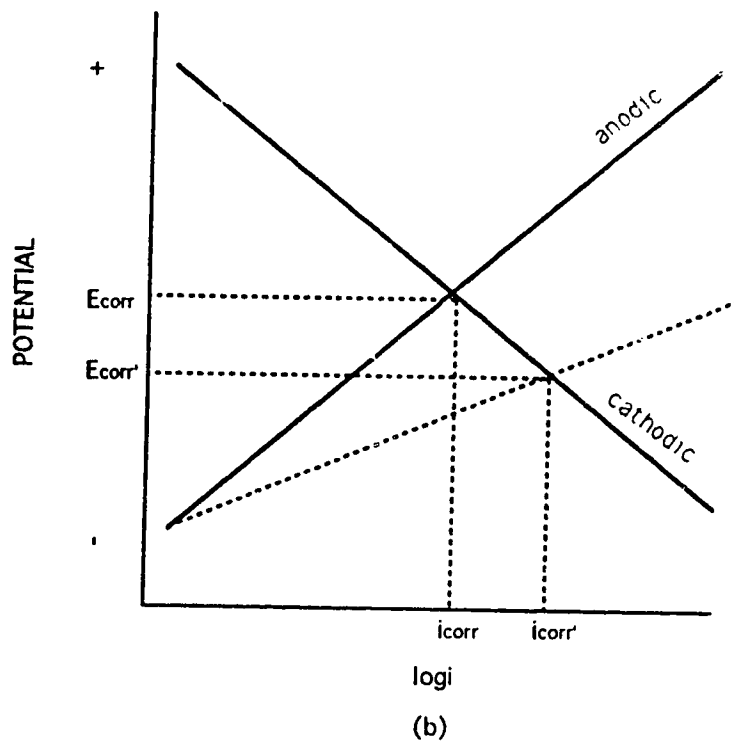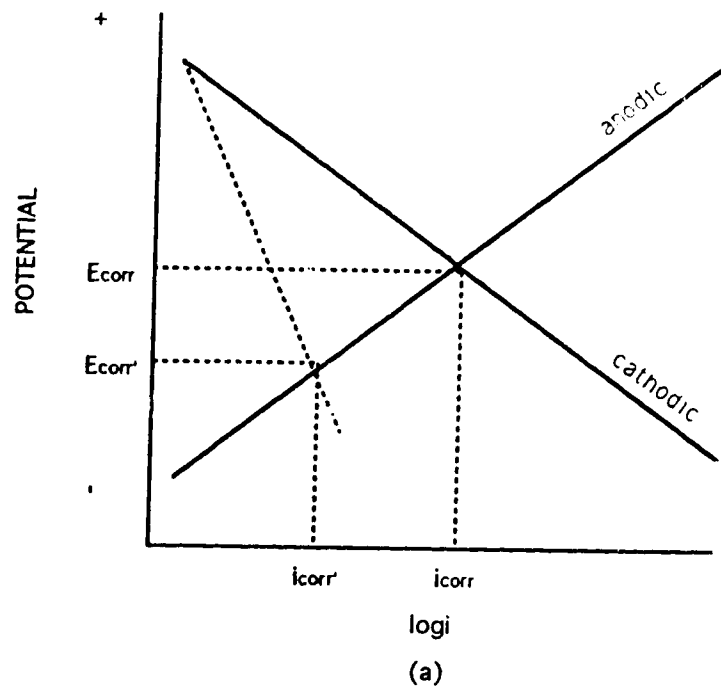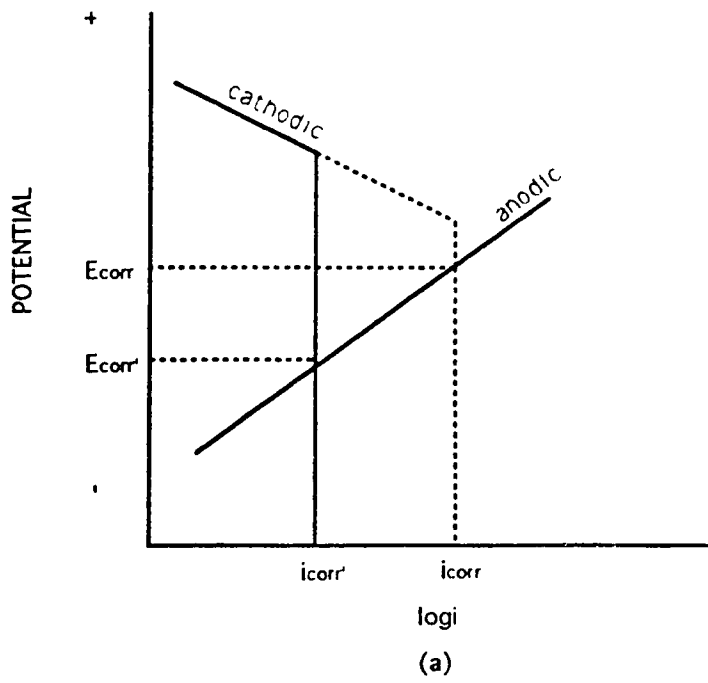
Figure 25. Increase of corrosion potential caused by (a) cathodic
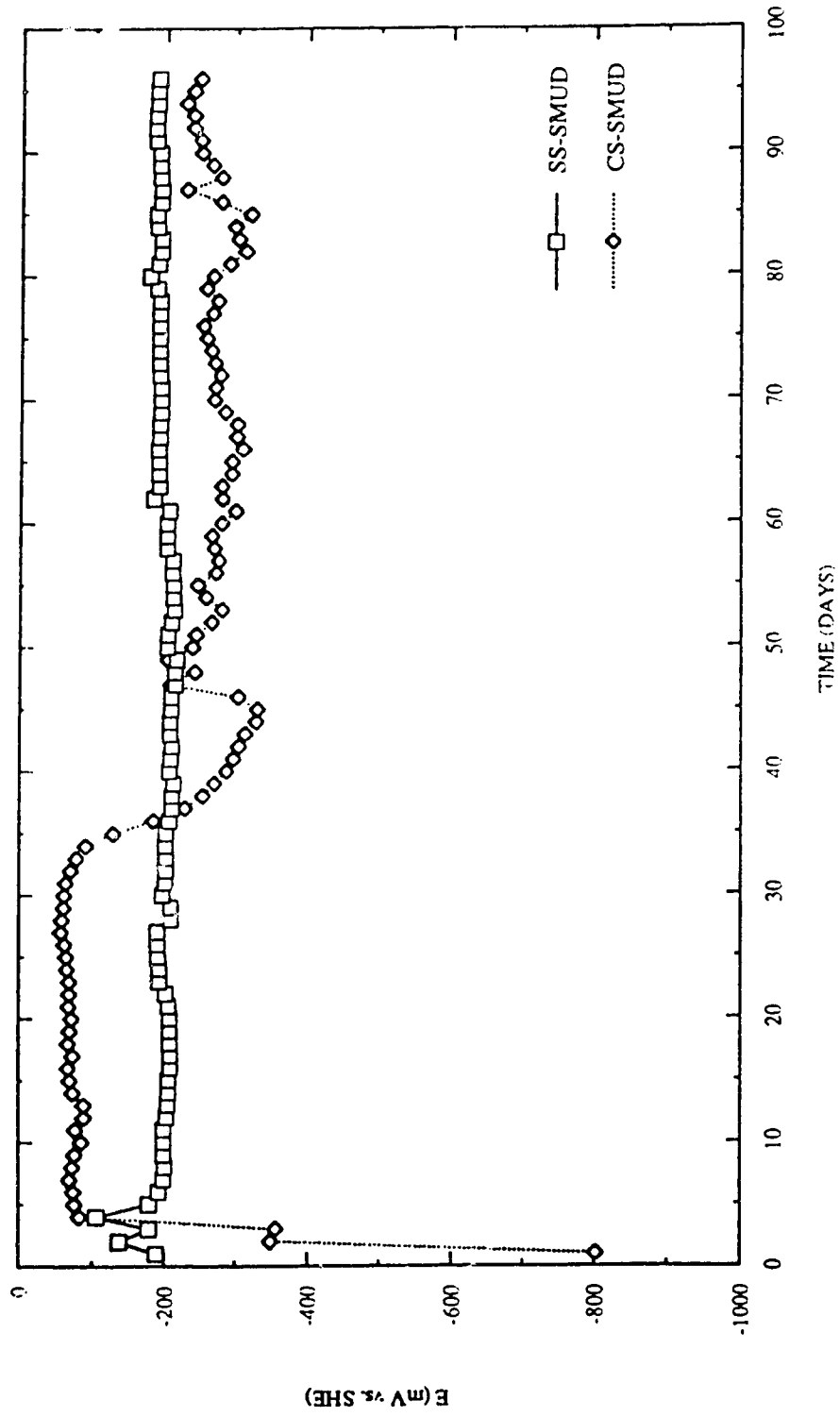shift; and (b) anodic shift.
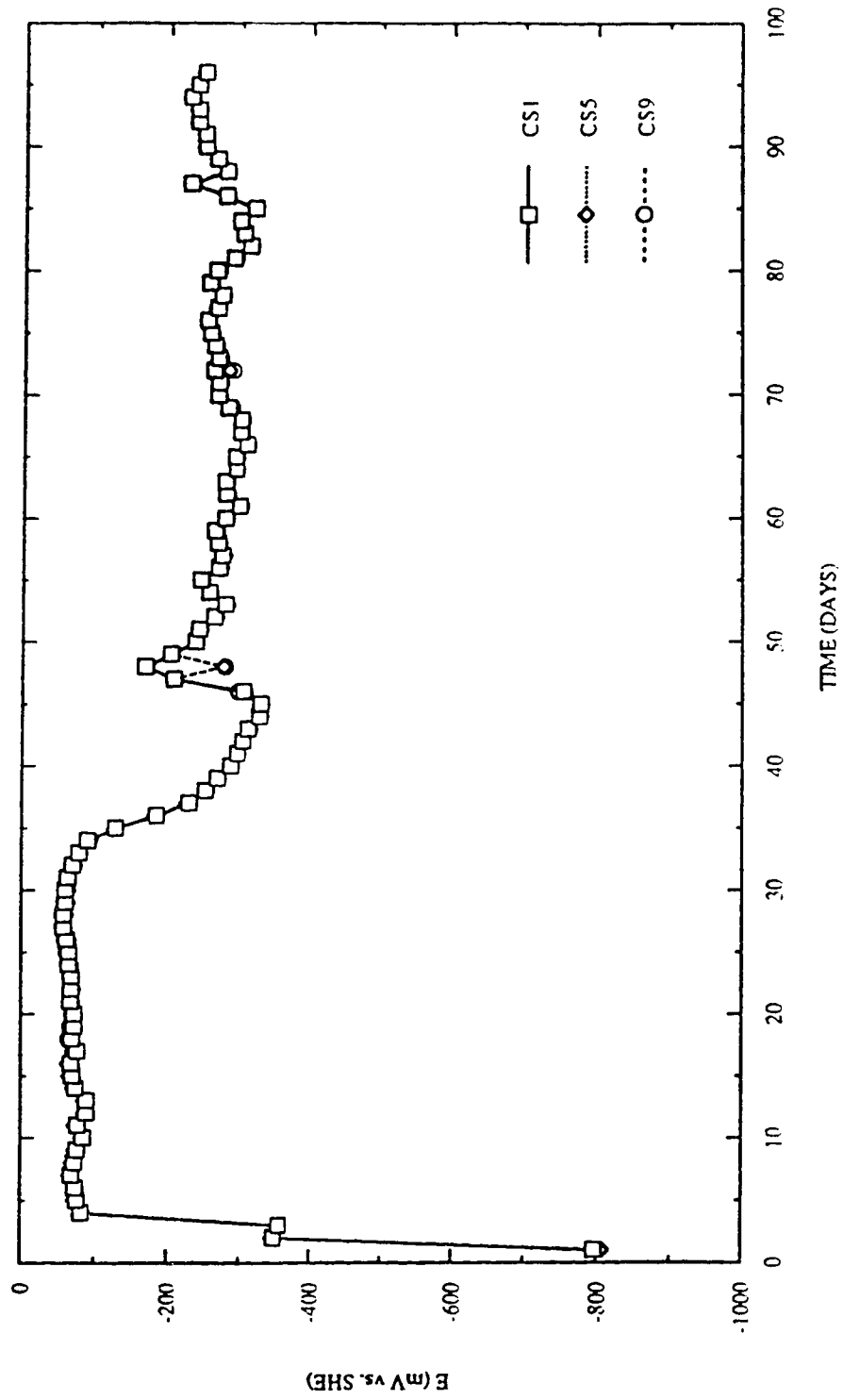
Figure 26. Corrosion potential vs. time for A513L carbon steel in medium containing mud sterilized by heat.
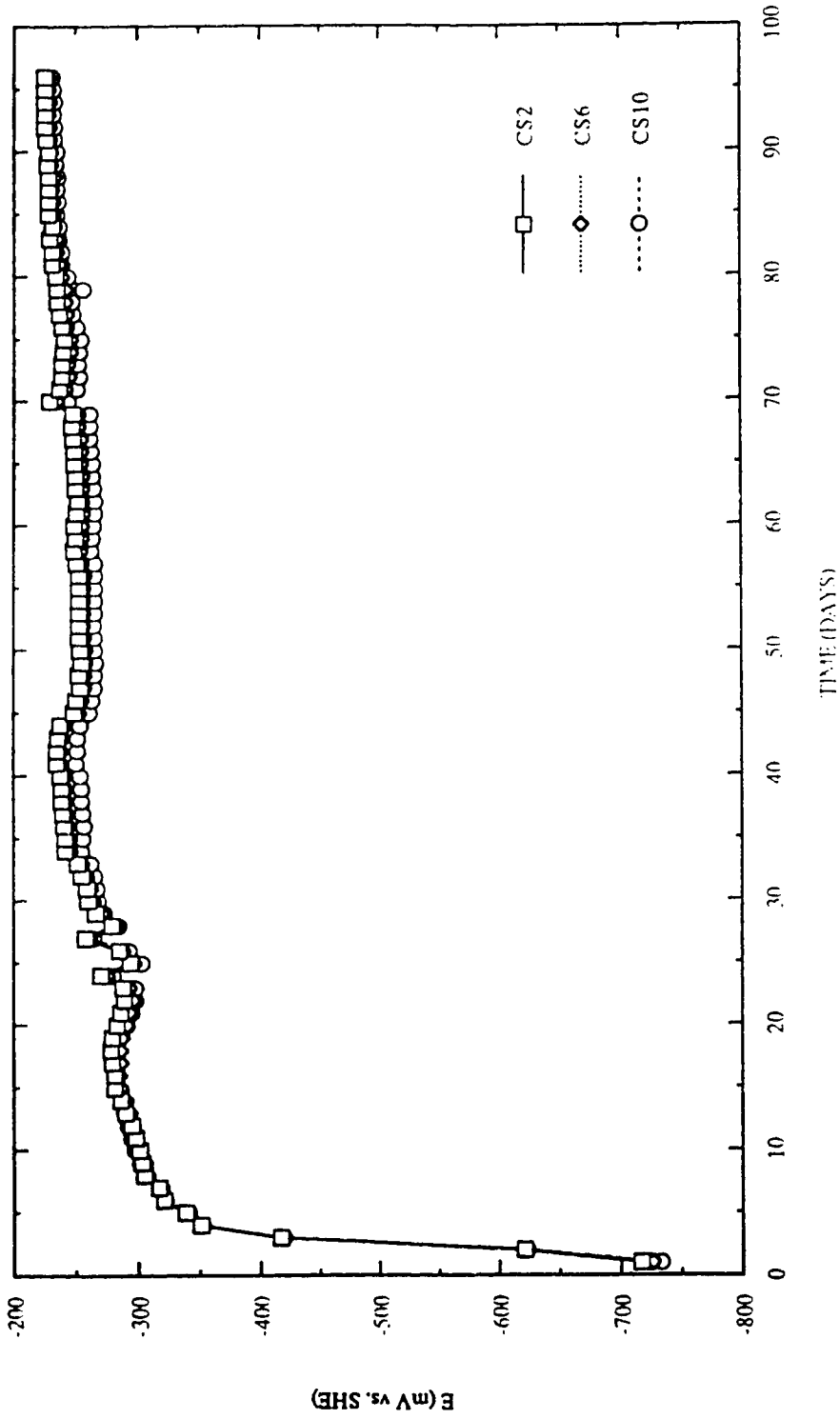
Figure 27. Corrosion potential vs. time for A513L carbon steel in medium containing mud.
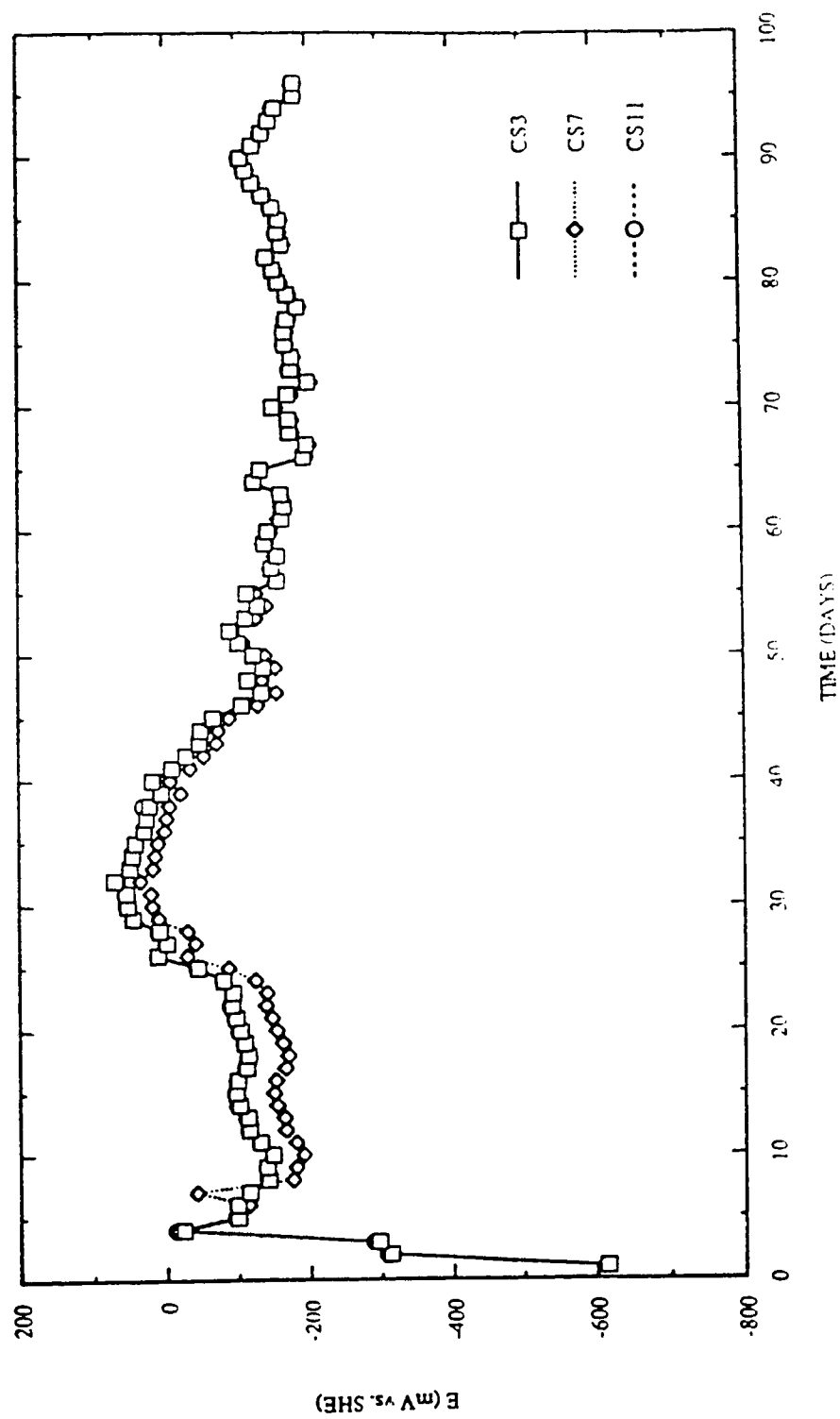
Figure 28. Corrosion potential vs. time for A513L carbon steel in sterile medium containing heat-killed *D. desulfuricans*.
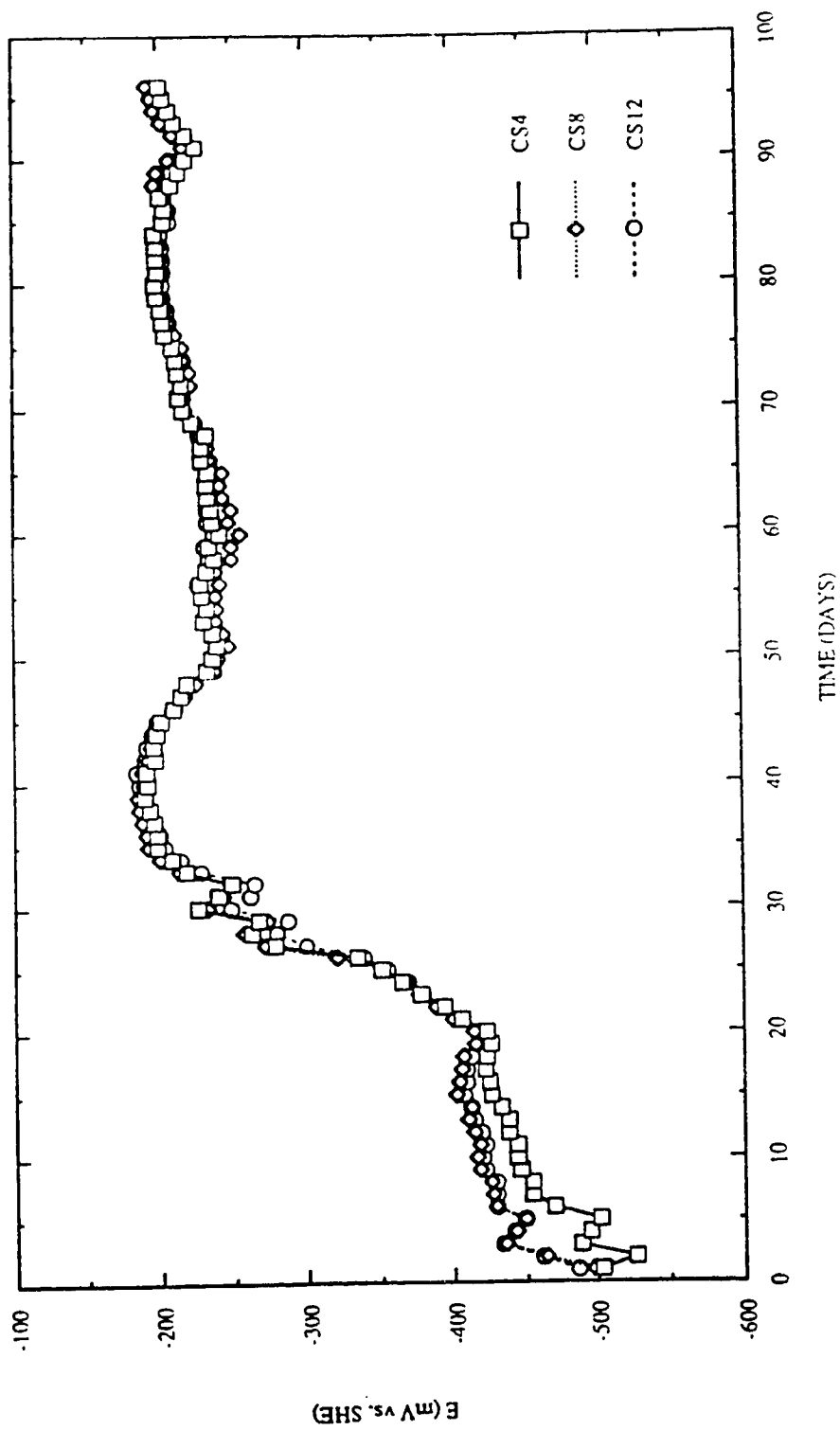
Figure 29. Corrosion potential vs. time for A513L carbon steel in medium containing viable *D. desulfuricans*.
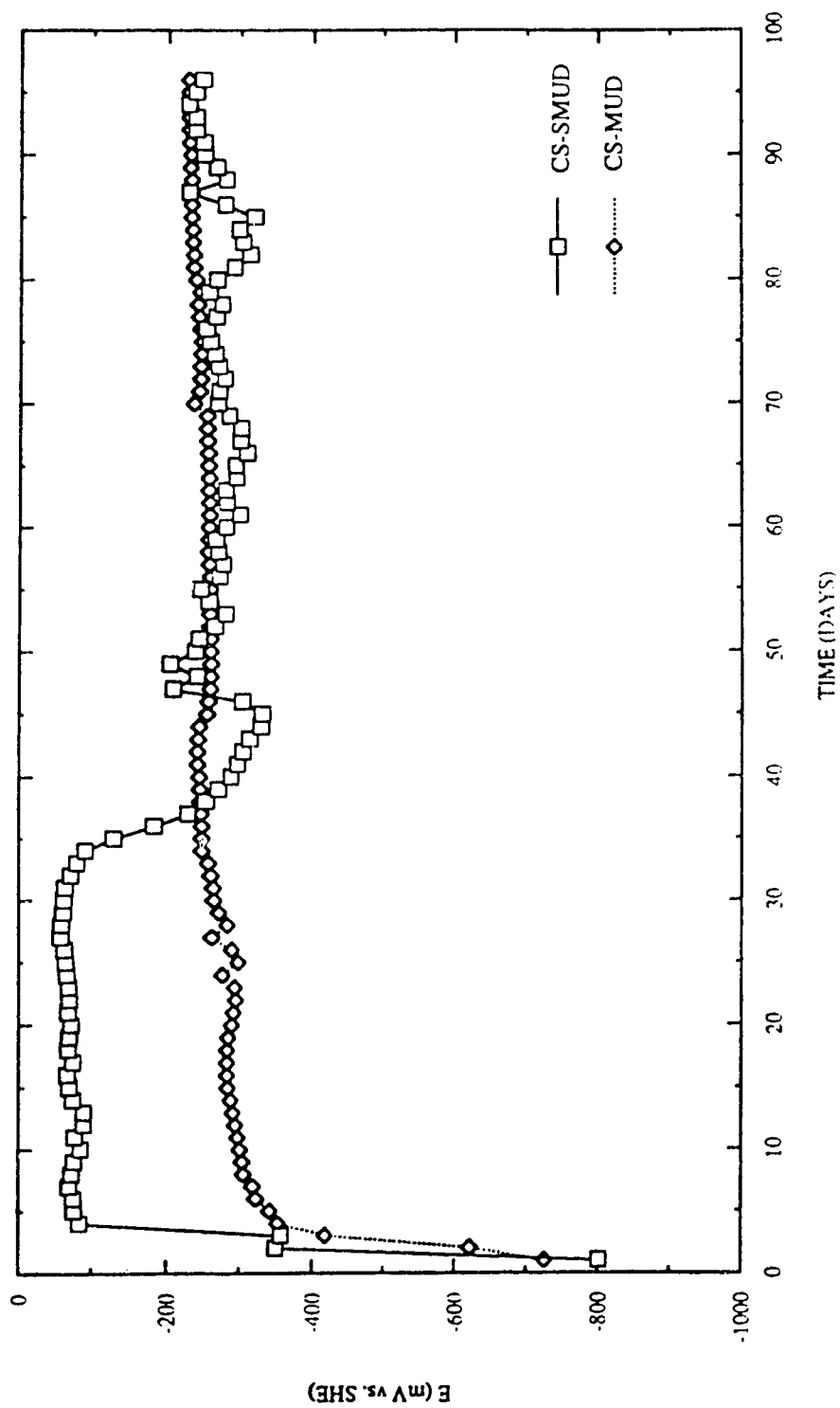
Figure 30. Corrosion potential vs. time for A513L carbon steel in medium containing mud sterilized by heat (CS-SMUD) and in medium containing mud (CS-MUD).
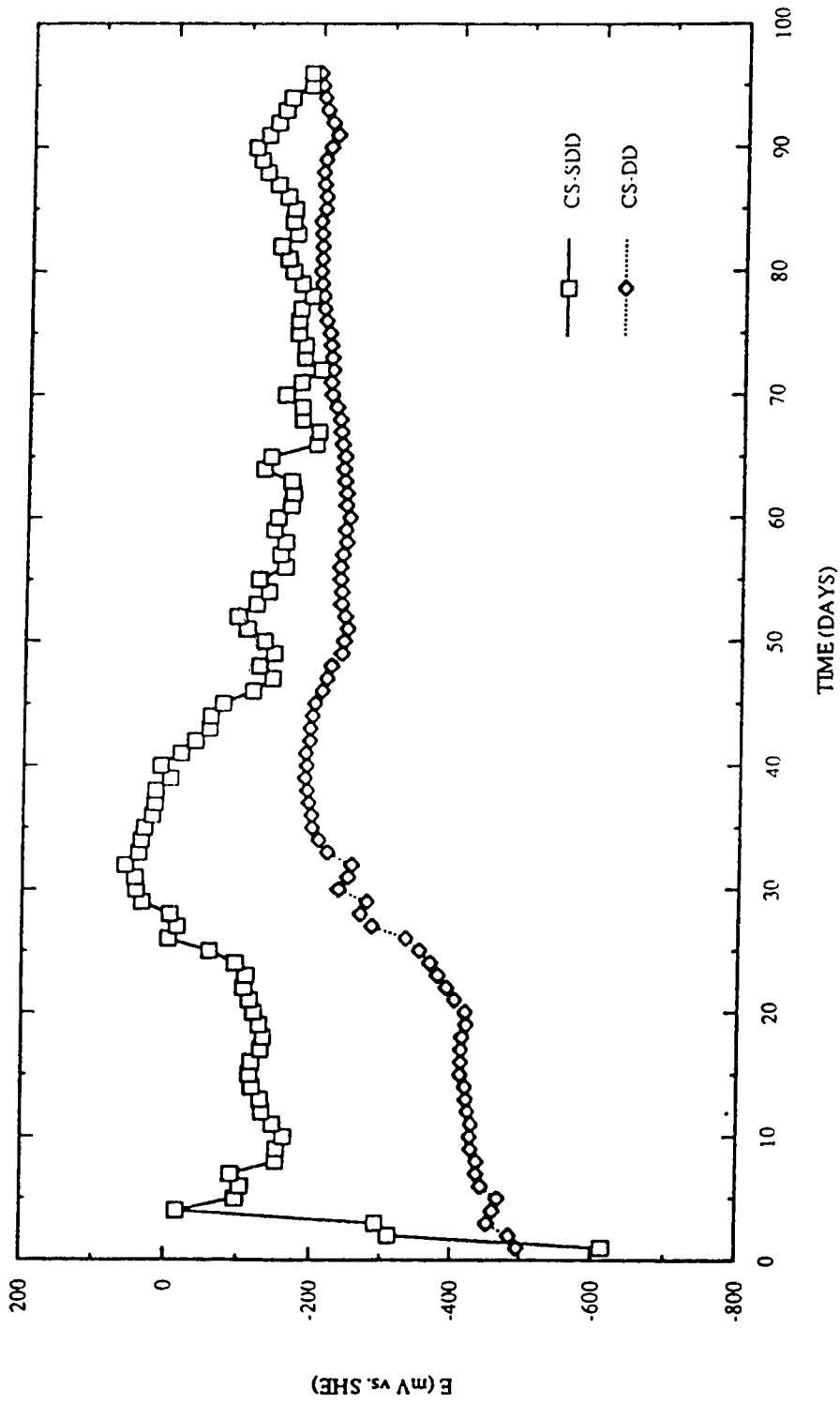
Figure 31. Corrosion potential vs. time for A513L carbon steel in sterile medium containing heat-killed *D. desulfuricans* (CS-SDD) and in medium containing viable *D. desulfuricans* (CS-DD).
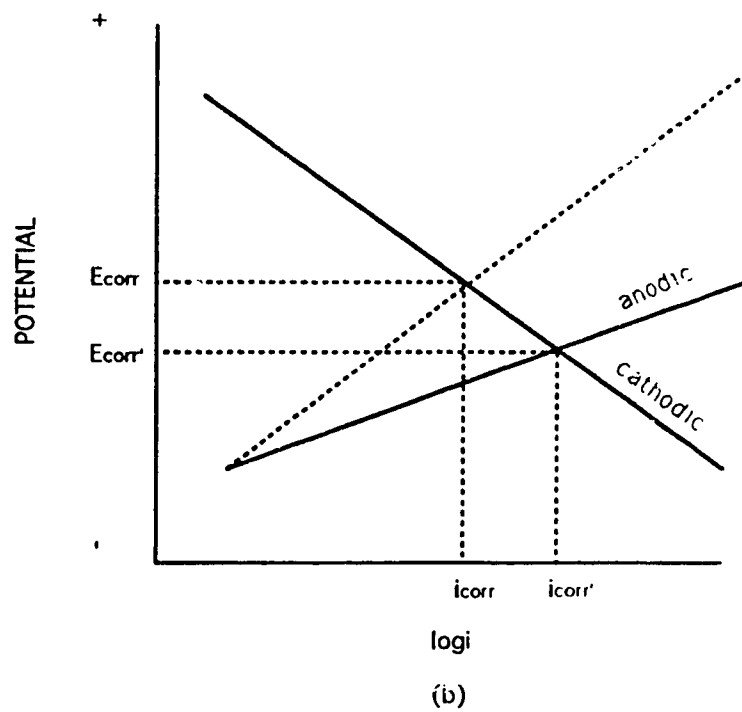
Figure 32. Increase of corrosion potential caused by (a) cathodic shift; and (b) anodic shift.

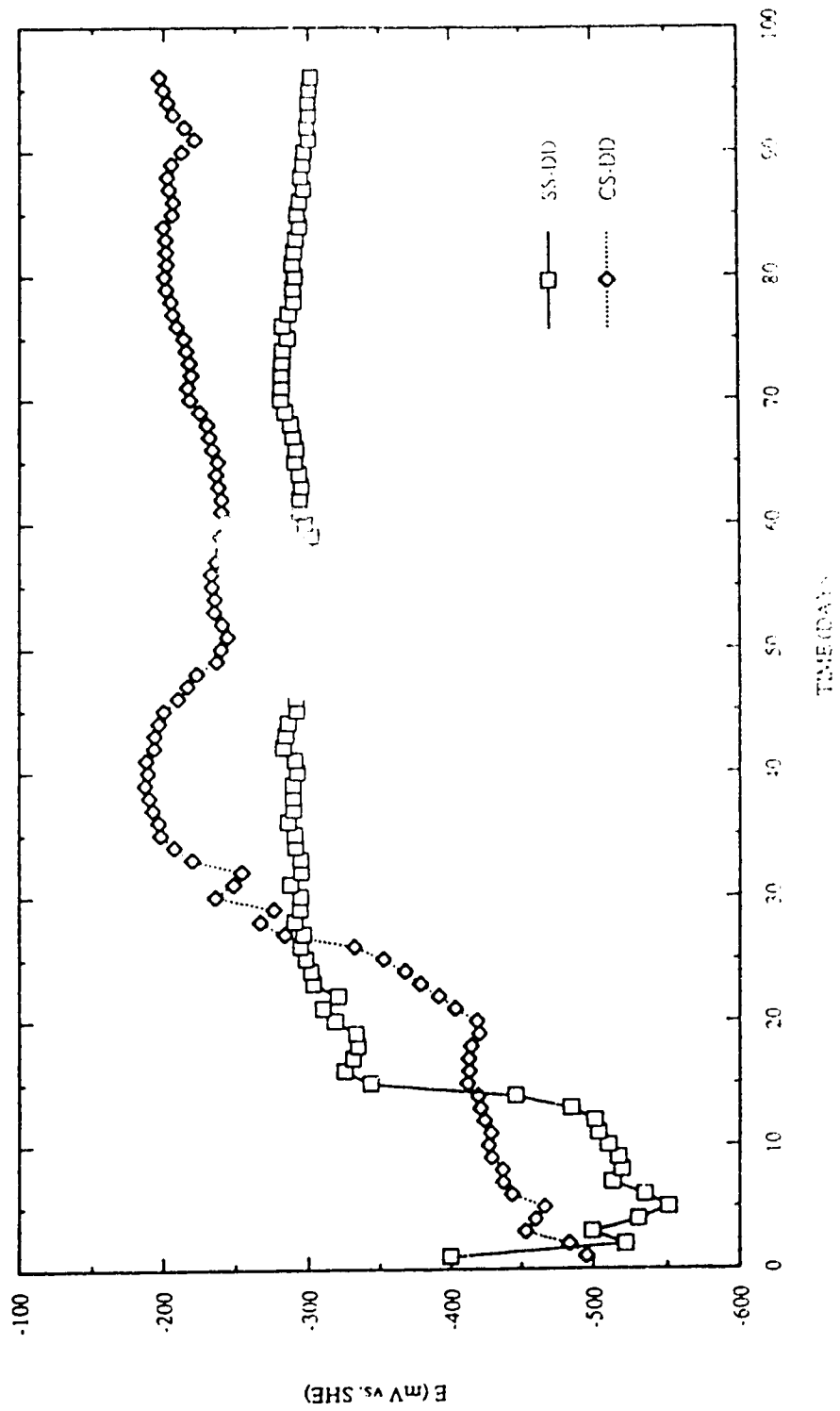Figure 33. Corrosion potential vs. time for type 304L stainless steel (SS-SMUD) and A513L carbon steel (CS-SMUD) in medium containing mud sterilized by heat.
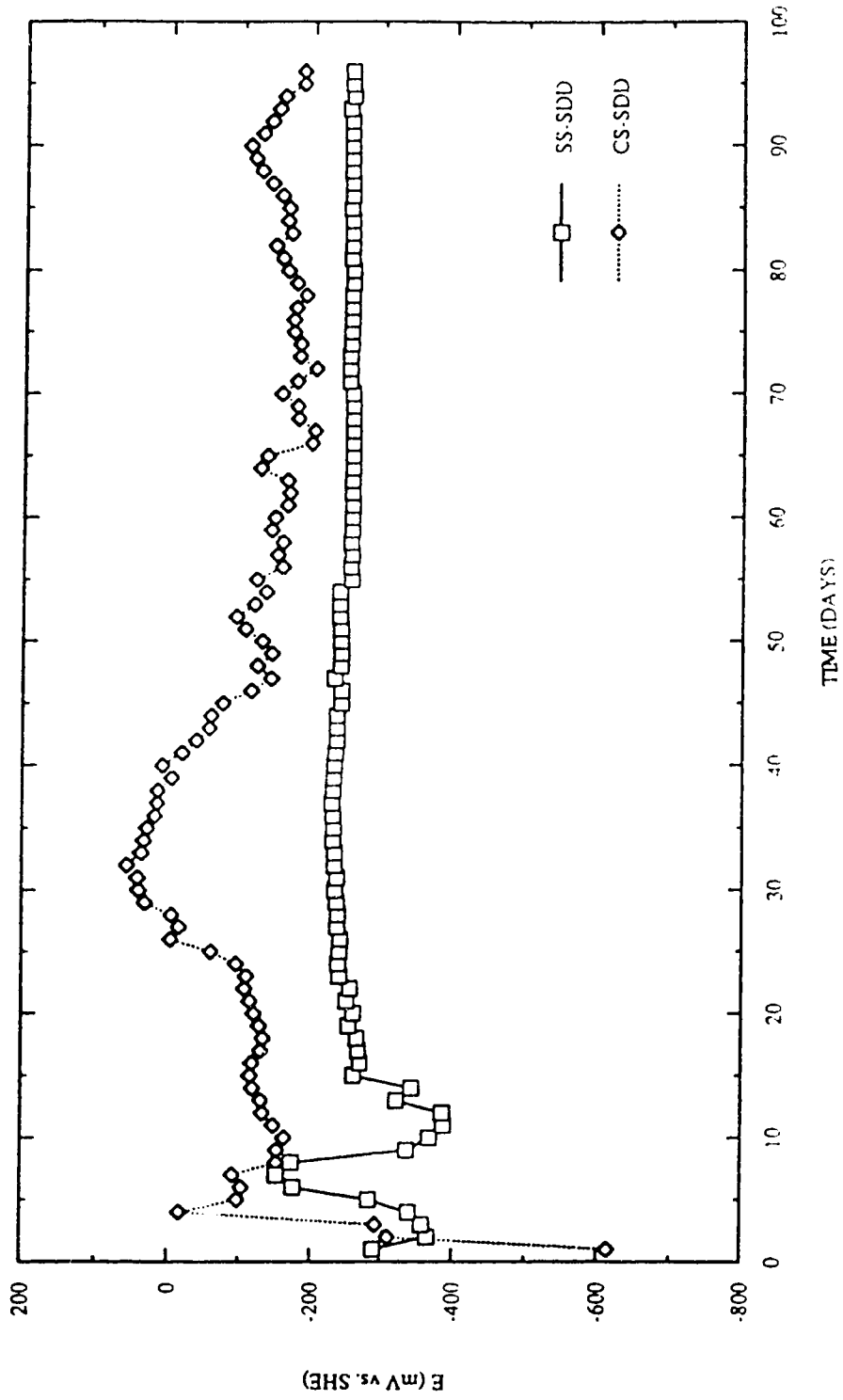
Figure 34. Corrosion potential vs. time for type 304L stainless steel (SS-SDD) and A513L carbon steel (CS-SDD) in sterile medium containing heat-killed *D. desulfuricans.*
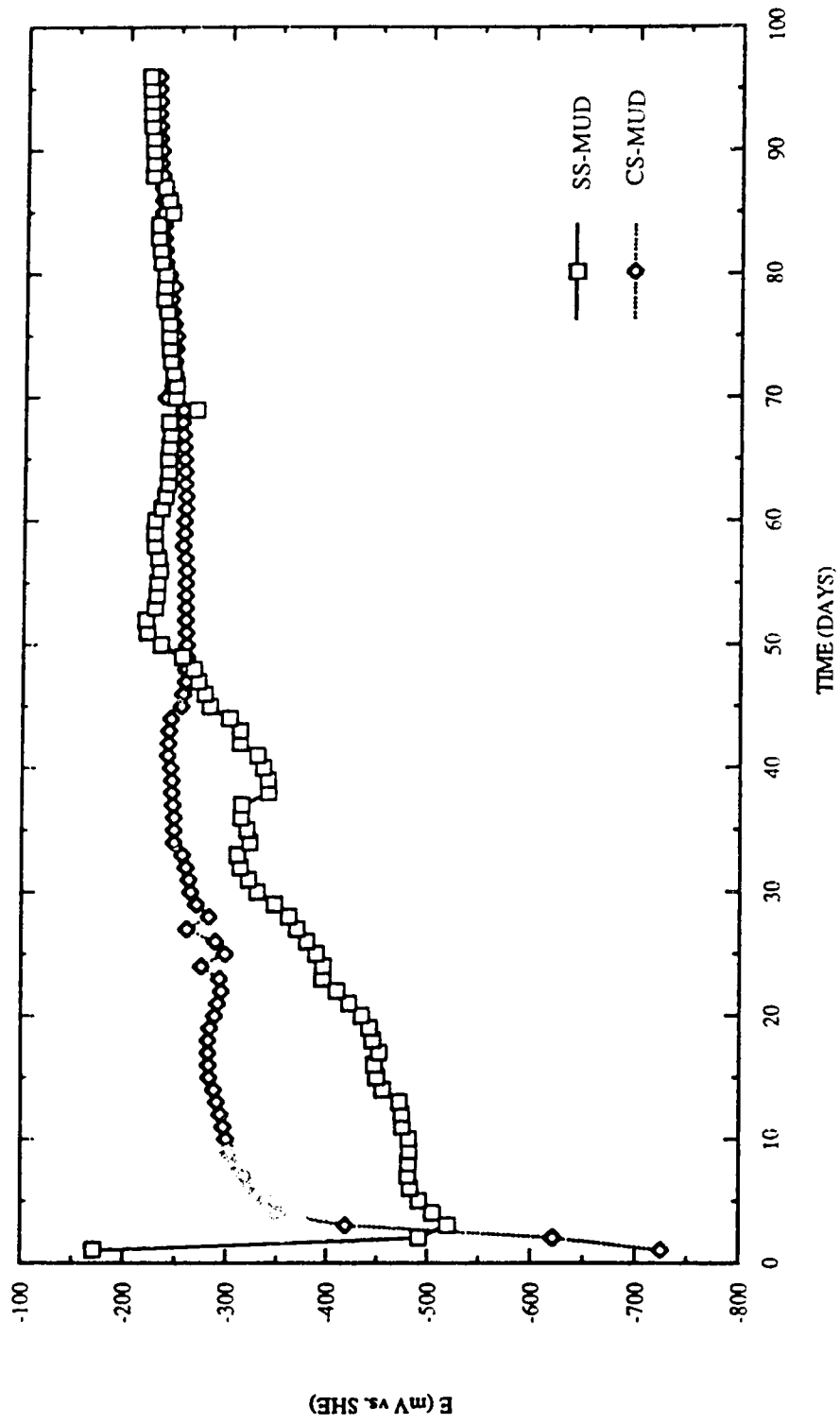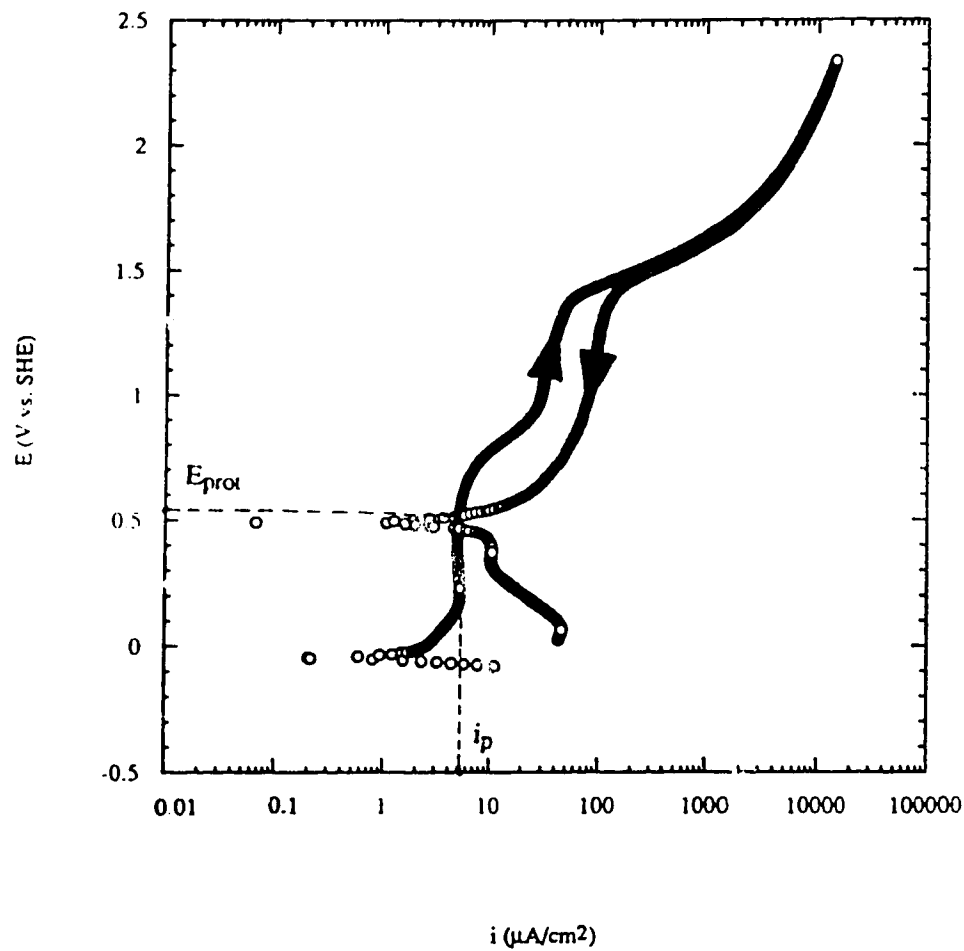
Figure 35. Corrosion potential vs. time for type 304L stainless steel (SS-MUD) and
A513L carbon steel (CS-MUD) in medium containing mud.

Figure 36. Corrosion potential vs. time for type 304L stainless steel (SS-DD) and A513L carbon steel (CS-DD) in medium containing viable *D. desulfuricans*.

Figure 37. Cyclic potentiodynamic polarization curves for type 304L stainless steel in medium containing mud sterilized by heat.
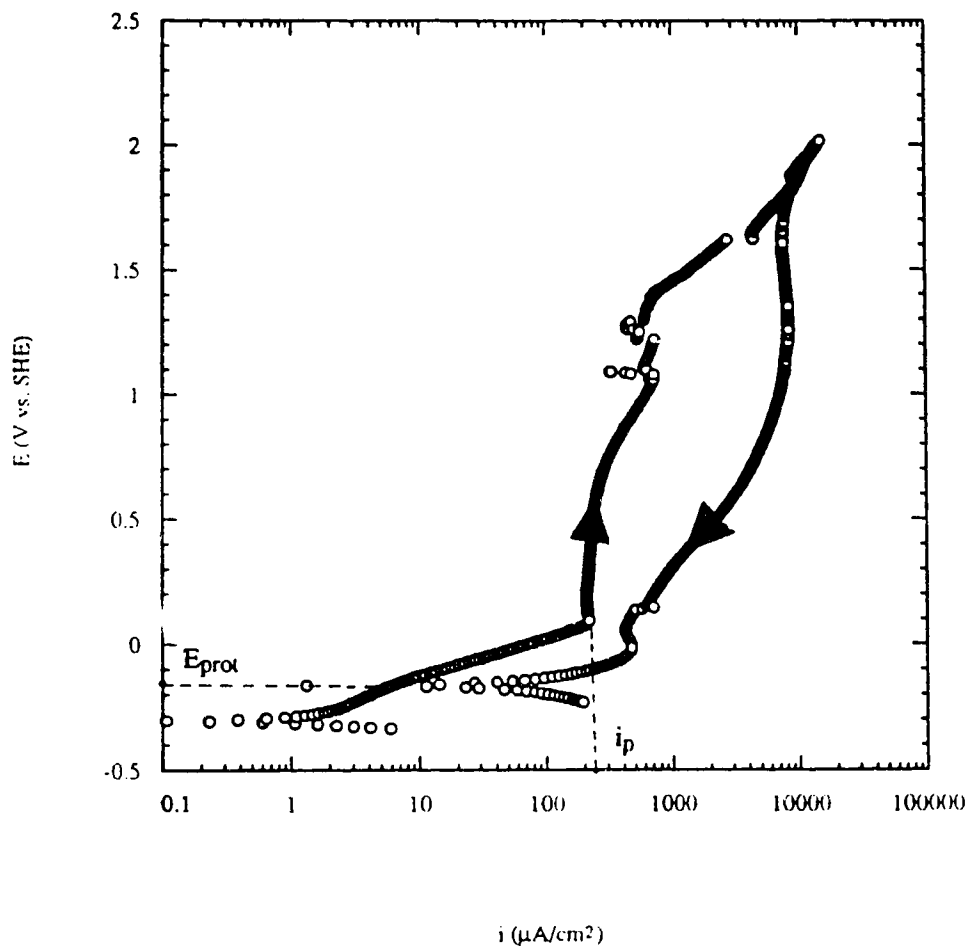
Figure 38. Cyclic potentiodynamic polarization curves for type 304L stainless steel in medium containing mud.
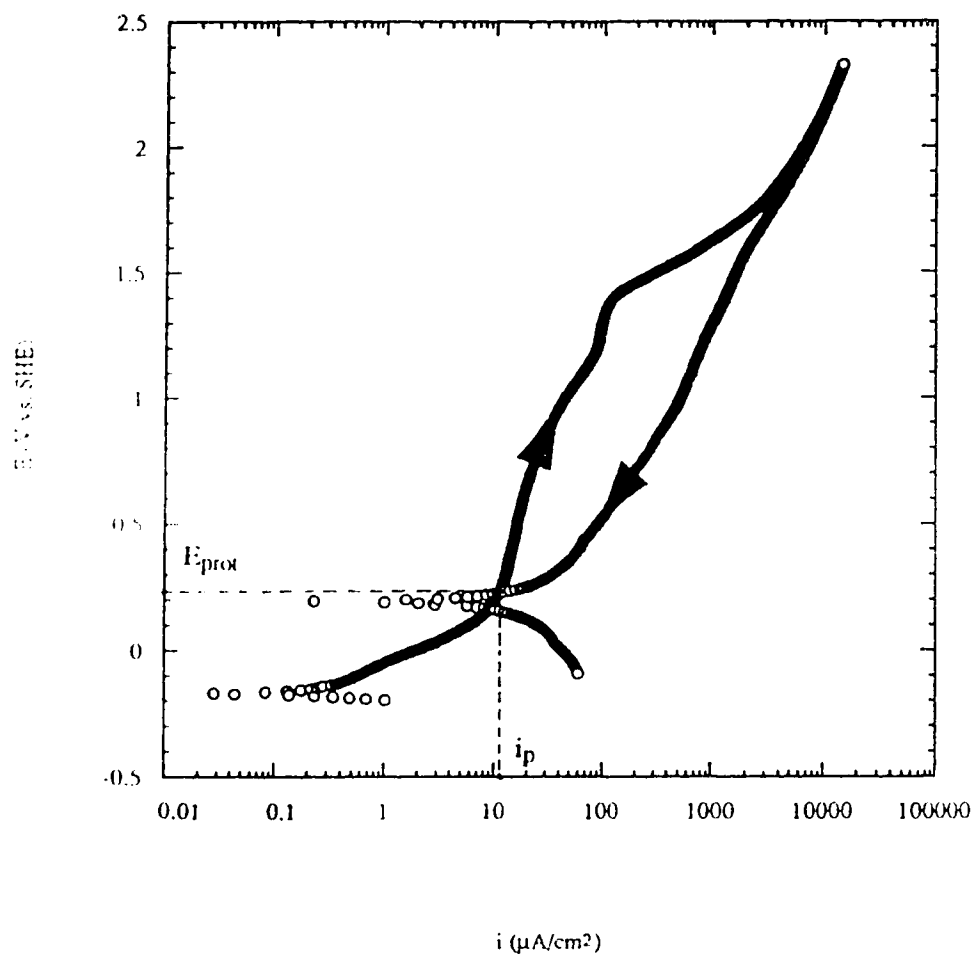
Figure 39. Cyclic potentiodynamic polarization curves for type 304L stainless steel in sterile medium containing heat-killed *D. desulfuricans*.
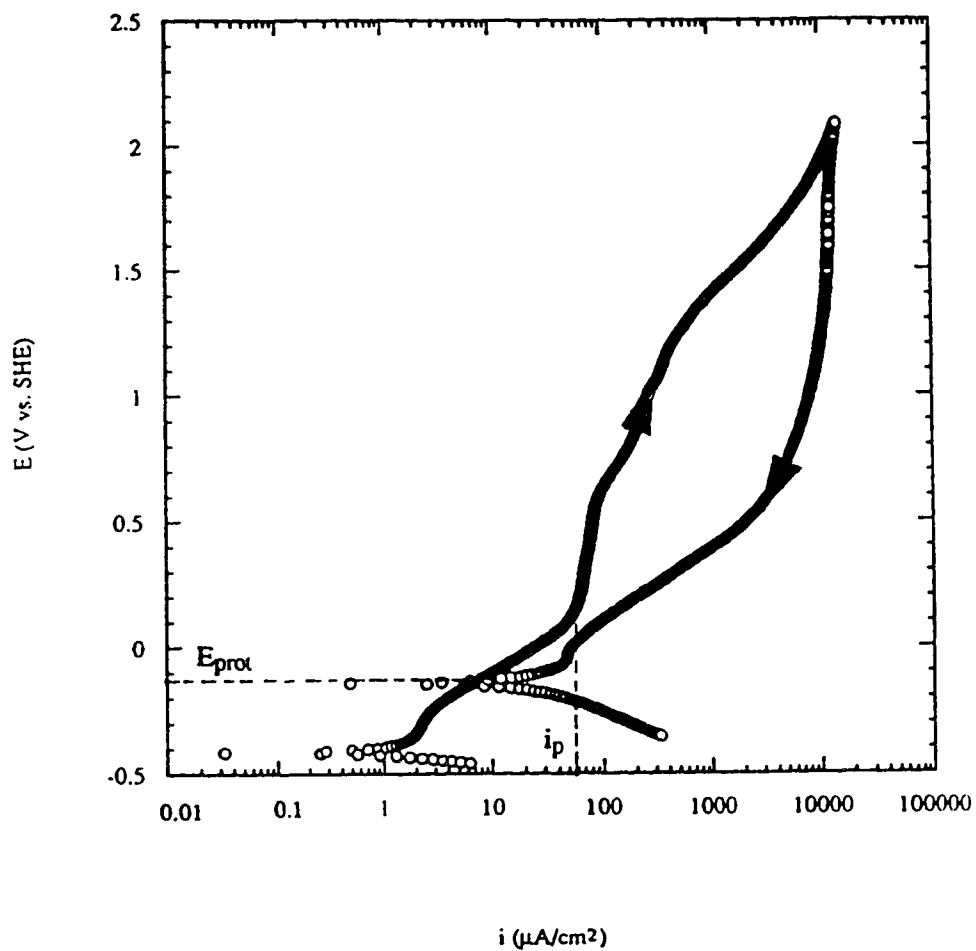
Figure 40. Cyclic potentiodynamic polarization curves for type 304L stainless steel in medium containing viable *D. desulfuricans.*
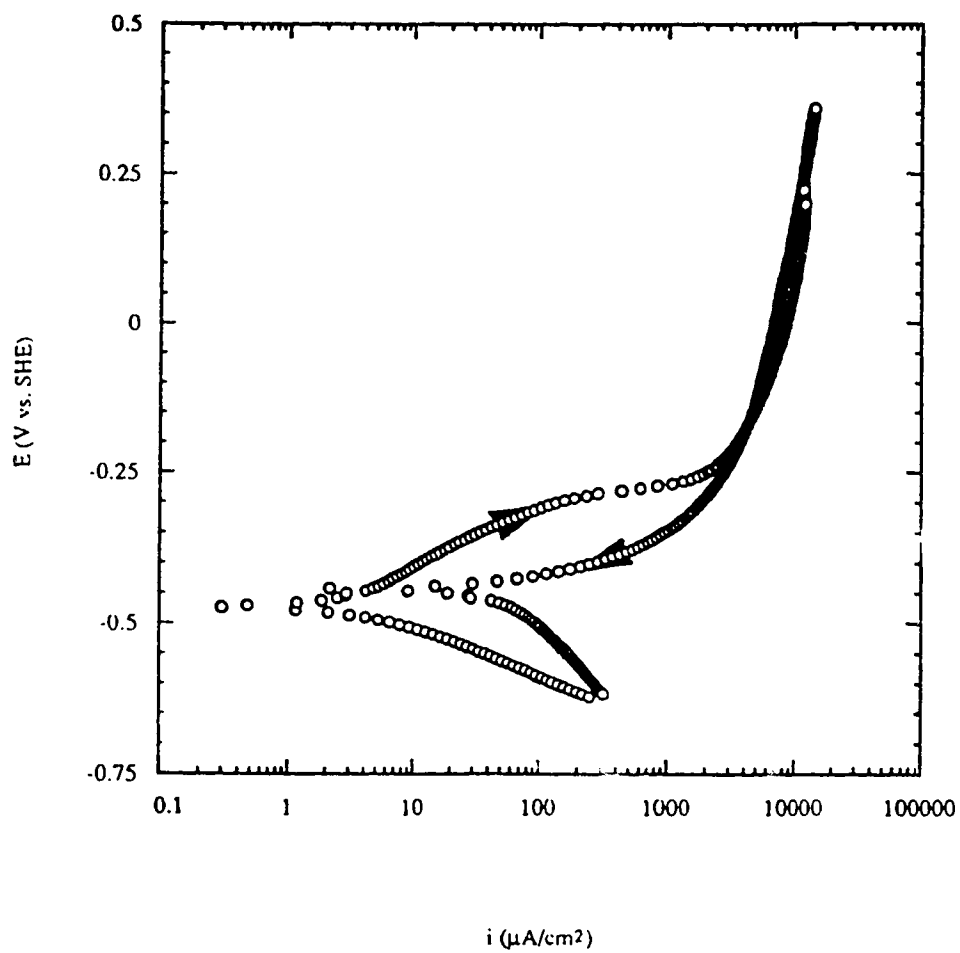
Figure 41. Cyclic potentiodynamic polarization curves for A513L carbon steel in medium containing mud sterilized by heat.
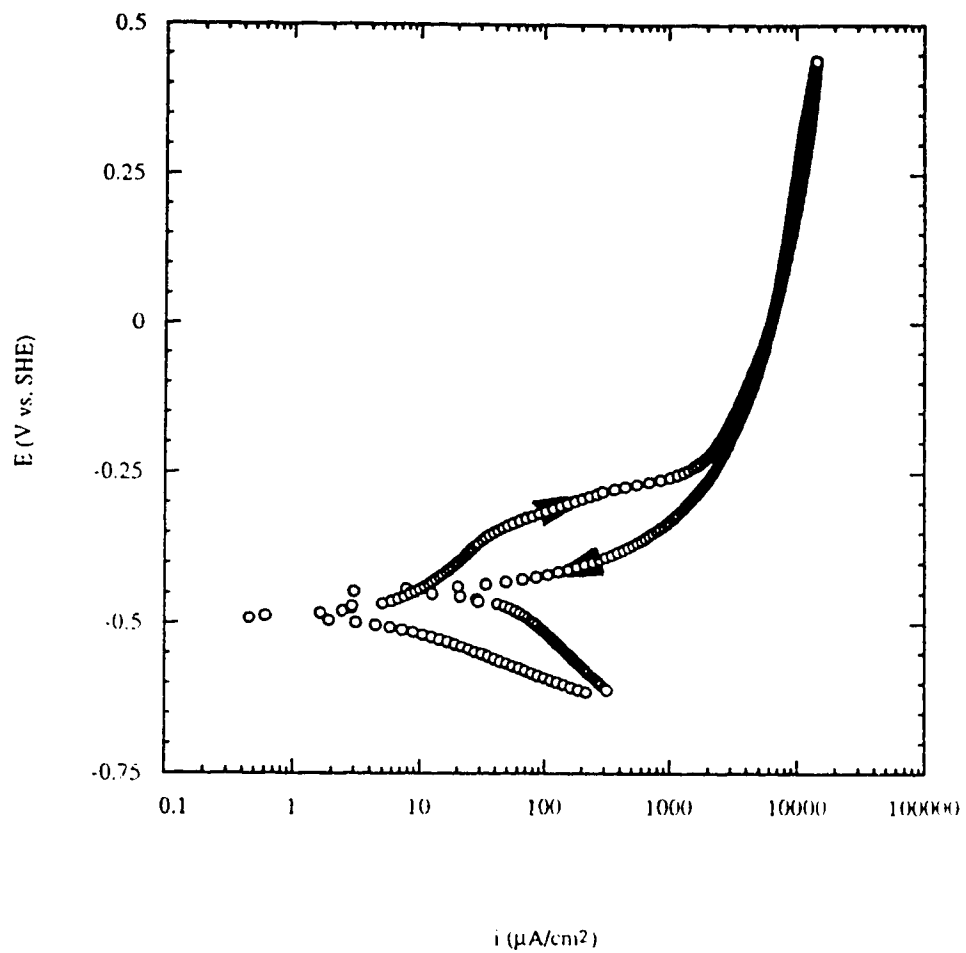
Figure 42. Cyclic potentiodynamic polarization curves for A513L carbon steel in medium containing mud.
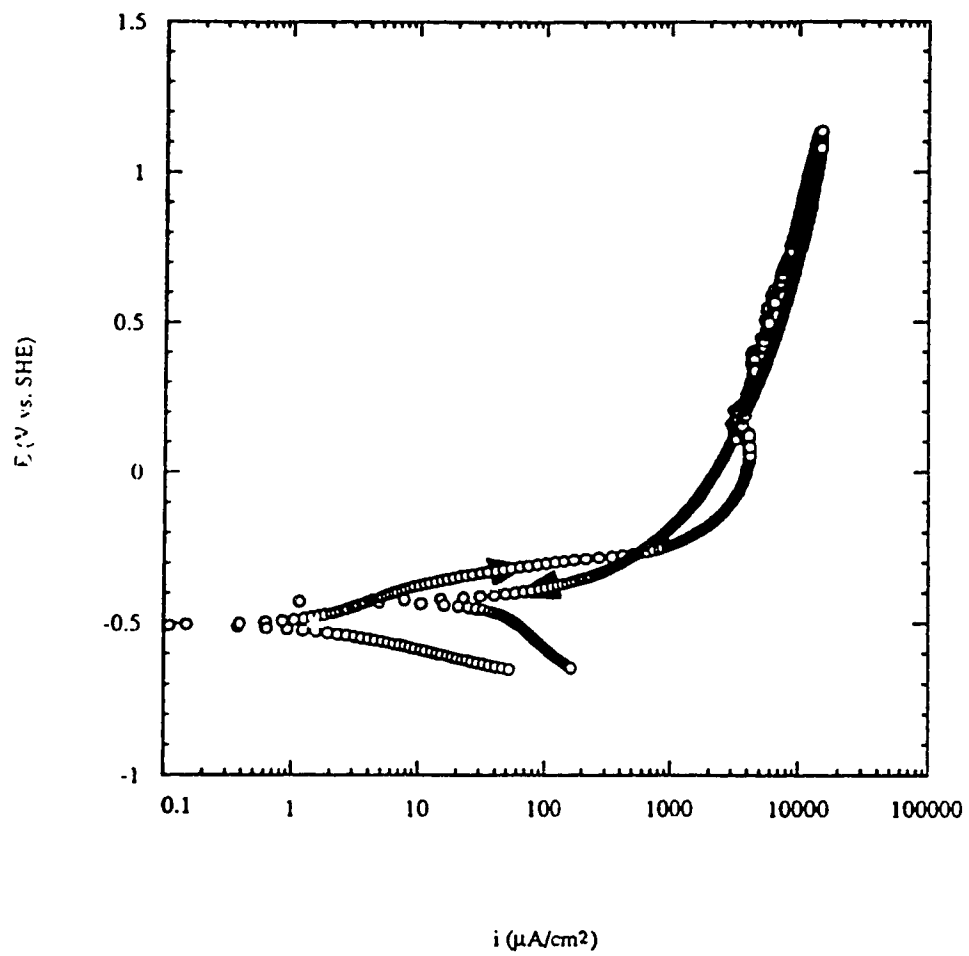
Figure 43. Cyclic potentiodynamic polarization curves for A513L carbon steel in sterile medium containing heat-killed *D. desulfuricans*.
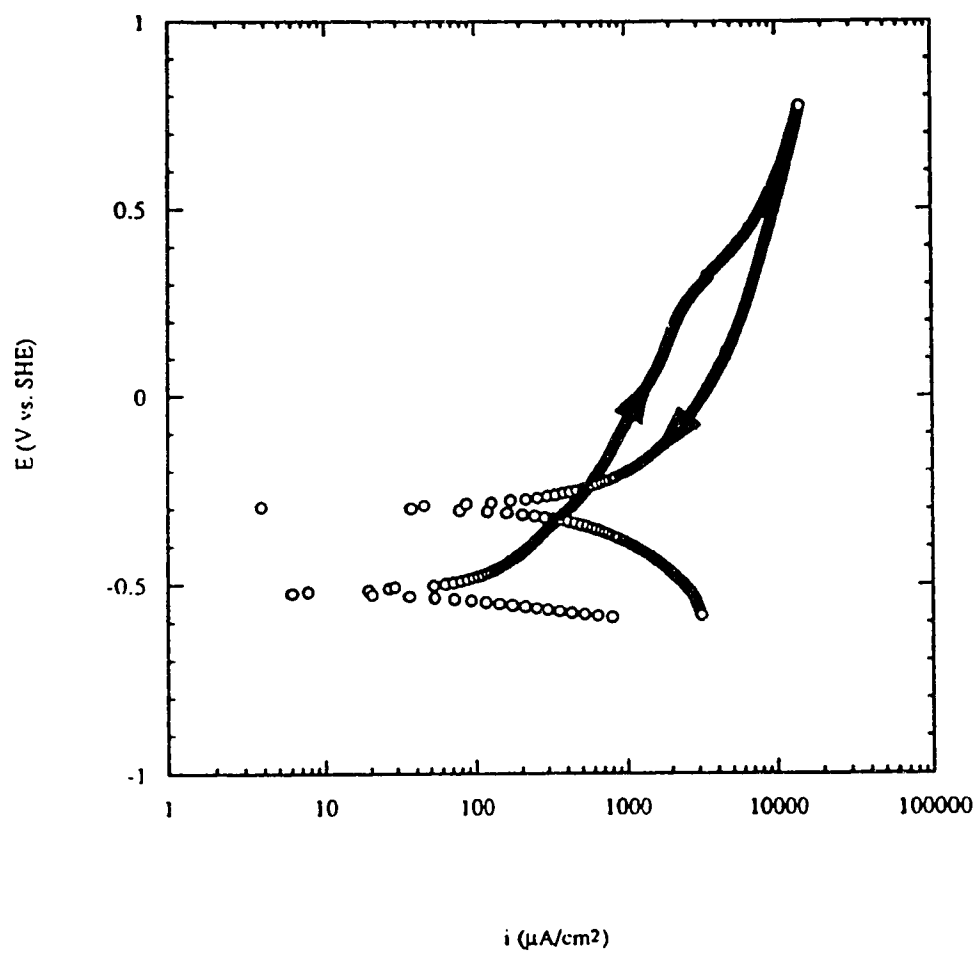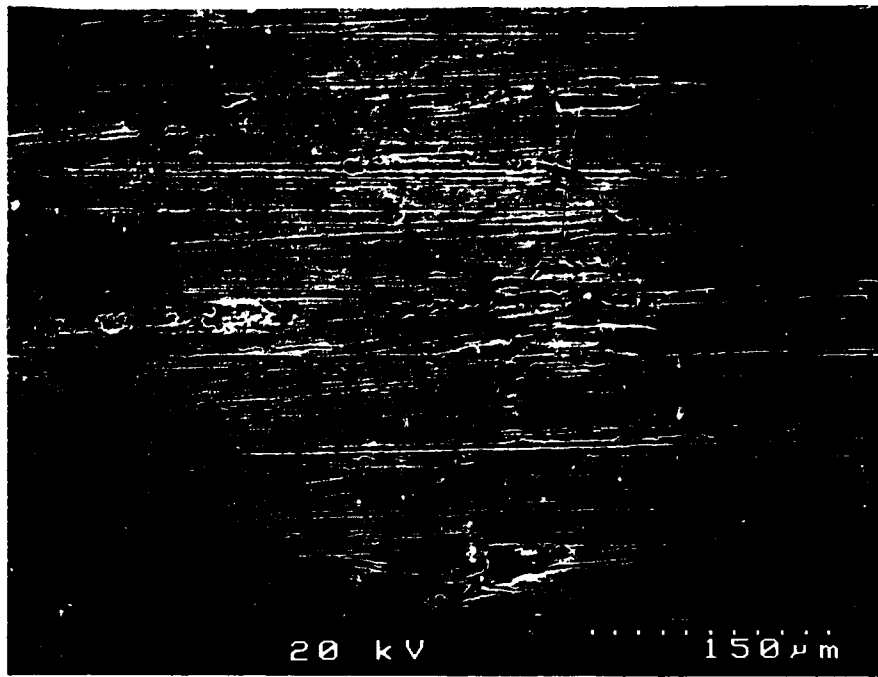
Figure 44. Cyclic potentiodynamic polarization curves for A513L carbon steel in medium containing viable *D. desulfuricans.*

(a)
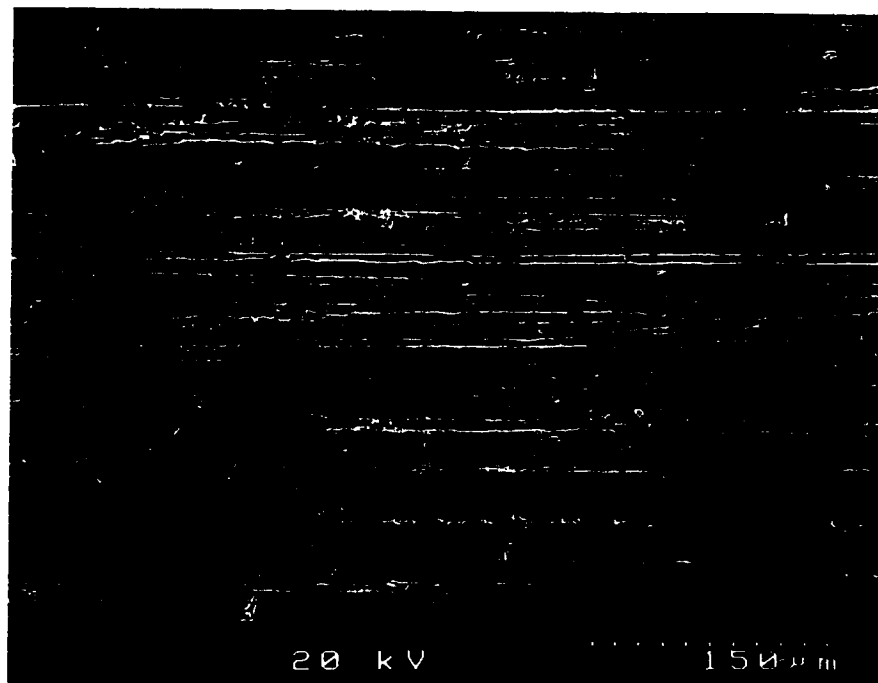
(b)

(c)

Figure 45. SEM micrographs for the carbon steel specimens after immersion test in a solution for corrosion product cleaning for (a) 0 minute (x200); (b) 10 minutes (x200); and (c) 120 minutes (x200).
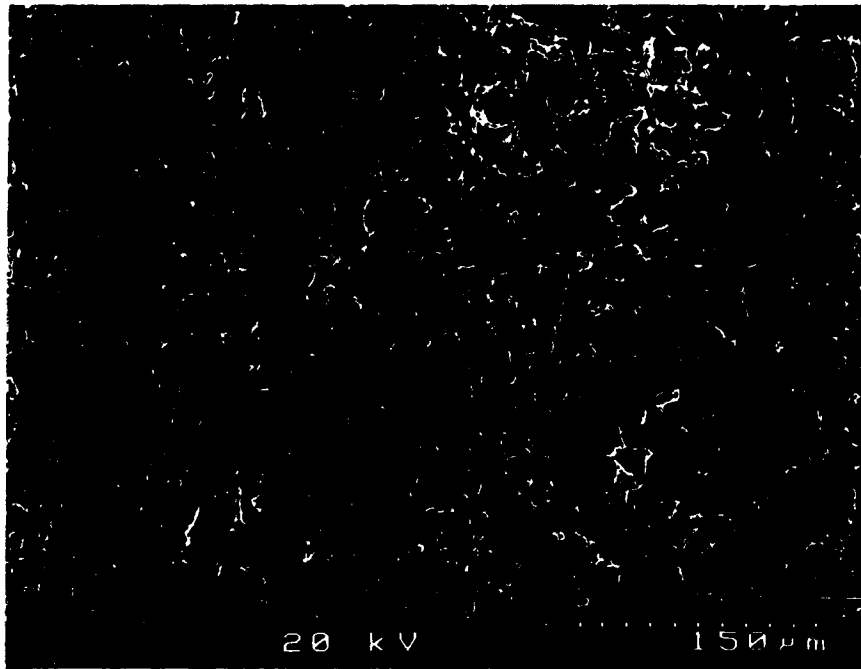
(a)
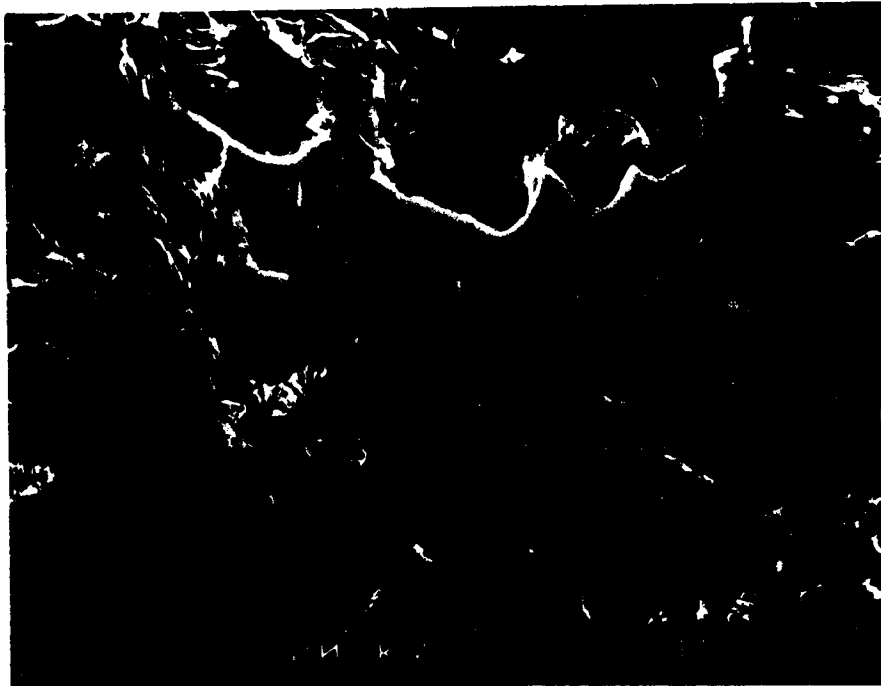
(b)

Figure 46. SEM micrographs for the carbon steel specimen after the immersion test in the medium containing mud sterilized by heat: (a) x200; and (b) x2000.

(a)

(b)

Figure 47. SEM micrographs for the carbon steel specimen after the immersion test in the medium containing mud: (a) x200; and (b) x2000.

(a)

(b)

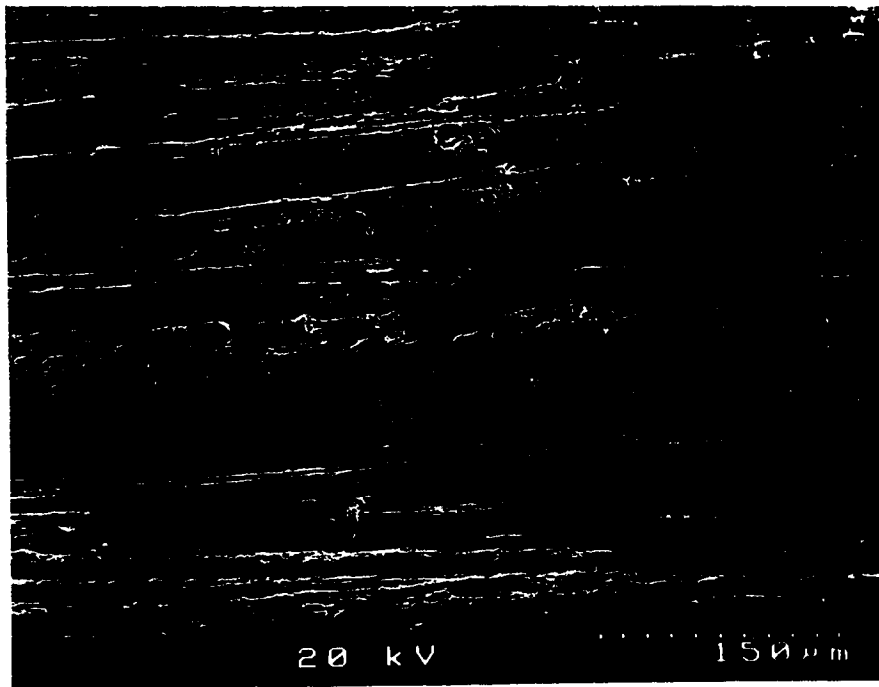Figure 48. SEM micrographs for the carbon steel specimen after the immersion test in the sterile medium containing heat-killed *D. desulfuricans:* (a) x200; and (b) x2000.
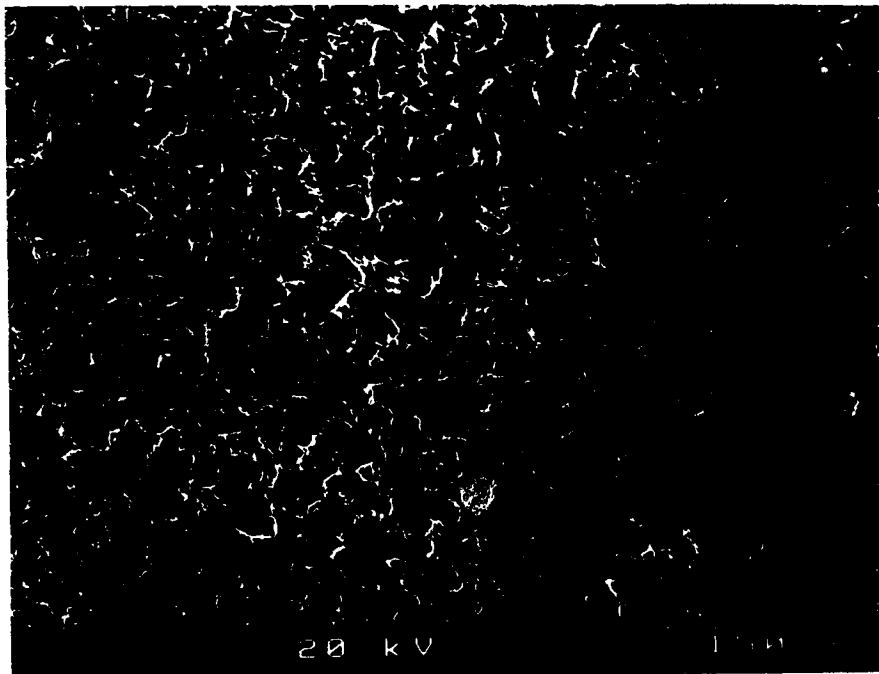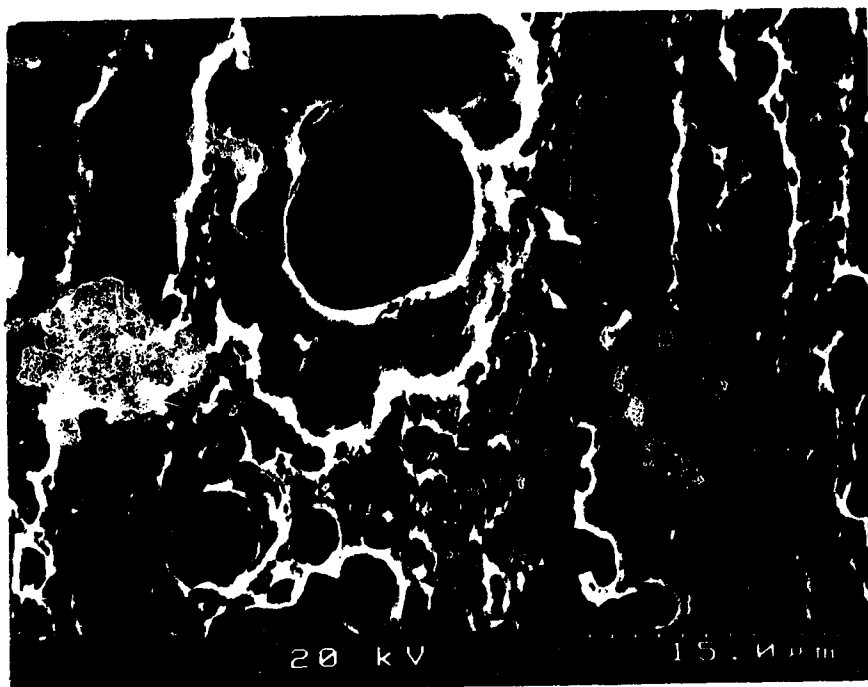
(a)

(b)

Figure 49. SEM micrographs for the carbon steel specimen after the immersion test in the medium containing viable *D. desulfuricans:* (a) x200; and (b) x2000.
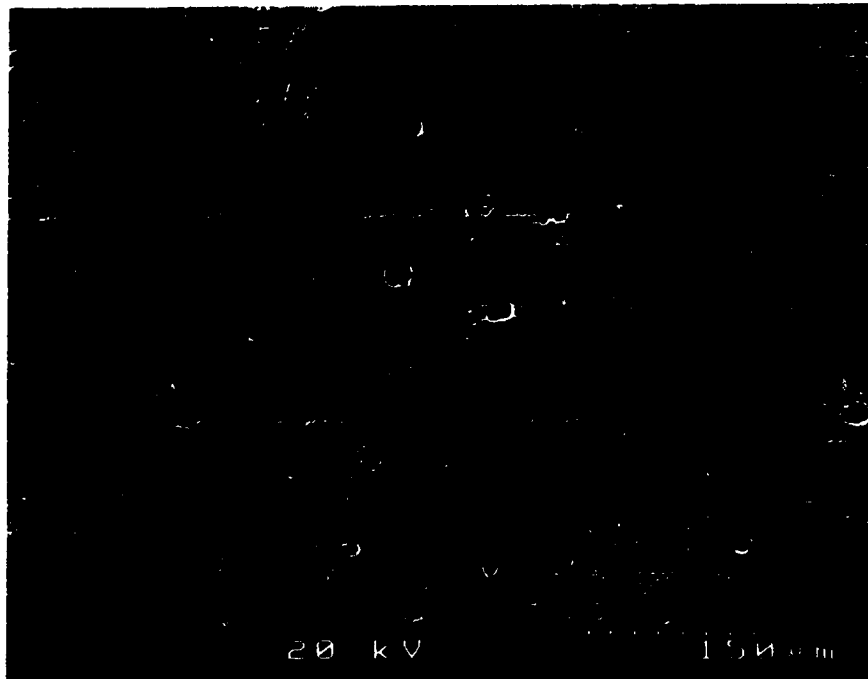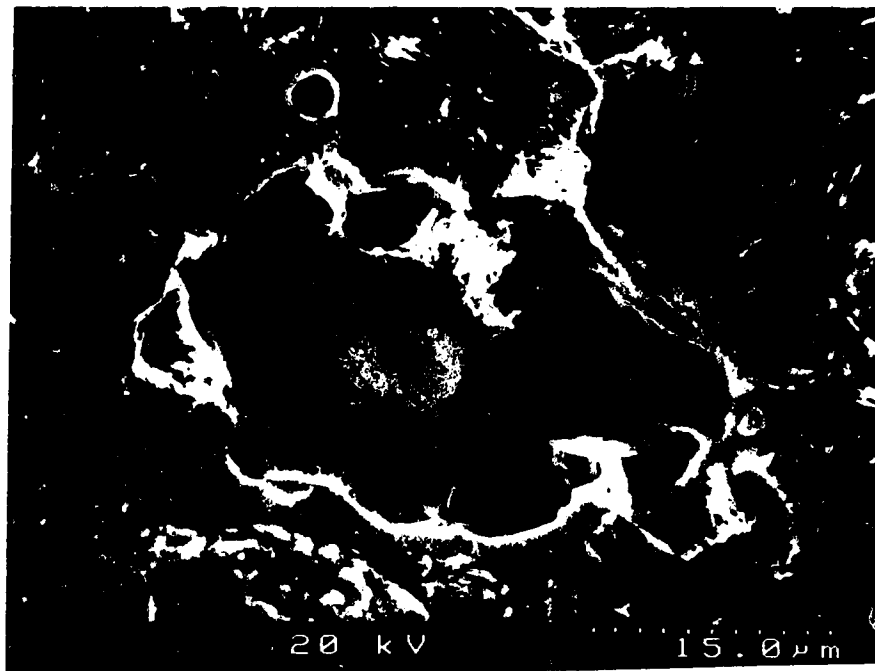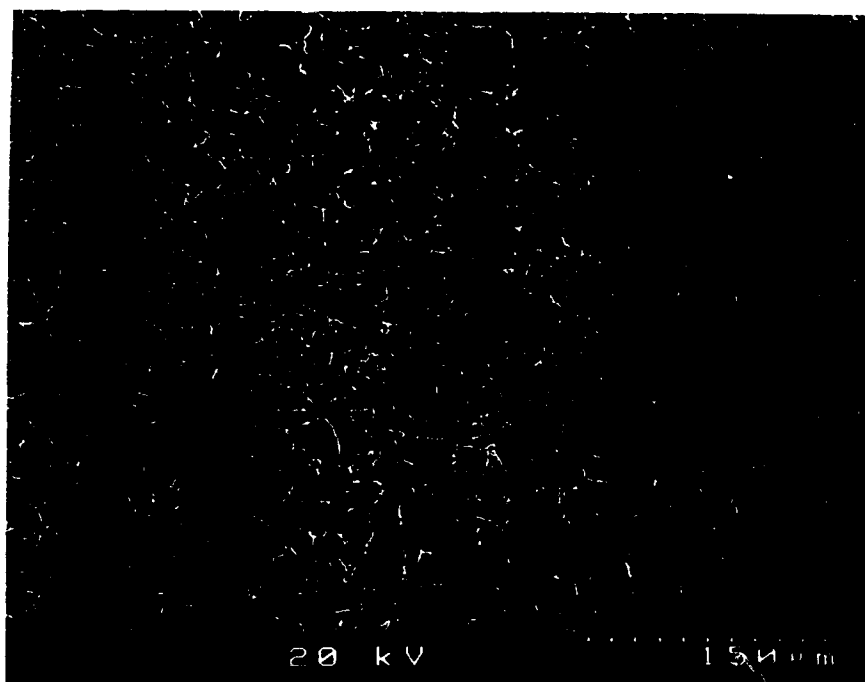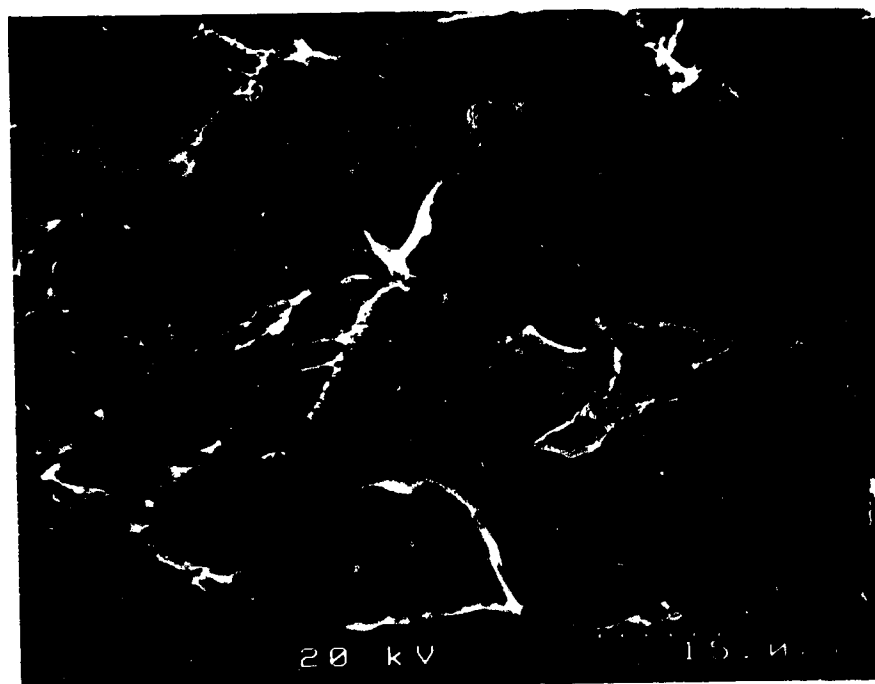
References

Arnold, R.G., Hoffmann, M.R., Christina, T.J. and Ricardal, F.W., "Regulation of Dissimilatory Fe (III) Reduction Activity in *Shewanella putrefaciens*", Applied Environmental Microbiology, 56(1990): p2811.

Azhogin, F.F., "Stress-Corrosion Cracking of High Strength Steels", in 3rd International Congress on Metallic Corrosion, Moscow, Vol II, MIR, p140, 1966.

Borenstein, S.W., "Microbiologically Influenced Corrosion Failures of Austenitic Stainless Steel Welds", Materials Performance, 27(1988): p62.

Borenstein, S.W., "Microbiologically Influenced Corrosion of Austenitic Stainless Steel Weldments", Materials Performance, 30(1991): p52.

Bos, P. and Kuenen, J.G., "Microbiology of Sulphur-Oxidizing Bacteria", in Microbial Corrosion, The Metals Society, London, p18, 1983.

Campbell, J.E., "Effects of Hydrogen Gas on Metals at Ambient Temperature", DMIC Report S-31, 1970.

Characklis, W.G., "Process Analysis in Microbial Systems: Biofilms as a Case Study", in Mathematics in Microbiology, edited by M. Bazin, Academic Press, London, p171, 1983.

Ciaraldi, S.W., "Stress-Corrosion Cracking of Carbon and Low-Alloy Steels", in Stress-Corrosion Cracking, Edited by R.H. Jones, ASM International, p41, 1992.

Cloete, T.E. and Brözel, V.S., "Practical Aspects of Biofouling Control in Industrial Water Systems", International Biodeterioration and Biodegradation, 29(1992): p299.

Cooper, G.L., "Proper Electrical Resistance Corrosion Probe Span", in Electrochemical Techniques for Corrosion Engineering, edited by R. Baboian, NACE, Houston, p327, 1986.

de Mele, M.F.L., Moreno, D.A., Ibars, J.R. and Videla, H.A., "Effect of Inorganic and Biogenic Sulfide on Localized Corrosion of Heat-Treated Type 304 Stainless Steel", Corrosion, 47(1991): p24.

Danilatos, G.D., "Review and Outline of Environmental SEM ~* Present", Journal of Microscopy, 162(1991): p391.

Delanty, B. and O'Beirne, J., "Major Field Study Compares Pipeline SCC with Coatings", Oil and Gas Journal, 90(1992): p39.

Devorecek, L.M., "Sulfide Stress Corrosion Cracking of Steels", Corrosion, 26(1970): p177.

Dexter, S.C., "Appendix: Biological Effects", in ASM Handbook, vol.13, ASM International, p41, 1992.

Dexter, S.C., Duquette, D.J., Siebert, O.W. and Videla, H.A., "Use and Limitations of Electrochemical Techniques for Investigating Microbiological Corrosion", Corrosion, 47(1991): p308.

Dexter, S.C. and Gao, G.Y., "Effect of Seawater Biofilms on Corrosion Potential and Oxygen Reduction of Stainless Steel", Corrosion, 44(1988): p717.

Fischer, W., Paradies, H.H., Wagner, D. et al., "Copper Deterioration in Water Distribution System of a County Hospital in Germany Caused by Microbially Induced Corrosion - I. Description of the problem", Werkstoffe und Korrosion, 43(1992): p56.

Ford, T. and Mitchell, R., "The Ecology of Microbial Corrosion", Advanced Microbial Ecology, 11(1990): p231.

Franklin, M.J., White, D.C. and Isaacs, H.S., "Pitting Corrosion by Bacteria on Carbon Steel, Determined by the Scanning Vibrating Electrode Technique", Corrosion Science, 9(1991): p945.

Gallagher, P., Malpas, R.E. and Shone, E.B., "Corrosion of Stainless Steels in Natural, Transported and Artificial Seawaters, British Corrosion Journal, 23(1988): p229.

Gangloff, R.P., and Kelly, R.G., "Microbe-Enhanced Environmental Fatigue Crack Propagation in HY130 Steel", Corrosion, 50(1994): p345.

Gerchakov, S.M., Little, B.J. and Wagner, P., "Probing Microbiologically Induced Corrosion", Corrosion, 42(1986): p689.

Gerristead, W.R. Jr. and Link, L.F., "In-situ Corrosion Studies of Material Surfaces", Scanning, 2(1992): p14:II.

Goldstein, J.I., Newbury, P.E., Joy, D.C. et al., Scanning Electron Microscopy and X-Ray Microanalysis, Plenum Press, New York, p417, 1992.

Hadley, R.F., "The Influence of *Sporovibrio desulfuricans* on the Current and Potential Behavior of Corroding Iron", National Bureau of Standards Corrosion Conference, 1943.

Haufman, W., and Rouls, W., "Ductility of Steel Under the Influence of External High Pressure Hydrogen", Welding Journal, 44(1965): p225-s.

Ishizuki, H. and Onishi, K., Japan Chemistry Quarterly, 3(1967): p30.

Issacs, H.S. and Ishikawa, Y., "Application of the Vibration Probe to Localized Current Measurements," Corrosion/85, Paper No.55, National Association of Corrosion Engineers, Houston, TX, 1985.

Iverson, W.P., "Microbial Corrosion of Metals", Advanced Applied Microbiology, 32(1987): p1.

Izumiya, M., Shimizu, N. and Yamamoto, M., "Stress-Corrosion Cracking of Mild Steel in a Cooling Water System Due to Nitrobacteria", Key Engineering Materials, 20(1988): p2001.

Johnsen, R. and Bardal, E., "Cathodic Properties of Different Stainless Steels in Natural Seawater", Corrosion, 41(1985): p296.

Jones, D.A., Principles and Prevention of Corrosion, Macmillan Publishing Company, New York, p373, 1992a.

.e., D.A., Principles and Prevention of Corrosion, Macmillan Publishing Company, New York, p93, 1992b.

Jones, D.A., Principles and Prevention of Corrosion, Macmillan Publishing Company, New York, p376, 1992c.

Jones, R.H. and Ricker, R.E., "Mechanisms of Stress-Corrosion Cracking", in Stress-Corrosion Cracking, edited by R.H. Jones, ASM International, p1, 1992.

Jones-Meehan, J., Walch, M. et al., "ESEM/EDS, SEM/EDS and EIS Studies of Coated 4140 Steel Exposed to Marine, Mixed Microbial Communities Including Sulfate-Reducing Bacteria (SRB)", American Society of Mechanical Engineers, p1, 92-JPGC-NE-7, 1992.

Kendig, M.W., Allen, A.T. et al., "Application of Impedance Spectroscopy to the Evaluation of Corrosion Protection by Inhibitors and Polymer Coatings," in Electrochemical Techniques for Corrosion Engineering, edited by R. Baboian, NACE, Houston, TX, p151,1986.

Lee, W., "AC Impedance and Microbial Corrosion", in IPA Industrial Associates Report, Montana State University, Bozeman, p2, 1986.

LeRoux, N.W., "Mineral Attack by Microbial Processes", in Microbial Aspects of Metallurgy, edited by J.D. Miller, American Elsevir Publishing Co., Inc., New York, p173, 1971.

Little, B., Wagner, P., Gerchakov, S.M. et al., "The Involvement of a Thermophilic Bacterium in Corrosion Processes", Corrosion, 42(1986): p533.

Little, B., Wagner, P. and Mansfeld, F., "Microbiologically Influenced Corrosion of Metals and Alloys", International Materials Reviews, 36(1991a): p253.

Little, B., Wagner, P., Ray, R., Pope, R. and Scheetz, R., "Biofilms: an ESEM evaluation of artifacts introduced during SEM preparation", Journal of Industrial Microbiology, 8(1991b): p213.

Little, B., and Wagner, P., "Advances in MIC Testing," in Microbiologically Influenced Corrosion Testing, ASTM STP 1232, edited by J. R. Kearns and B.J. Little, American Society for Testing and Materials, Philadelphia, p1, 1994.

Mansfeld, F., "The Relationship Between Galvanic Current and Dissolution Rates", Corrosion, 29(1973): p403.

Mansfeld, F., "The Polarization Resistance Technique for Measuring Corrosion Currents", Advances in Corrosion Science and Technology, Plenum Press, New York , Vol.6, p163, 1976.

Mansfeld, F. and Little, B., "A Technical Review of Electrochemical Techniques Applied to Microbiologically Influenced Corrosion", Corrosion Science, 3(1991): p247.

Marsh, P.G. and Gerberich, W.W., "Stress-Corrosion Cracking of High-Strength Steels (Yield Strengths Greater Than 1240 MPa)", in Stress-Corrosion Cracking, edited by R.H. Jones, ASM International, p63, 1992.

Mollica, A., "Biofil and Corrosion on Active-Passive Alloys in Seawater", International !   eterioration and Biodegradation, 29(1992): p213.

Mollica, A., Trevi: .., Traverso, E. et al., "Interaction Between Biofouling and Oxygen Reduction Rate on Stainless Steel in Sea Water", in Proc. 6th Int. Cong. Marine Corrosion and Fouling, Athens, Greece, p269, 1984.

NACE (National Association of Corrosion Engineers), A State of the Art Review, MIT Publication series no.13, National Corrosion Engineering, p1-76,1984.

Obuekwe, C.O., Westlake, D.W.S., Cook, F.D. and Costerton, J.W., "Surface Changes in Mild Steel Coupons From the Action of Corrosion-causing Bacteria", Applied Environmental Microbiology, 41(1981): p66.

Pankhania, I.P., "Hydrogen Metabolism in Sulphate-Reducing Bacteria and Its Role in Anaerobic Corrosion", Biofouling, 1(1988): p27.

Pope, D.H., Duquette, D.J., Johannes, A.H. and Wayner, P.C., "Microbiologically Influenced Corrosion of Industrial Alloys", Materials Performance, 23(1984): p4.

Pope, D.H. and Zintel, T.P., "Methods for Investigating Underdeposit Microbiologically Influenced Corrosion", Materials Performance, 11(1989): p46.

Postgate, R., The Sulfate Reducing Bacteria, 2nd edition, Cambridge University Press, p31, 1984.

Purkiss, B.E., "Corrosion in Industrial Situations by Mixed Microbial Floras", in Microbial Aspects of Metallurgy, edited by J.D.. Miller, American Elsevir Publishing Co., Inc., New York, p107, 1971.

Ringas, C. and Robinson, F.P.A., "Corrosion of Stainless Steel by Sulfate-Reducing Bacteria--Electrochemical Techniques", Corrosion, 6(1987): p386.

Seed, L.J., "The Significance of Organisms in Corrosion", Corrosion Reviews, 9(1990): p1.

Schutz, R.W., "A Case for Titanium's Resistance to Microbiologically Influenced Corrosion", Materials Performance, 30(1991): p58.

Sedriks, A.J., "Stress-Corrosion Cracking of Stainless Steels", in Stress-Corrosion Cracking, edited by R.H. Jones, ASM International, p91, 1992.

Shackelford, J.F., Introduction to Materials Science for Engineers, 3rd Edition, Macmillan Publishing Company, New York, p340, 1992.

Singleton, Jr., R., "The Sulfate-Reducing Bacteria: An Overview", in The Sulfate-Reducing Bacteria: Comtemporary Perspectives, edited by J.M. Odom and R. Singleton, Jr., Springer-Verlag New York Inc., p11, 1992.

Sprowls, D.O., "Evaluation of Stress-Corrosion Cracking ", in Stress-Corrosion Cracking, edited by R.H. Jones, ASM International, p 363, 1992.

Tatnall, R.E., "Microbiologically Induced SCC?", Materials Performance, 2(1994): p68.

Thomas, C.J., Edyvean, G.J., Brook, R. et al., "The Effects of Microbially Produced Hydrogen Sulphide on the Corrosion Fatigue of Offshore Structural Steels", Corrosion Science, 27(1987): p1197.

Tiller, A.K., "A Review of the European Research Effort on Microbial Corrosion Between 1950 and 1984", Proc. Int. Conf. 'Biologically Induced Corrosion', NACE-8, p.121, 1986.

Tortora, G.J., Funke, B.R. and Case, C.L., Microbiology - An Introduction, The Benjamin/Cummings Publishing Company, Inc., Redwood City, CA. p16, 1989a.

Tortora, G.J., Funke, B.R. and Case, C.L., Microbiology - An Introduction, The Benjamin/Cummings Publishing Company, Inc., Redwood City, CA, p18, 1989b.

Tortora, G.J., Funke, B.R. and Case, C.L., Microbiology - An Introduction, The Benjamin/Cummings Publishing Company, Inc., Redwood City, CA. p74-76, 1989c.

Treseder, R.S., and Swanson, T.M., "Factors in Sulfide Corrosion Cracking of h Strength Steels", Corrosion, 24(1968): p31.

Troiano, A.R., "The Role of Hydrogen and Other Interstitials in the Mechanical Behavior of Metals", Transactions of American Society for Metals, 52(1960): p54.

Videla, H.A. and Characklis, W.G., "Biofouling and Microbially Influenced Corrosion", International Biodeterioration and Biodegradation, 29(1992): p195.

Voordouw, G., "From the Molecular Biology of *desulfovibrio* to a Nobel Method for Defining Bacterial Communities in Oil Field Environments", Fuel Processing Technology, 40(1994): p331.

Voordouw, G., Jack, T.R., Foght, J.M. et al., "Application of Reverse Sample Genome Probing to the Identification of Sulfate-reducing Bacteria", Proceedings of the Symposium on Microbiologically Influenced Corrosion Testing, ASTM Special Technical Publication, n1232, p188, 1994.

Wagner, P.A., "Investigations of Microbiologically Influenced Corrosion Using Environmental Scanning Electron Microscopy", Corrosion/92, Paper No.185, NACE, Houston, TX, 1992.

Walch, M., "Microbiological Influences on Marine Corrosion", Sea Technology, 32(1991): p31.

Walch, M., "Microbial Corrosion", in Encyclopedia of Microbiology, Academic Press, London, Vol.1, p585, 1992.

Wanklin, J.N. and Spruit, C.I.P., " Influence of Sulphate-Reducing Bacteria on the Corrosion Potential of Iron", Nature, 169(1952): p928.

Water, R.J., and Chandler, W.T., "Influence of Hydrogen Pressure and Notch Severity on Hydrogen-environment Embrittlement at Ambient Temperatures", Material Science and Engineering, 8(1971): p90.

Weimer, P.J., Van Kavelaar, M.J., Michel, C.B. et al., "Effect of Phosphate on the Corrosion of Carbon Steel and on the Compostion of Corrosion Products in Two-stage Continuous Cultures of *Desulfovibrio desulfuricans*", Applied Environmental Microbiology, 54(1988): p386.

Widdel, F. and Pfennig, N., "Dissimilatory Sulfate- or Sulfur-reducing Bacteria", in Bergey's Manual of Systematic Bacteriology, Williams & Wilkins, Baltimore, vol.1, p6 ,3, 1984.

Williams, D.P., and Nelson, H.G., "Embrittlement of 4130 Steel by Low-Pressure Gaseous Hydrogen", Metallurgical Transactions, 1(1970): p63.

Appendix A

A FORTRAN program to calculate the final diameter required to give the desired

stress for stainless steel C-ring specimens.

PROGRAM CRING1

****

*Purpose: This FORTRAN program calculates the final diameter required to

*give the desired stress for stainless steel C-rings using a given equation.

*Parameters: I, J ------------ integers:

*   DT ------------ D/T:

*   PI ------------ constant:

*   ODT ---------- actual measurements of OD or T:

*   OD ------------ average outside diameter:

*   T -------------- average thickness:

*   E -------------- elastic modulus:

*   YS ------------ yield strength:

*   F -------------- desired stress:

*   DELTA ------ change of OD giving desired stress:

*   ODF ---------- outside diameter of stressed C-ring:

*   D -------------- mean diameter (OD - t):

*   Z -------------- correction factor for curved beams.

****

```
      INTEGER I, J
      REAL  DT, PI, ODT(12,8), OD, T, YS, F, DELTA, ODF, D, E, Z
      REAL FACT
```

```
* PRINT THE TITLE OF FINAL RESULTS

        PRINT*, 'THE FINAL RESULT IS:'

        PRINT 1

1       FORMAT (1X, 'OD T DT Z DELTA ODF')


        OPEN (UNIT = 12, FILE='DATA1', STATUS ='OLD')


        DO 5 I = 1, 14

            READ (12, *) (ODT(I,J), J=1, 8)

5       CONTINUE


        DO 8 I = 1, 12

                ODI = 0.0

                TI = 0.0

        DO 10 J=1, 4

            ODI=ODI+ ODT(I,J)

10      CONTINUE


        DO 11 J=5, 8

                TI=TI+ODT(I,J)

11      CONTINUE


        OD = ODI/4.0

        T =TI/4.0


        D = OD - T
```

```
      DT = D/T

      Z = FACT(DT)

      E = 0.28E8

      YS = 0.4E5

      F = YS*0.85

      PI = 3.1416

      DELTA = F*PI*D*D/(4.0*E*T*Z)

      ODF = OD - DELTA


      PRINT 30, I, OD,T, DT, Z, DELTA, ODF
30    FORMAT (1X,'(',I2.')',5X, 6(F7.4,5X))
8         CONTINUE
      END


******************************************************************

      REAL FUNCTION FACT(DT)
      REAL DT
      IF (DT.GE.11.33.AND.DT.LE.11.67) THEN
            FACT = 0.9440
      ELSEIF (DT.LE.12.00) THEN
            FACT = 0.9453
      ELSEIF (DT.LE.12.33) THEN
            FACT = 0.9473
      ELSEIF (DT.LE.12.67) THEN
            FACT = 0.9487
      ELSEIF (DT.LE.13.00) THEN
```

```
        FACT = 0.9500

ELSEIF (DT.LE.13.33) THEN

        FACT = 0.9513

ELSEIF (DT.LE.13.67) THEN

        FACT = 0.9520

ELSEIF (DT.LE.14.00) THEN

        FACT = 0.9533

ELSEIF (DT.LE.14.33) THEN

        FACT = 0.9540

ELSEIF (DT.LE.14.67) THEN

        FACT = 0.9547

ELSEIF (DT.LE.15.00) THEN

        FACT = 0.9560

ELSEIF (DT.LE.15.33) THEN

        FACT = 0.9573

ELSE

        PRINT*, 'BEYOND THE EXPECTED RANGE'

        STOP

ENDIF

RETURN

END
```